CHEMICAL REVIEWS

pubs.acs.org/CR

Review

Metal–Organic Framework-Based Hierarchically Porous Materials: Synthesis and Applications

Guorui Cai,[†] Peng Yan,[†] Liangliang Zhang, Hong-Cai Zhou, and Hai-Long Jiang*

Cite This: *Chem. Rev.* 2021, 121, 12278–12326

Read Online

ACCESS | Metrics & More | Article Recommendations

ABSTRACT: Metal–organic frameworks (MOFs) have been widely recognized as one of the most fascinating classes of materials from science and engineering perspectives, benefiting from their high porosity and well-defined and tailored structures and components at the atomic level. Although their intrinsic micropores endow size-selective capability and high surface area, etc., the narrow pores limit their applications toward diffusion-control and large-size species involved processes. In recent years, the construction of hierarchically porous MOFs (HP-MOFs), MOF-based hierarchically porous composites, and MOF-based hierarchically porous derivatives has captured widespread interest to extend the applications of conventional MOF-based materials. In this Review, the recent advances in the design, synthesis, and functional applications of MOF-based hierarchically porous materials are summarized. Their structural characters toward various applications, including catalysis, gas storage and separation, air filtration, sewage treatment, sensing and energy storage, have been demonstrated with typical reports. The comparison of HP-MOFs with traditional porous materials (e.g., zeolite, porous silica, carbons, metal oxides, and polymers), subsisting challenges, as well as future directions in this research field, are also indicated.

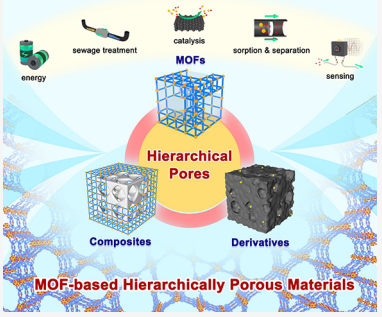

CONTENTS

Received: March 23, 2021
Published: July 19, 2021

https://doi.org/10.1021/acs.chemrev.1c00243
Chem. Rev. 2021, 121, 12278–12326

1. INTRODUCTION

Porous materials play significant roles in our daily activities. They have attracted great attention in various fields from structural materials to energy technologies, covering applications in catalysis, adsorption/separation, biomedicine, energy, etc. Classical porous materials, for example, zeolite, mesoporous silica, carbon, metal oxide, and polymer, are usually either fully organic or inorganic materials.[1−8] Most of them are amorphous porous solids suffering from undefined structures, irregular pores, and are, thus, unfavorable for understanding structure−property relationships. Specifically, zeolites, a class of crystalline porous solids with superior stability, periodic structure, and intrinsic acidity, have found wide applications in industrial adsorption and catalysis. Unfortunately, the rational control of acidic site distribution is challenging, and the limited kinds of pore structures are disadvantageous factors. Consequently, the exploration of advanced porous materials with well-defined, numerous, readily tailored structures toward various applications continues to be an intense area of scientific research.

Metal−organic frameworks (MOFs), a class of organic−inorganic hybrid and crystalline porous materials, have significantly enriched the domain of porous materials.[9−17] In general, their framework structures, pore environment, and functionality can be finely adjusted by elaborately choosing desirable metal nodes and organic linkers, the rational design of topological structures (the way how they are assembled), and postsynthetic modification of MOF skeletons. Therefore, compared with the traditional porous materials, MOFs integrate their particular advantages. For example, (1) their crystalline nature endows MOFs with well-defined structures, which are of great importance to understand the underlying mechanism and relationship between structural features and resulting performance. (2) The organic−inorganic hybrid structures not only combine the respective beneficial characters of organic and inorganic components, but also endow exceptional properties beyond a simple mixture of their components. (3) Their high surface area and porosity ensure abundant and available functional sites, which favor the adsorption and enrichment of substrate molecules around the active sites. (4) The uniform pore size/shape allows the accessibility of reaction substrates and products with specific size/shape, thereby enabling the size-selective permeability of MOFs. (5) The tunable pore wall environment at atomic/molecular level, in a de novo or postsynthetic manner, enables the recognition and transportation of substrates and products, as well as the adjustment of the interaction between substrates with active sites. (6) Given MOFs are compatible with various kinds of materials (e.g., metal nanoparticles, biomolecules, polymers), the permanent pore space of MOFs provides congenital conditions for the incorporation of functional species, generating MOF composites for diverse ends. (7) Owing to the coexistence and homogeneous dispersion of metal ions and organic linkers in a highly porous structure, MOFs are excellent precursors/templates for various porous carbons, metal-based compounds and their composites.

Despite the above structural advantages, the pore sizes of MOFs are mainly tunable in the microporous regime (<2 nm). To some extent, micropores are necessary to ensure the high surface area, abundant active sites, strong interaction between substrates and MOFs, heterogenization/stabilization of small-sized active species, and size-selective effects. On the other hand, their inherent microporosity brings about the hindrance of mass transfer and restricts their applications involving large species.[18−22] Therefore, it is of great importance to extend the pore sizes of MOFs to a larger regime, including mesopore and even macropore to meet the growing demands in diverse ends, especially large-species-involved (e.g., large drug molecules, bioenzymes, proteins) and mass diffusion related (e.g., continuous separation, batch/flow reactors) applications.[18−23] As a matter of fact, many MOFs exhibit mesoporous cages within their inherent structures. However, in the majority of cases, these large cavities are accessed via much smaller apertures which limit the size of molecules that can diffuse into the functional mesoporous spaces. In addition, the construction of mesopores by elongated linkers easily leads to framework interpenetration, and the resulting mesoporous structures are prone to collapse after removing the templates or guest solvent molecules.[24−27]

Hierarchically porous materials, referring to multiple-level-pore-containing materials, integrate the strengths of microporous and meso-/macroporous materials, thereby offering an original path to solve mass transfer issues. In fact, hierarchically porous structures, formed by long-term biological evolution, play an essential part in maintaining the function of living organisms, as well as enhancing the adaptivity to environmental changes.[28−30] Generally, the pores of functional materials are divided into three categories, namely micropores (<2 nm), mesopores (2−50 nm) and macropores (>50 nm). In the field of MOF research, pores with a diameter larger than 2 nm is of particular interest. In this Review, we will focus on hierarchically porous MOFs (HP-MOFs) and related materials possessing two or all the three categories of pores. Materials integrating different kinds of mesopores or macropores are also mentioned.[1,2,31−33] The development of HP-MOFs will not only keep the function of micropores which ensure the high surface area, but also build mesopores/macropores across the microporous matrix, which contribute to the required accessibility/space toward large-size species and minimize diffusion barriers. Given their adjustable components and structures in atomic/molecular level, HP-MOFs enable precise control of various variables of hierarchy including porosity variables (bimodal, trimodal, or multimodal pores and pore size at each porous level), structural variables (the topology structures of metal clusters and organic linkers, as well as the way how they assemble, crystalline phase, and interfaces at all

https://doi.org/10.1021/acs.chemrev.1c00243
Chem. Rev. 2021, 121, 12278−12326

levels), component variables (atomic and molecular chemical composition and distribution), and morphological variables (shape, grain size, and orientation distributions).

Owing to the intrinsic features of MOF powders, HP-MOFs still suffer from similar issues to conventional MOFs toward practical applications, such as poor processability, low conductivity, and mediocre stability. To address these issues, the incorporation of MOFs with additional porous materials with flexible mechanical properties has been proven an alternative solution to supply MOFs with both hierarchically porous structures and good handleability.[34−37] On the other hand, the conversion of MOFs into corresponding porous carbon, metal-based compounds or their composites has been recognized as a promising way to enhance the stability and conductivity, as well as introduce additional porosity to the MOF-derived porous materials, while partially inheriting the characteristics of pristine MOFs.[38−42]

Given the rapid growth of MOF-based materials in recent years, there have been several review articles related to mesoporous MOFs or HP-MOFs because of the increasing importance of this topic.[18−22,25−27,43] Typically, there are several reviews summarizing the preparation methods of mesoporous MOFs or HP-MOFs. However, these summaries are mainly focused on one of the synthetic strategies, such as supramolecular templating or perturbation-assisted nanofusion synthesis.[19,20] Actually, the comprehensive discussions on diverse synthetic strategies for HP-MOFs, MOF-based hierarchically porous composites (hereafter, denoted as HP-composites) and MOF-based hierarchically porous derivatives (hereafter, denoted as HP-derivatives) have yet been reached up to now. In addition, after more than ten years of development, there have been also some review articles on the applications of MOF-based materials.[14,34,44,45] Unfortunately, they almost do not systematically summarize the structure−performance relationships between hierarchical pores in various MOF-based materials and the targeted applications. Therefore, it is timely and highly expected to compose a comprehensive review article summarizing the rational fabrication and enhanced applications of all types of MOF-based hierarchically porous materials.

To discuss the relationship between the specific hierarchically porous structures and enhanced applications in a logical way, the reported MOF-based hierarchically porous materials are divided into three categories based on their structural features and origin of hierarchical pores, including HP-MOFs, MOF-based HP-composites, and MOF-based HP-derivatives (Figure 1). In this Review, the significant progress in the design and synthesis of different types of MOF-based hierarchically porous materials is presented with typical reports. When discussing the functional applications of these materials, the relationship between their unique pore structures and the specific performance is highlighted to unravel the underlying mechanism. To further illustrate the strengths of multilevel porous structures, we make a comparison between MOF-based hierarchically porous materials and traditional porous materials. Finally, the challenges and outlook of this field are put forward to propose the future research direction. We believe that this Review will be able to help readers to gain a better understanding of the formation mechanism of hierarchical pores in different MOF-based porous systems, and the fundamental principles of how to design and fabricate HP-MOFs, MOF-based HP-composites, and MOF-based HP-derivatives toward targeted applications.

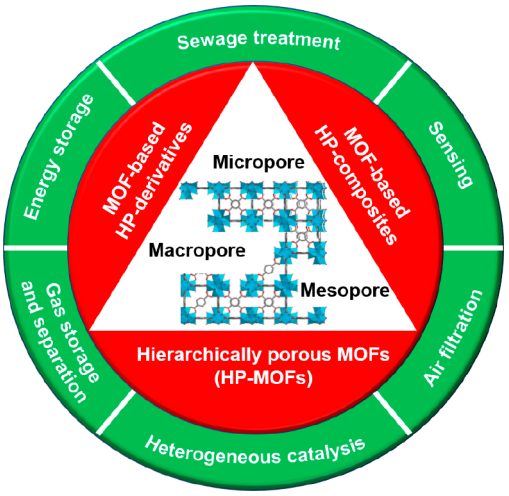

Figure 1. Schematic showing the construction of MOF-based hierarchically porous materials for various practical applications.

2. RATIONAL FABRICATION OF MOF-BASED HIERARCHICALLY POROUS MATERIALS

Depending on the origin of hierarchical pores, MOF-based hierarchically porous materials can be classified into three subgroups: 1) hierarchically porous MOFs (hierarchical pores based on the intrinsic pores in MOFs); 2) MOF-based hierarchically porous composites (hierarchical pores based on the integration of intrinsic pores in MOFs and additional porous materials); 3) MOF-based hierarchically porous derivatives (MOFs or/and MOF-based composites derived hierarchically porous materials).

2.1. Hierarchically Porous MOFs (HP-MOFs)

Although most MOFs are in the microporous regime, to some extent, their pore sizes can be extended to meso-/macroporous ranges by elaborate design of larger cages and wider channels or the introduction of additional defective mesopores and even hollow structures while maintaining the overall framework structures of the parent MOFs.[25−27,43] Corresponding synthetic strategies will be discussed in detail in the following three subsections: intrinsic, defective and hollow HP-MOFs.

2.1.1. Intrinsic HP-MOFs. The intrinsic HP-MOFs feature periodic structures and their hierarchical pores are fully composed of the intrinsic micropores and mesopores in MOFs, which are typically achieved by the reasonable choice of longer ligands, larger metal clusters, rational design of topological structures, etc.

2.1.1.1. Creating Mesoporous MOFs with Extended/Large Linkers and Large Metal Clusters. To address the drawbacks of microporous MOFs, many efforts have been made to create mesopores when designing new MOFs. A straightforward solution to fabricate larger pores in MOFs is the extension of the bridging linker length to afford mesopores while keeping the framework topology. IRMOF series are the first models to generate mesoporous MOFs by using linker extension strategy (Figure 2).[46] They are isoreticular analogues of MOF-5, in which the octahedral $Zn_4O(CO_2)_6$ clusters as nodes and ditopic linear carboxylate ligands as linkers are assembled into a cubic topology.[47] By the replacement of BDC (1,4-benzenedicarboxylate) with the extended linkers BPDC, HPDC, PDC, and TPDC (their molecular structures were shown in Figure 2), a series of IRMOFs with larger pore sizes can be obtained, respectively. The pore size of IRMOF-16 is as

https://doi.org/10.1021/acs.chemrev.1c00243
Chem. Rev. 2021, 121, 12278−12326

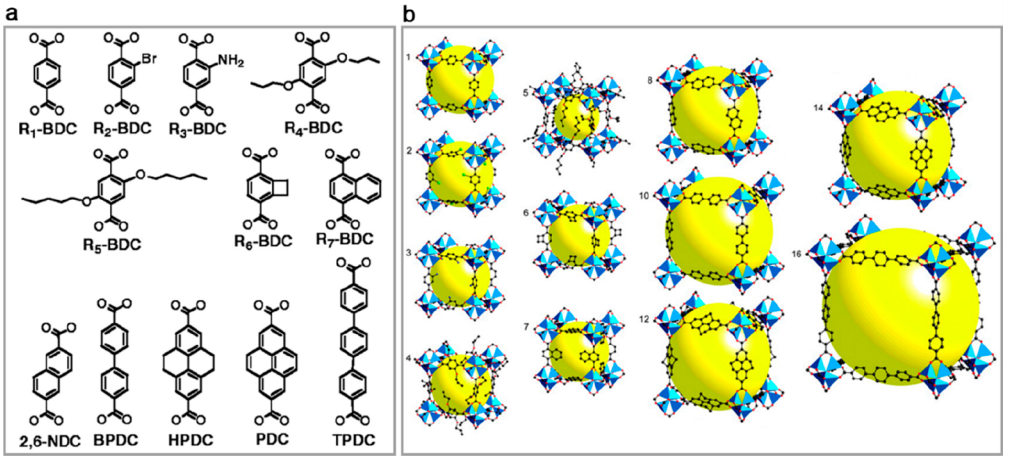

Figure 2. Schematic showing the (a) linear linkers and (b) single-crystal X-ray structures of IRMOF series. Adapted with permission from ref 46. Copyright 2002 The American Association for the Advancement of Science.

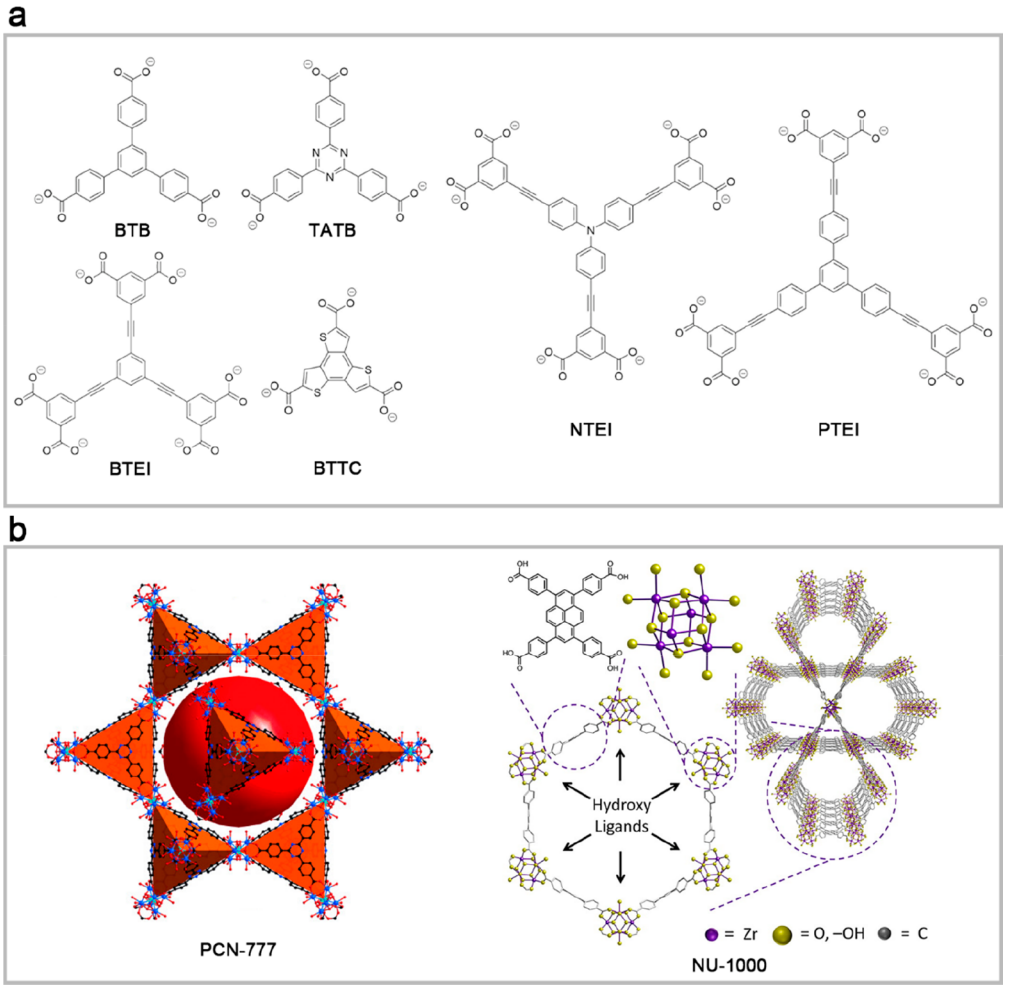

Figure 3. (a) Summary of tritopic linkers used for the construction of mesoporous MOFs. (b) Structure of typical mesoporous MOFs constructed with tritopic and tetratopic linkers. The illustration for PCN-777 is reproduced with permission from ref 52. Copyright 2014 John Wiley & Sons, Inc. The illustration for NU-1000 is reproduced from ref 69. Copyright 2013 American Chemical Society.

large as 2.88 nm. Unfortunately, the targeted products with extended linear linkers are mostly thermodynamically instable and tend to form an interpenetrated structure, which in turn reduces the pore sizes of the obtained MOFs.

To avoid the interpenetration effect of MOFs with extended linear ligands, Deng et al. further replaced octahedral $Zn_4O(CO_2)_6$ clusters with infinite rod-shaped metal carboxylate secondary building units (SBUs). Different from the cubic pores of IRMOFs, such SBUs are joined along the long and short axis by organic linkers to form MOF-74 with one-dimensional channel-typed structures, effectively eliminating the possibility of interpenetration. This specific construction

https://doi.org/10.1021/acs.chemrev.1c00243
Chem. Rev. 2021, 121, 12278−12326

guarantees the isoreticular expansion of pore sizes from 1.4 to 9.8 nm without interpenetration. However, the poor solubility of long linkers makes them incompatible with the common solvothermal synthetic conditions, which usually leads to more complicated synthetic procedures. The long linkers themselves are also difficult to synthesize, thereby impeding the practical use of these MOFs.[48] It must be pointed out that the above-mentioned MOFs might not be hierarchically porous in a narrow sense, since they only contain one level of pores (generally only mesopores). Nonetheless, these creative works definitely offer a controllable strategy to extend the tiny MOF pores to large-size regimes similar to the purpose of HP-MOFs.

In addition to longer linear linkers, bulky multitopic ligands have been recognized as excellent candidates for the construction of mesopores without interpenetration. As shown in Figure 3, derived from BTC (benzene-1,3,5-tricarboxylate), a series of tritopic linker analogues were developed to produce MOFs with large pore sizes, such as PCN-X (X = 308, 332, 333, 610, 777), BUT-12, BUT-13, NU-100, NU-1301, NU-1200, InPF-110, MOF-818, MOF-919, STMOF, etc.[49−59] Similarly, some tetratopic linkers, for example, tetrakis(4-carboxyphenyl)porphyrin) (TCPP), 1,3,6,8-tetrakis(*p*-benzoicacid)pyrene (TBAPy), were also used to construct mesopores in MOFs, such as PCN-X (X = 128W, 222, 228, 229, 300, 605, 606, 608),[60−64] NU-X (X = 1000, 1003, 1004, 1005, 1006, 1007, 1008, 1200),[65−69] MIT-25,[70] UMCM-313,[71] etc.

On the other hand, increasing the size of the metal nodes instead of the complexity of the extended linkers has been proven a promising alternative strategy for the introduction of large pore spaces. For example, Bio-MOF-100 with a 2.8 nm mesoporous channel was successfully synthesized by using the huge metal-biomolecule clusters (zinc-adeninate octahedral building units) as the metal node (Figure 4).[72]

2.1.1.2. Intrinsic HP-MOFs by Rational Design of Topological Structures. Although the long linkers and large clusters are able to provide great possibility for the formation of mesopores, the successful construction of a "real" HP-MOF requires a proper topology design to form at least two different kinds of pores. For example, MIL-101, MIL-88, and MIL-53 are all built by similar components of M_3O clusters and BDC linkers. Although MIL-53 and MIL-88 are microporous, MIL-101 has two types of mesoporous cages with diameters of 2.9 and 3.4 nm and microporous openings of 1.2 and 1.45 nm by 1.6 nm.[73−77] Later, Du et al. demonstrated a promising alternative strategy for the construction of mesopores through modulating the ligand symmetry rather than expanding the length of ligands (Figure 5). The 446-MOF with trigonal micropores (0.8 nm) and channel-type mesopores (3.0 nm) is achieved by the assembly of Zn_4(adeninate)$_8$ clusters with the C_3-symmetric organic linkers instead of C_2-symmetric ligands.[78]

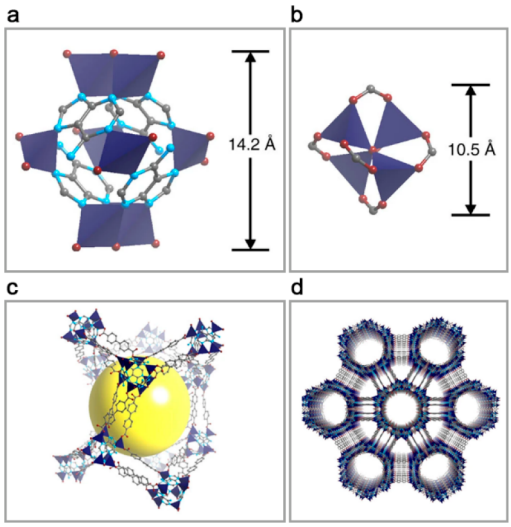

Figure 4. Comparison of (a) zinc-adeninate octahedral and (b) basic zinc-carboxylate building units. In the crystal structure of bio-MOF-100, one zinc-adeninate octahedral building unit is coordinated with 12 BPDC (biphenyldicarboxylate) linkers to produce the large (c) 3D cages and (d) 1D channels in the MOF. Reproduced with permission from ref 72. Copyright 2012 Nature Springer.

As an alternative solution, multiple ligands strategy has been also developed to build MOFs with hierarchical pores, in which two or more different organic ligands are more likely to be assembled into a framework with more than one kind of pores. Based on this strategy, Matzger group reported the synthesis of $Zn_4O(BDC)(BTB)_{4/3}$ (UMCM-1) by the assembly of zinc ions with two ligands, BDC and BTB (1,3,5-tris(4-carboxyphenyl)benzene), at a very early stage. The resulting UMCM-1 with an octahedral geometry possesses channel-type mesopores with the dimension of 2.7 nm × 3.2 nm.[79] Subsequently, a series of noninterpenetrated MOFs (e.g., UMCM-2, MOF-210, DUT-6, DUT-23, DUT-25, DUT-32) with hierarchically porous nature have been synthesized based on this strategy.[80−85]

2.1.2. Defective HP-MOFs. For defective HP-MOFs, their hierarchical pores are mainly constructed by introducing additional meso-/macropores into conventional microporous MOF skeletons, preserving the crystalline nature of the original MOFs. Related technologies can be divided into two subgroups: the de novo synthetic and postsynthetic strategies. The de novo synthetic strategies can be divided into two categories in terms of whether a template is used during the synthesis process. The template methods utilize soft, hard or even self-sacrificial templates to occupy spaces. Mesopores or macropores are generated when the templates are cleared up. The template-free methods include ligand fragment strategy, modulator-induced defect formation strategy, sol−gel strategy, 3D printing, etc. The postsynthetic strategies, comprising of chemical etching strategy, thermal decomposition strategy, stepwise ligand exchange strategy, metal ion metathesis strategy, phase transformation strategy, etc., produce additional defective sites and large pore spaces in originally defect-free MOFs.

2.1.2.1. De Novo Synthetic Strategy. Soft Template Methods. Similar to the synthesis of mesoporous silica, soft templates, generally formed by self-assembly of amphiphilic molecules, can also be used to create additional mesopores in the frameworks of conventional microporous MOFs.[86] The strategy was first employed to the synthesis of hierarchically porous HKUST-1 (HP-HKUST-1), by using cetyltrimethylammonium bromide (CTAB) as the structure-directing agent to form micellar templates (Figure 6a). The electrostatic interactions between positively charged micelles and the negatively charged BTC^{3-} ions would direct the final positioning of the nucleation and growth processes of microporous MOF crystals. After removal of the surfactants by an extraction treatment with ethanol, HP-HKUST-1 with mesopores as large as 5.6 nm can be obtained.[87]

https://doi.org/10.1021/acs.chemrev.1c00243
Chem. Rev. 2021, 121, 12278−12326

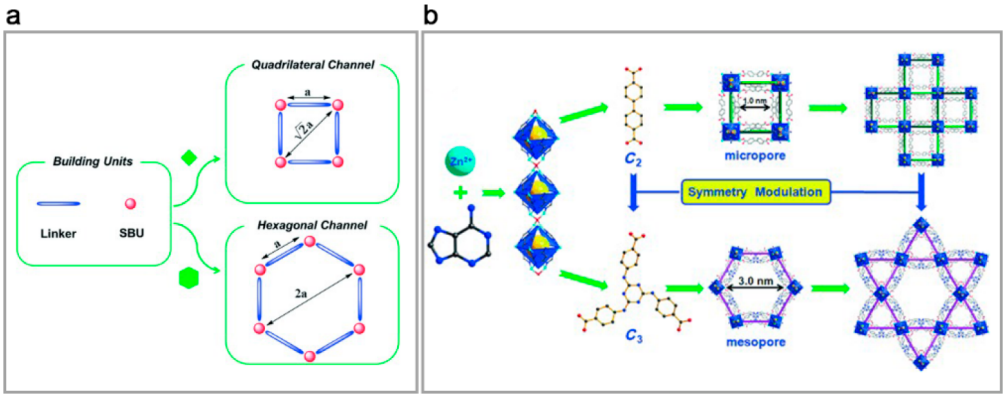

Figure 5. Schematic representation of the design strategy for (a) the construction of mesopores and (b) the structures of MOFs based on the linkers with different symmetries. Reproduced with permission from ref 78. Copyright 2015 John Wiley & Sons, Inc.

However, the weak interaction between surfactants and MOF precursors is prone to cause a phase separation between them during the self-assembly, resulting in the exclusion of micellar templates from the microporous MOF skeletons. To impede this tendency, a co-template was utilized as a chelating reagent to enhance their interaction, in which the surfactant molecules formed micelles and the chelating agent bridged the MOF precursors and the micelles, thereby ensuring a cooperative self-assembly and directed crystal growth. The citric acid (CA) was employed to rationally adjust the interactions between the micellar templates and the MOF precursors, where the multianionic CA could increase such interactions via both electrostatic interactions and the chelation of the metal ions (Figure 6b). In this way, the HP-HKUST-1 was prepared with a maximum mesopore diameter of 19.6 nm.[88]

Because of the strong tendency of self-nucleation of MOFs during the synthesis process, it is hard to introduce additional mesopores with uniform long-range periodicity by solely using surfactants. To optimize the kinetics of self-assembly, crown ether was utilized as a chelating reagent to controllably release metal ions, thereby slowing down the self-nucleation process (Figure 6c). In this way, hierarchically porous Cd-MOFs with ordered mesopores are synthesized by using crown ether 1,10-diaza-18-crown-6 (NC) to slowly release the Cd^{2+} during the surfactant self-assembly and MOF crystal growth.[89]

In recent years, various surfactants and block copolymers have been employed as the soft templates for the fabrication of various HP-MOFs, for example, ionic liquid (IL), block copolymers (F127 and P123), cationic surfactants (CTAC and CTAB), etc.[86−91,93−114] However, the micelles assembled from them suffer from limited sizes. Adding the swollen reagent into their interior to enlarge the size of micelles represents an alternative solution. For example, the incorporation of a hydrophobic organic compound, 1,3,5-trimethylbenzene (TMB), as an auxiliary structure-directing agent to swell the CTAB micelles causes the increase of the mesopore sizes in the resulting meso-MOFs.[87] Besides liquid reagents, gas molecules can also function as the swollen reagent. For instance, a series of HP-MOFs with adjustable mesopores were prepared by combining the advantages of IL and supercritical CO_2, in which IL forms the micelles and supercritical CO_2 is dissolved in the IL to swell the micelles (Figure 6d).[90]

To synthesize a hierarchically porous UiO-66-NH_2, the Gu group designed an amphoteric surfactant with bifunctional hydrophilic headgroup based on the combination of carboxylate group and quaternary ammonium, in which the former attaches the surfactant to MOFs' metal clusters strongly, while the latter ensures high solubility for the otherwise insoluble fatty acid in aqueous solution (Figure 6f). Therefore, this bifunctional surfactant not only serves as the soft template but also chemically bonds to MOF precursors, thereby avoiding the phase separation of surfactant assemblies during the formation of MOFs. The excellent stability of UiO-66-NH_2 prevent itself from decomposing when soaking in the methanol solution of hydrochloric acid to remove the templates.[91] In addition, the same group developed a series of stable HP-MOFs with large mesopores (>10 nm) by combining the synergistic effects of triblock polymer and hofmeister ion. They found that the introduction of Hofmeister ions (e.g., ClO_4^-) could promote the nucleation and growth of stable MOFs (e.g., Ce-UiO-66, Zr-UiO-66-NH_2) in aqueous phase and the in situ crystallization of MOFs around templates, thus opening the possibility of stable HP-MOFs obtained in mild reaction condition and aqueous solution (Figure 6e).[92,115,116]

The selection and compatibility of desirable soft template and proper solvent are essential for the formation of stable micellar templates with specific sizes and shapes (e.g., spheric pores, 1D cylindrical pores, etc.). Once the template is chosen, the size of resulting micelles can be readily adjusted to some extent by altering the length of the surfactant's carbon skeleton. Liquid or gas phase swollen agents can be added to further expand the pore size. Additionally, the concentration of surfactants poses a direct influence toward the number of micelles, thereby providing a straightforward method to tune the mesoporosity of HP-MOFs. Despite these features, the tailorability of this method is relatively limited. For example, the soft-template strategy restricts the synthesis mixture to aqueous or alcoholic systems (although some reports demonstrate W/O emulsion systems successfully extend this method to organic solvents),[99] because the frequently used surfactants tend to dissolve rather than assemble to micelles in organic solvents. However, many MOFs, especially stable MOFs, require an organic solvothermal condition to crystallize. Therefore, the soft-template strategy is limited to a small volume of MOFs.

Hard Template Methods. Different from cooperative coassembly of soft templates, hard-template methods involve the direct addition of preformed templates into the precursor solution of MOFs, and MOF crystals are subsequently directed grown on the surface of hard templates. After selectively

https://doi.org/10.1021/acs.chemrev.1c00243
Chem. Rev. 2021, 121, 12278−12326

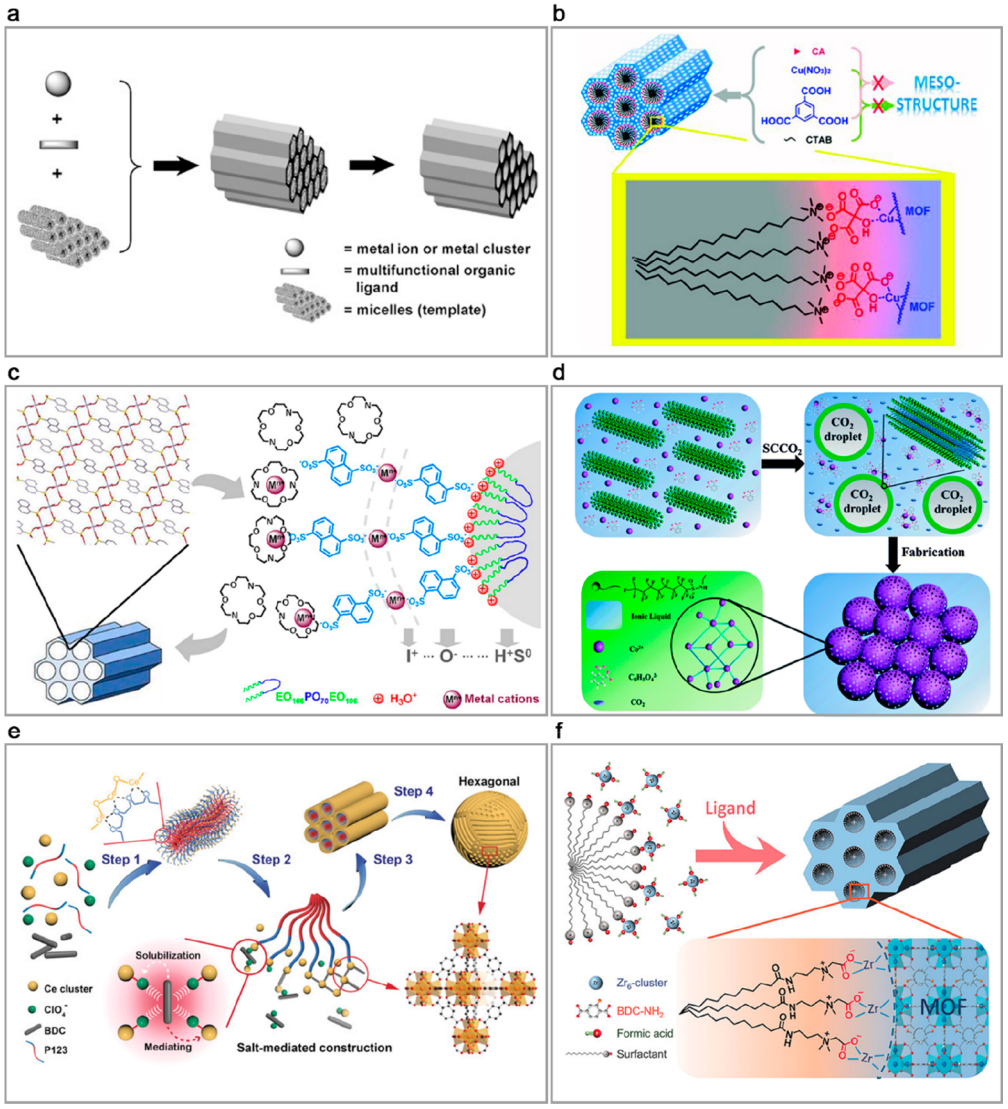

Figure 6. (a) Schematic showing the construction of mesopores in MOFs based on the self-assembly of amphiphilic molecules. Reproduced with permission from ref 87. Copyright 2008 John Wiley & Sons, Inc. (b) Schematic showing the mechanism of chelating reagent to enhance the interaction of soft template and MOFs. Reproduced with permission from ref 88. Copyright 2012 American Chemical Society. (c) Schematic showing the mechanism of controllable releasing metal ions. Reproduced with permission from ref 89. Copyright 2012 American Chemical Society. (d) Schematic representation of the design strategy for expanding the sizes of micellar templates based on the supercritical CO_2 as the swollen reagent. Reproduced with permission from ref 90. Copyright 2015 Royal Society of Chemistry. (e) Illustration for the construction of HP-MOFs based on the synergistic effects of Hofmeister ion and triblock polymer. Reproduced with permission from ref 92. Copyright 2020 John Wiley & Sons, Inc. (f) Illustration for the construction of stable HP-MOFs (mesoUiO-66-NH_2) based on a bifunctional surfactant. Reproduced with permission from ref 91. Copyright 2018 John Wiley & Sons, Inc.

etching the hard templates, HP-MOFs with inverse-template porous structures will be obtained. Two prerequisites are important for this strategy: one is heterogeneous nucleation and oriented growth of MOFs on the template surface, and the other is the selective removal of the hard templates from template/MOFs composites.[117−122]

In order to control the growth position of MOF crystals, some special functional groups, acting as the coordinating/anchoring sites to induce the nucleation of MOFs, are necessarily employed to modify the surface of selected templates. For example, Li et al. reported a HP-HKUST-1 membrane with ordered macroporous structures based on a colloidal crystal templating method. The polystyrene (PS) latex with a carboxylic acid terminated surface was utilized to form a hard template. A clear solution of MOF precursors was infiltrated into it and followed by solvent evaporation for MOF crystallization. After the dissolution of PS in tetrahydrofuran (THF), a large volume of macropores with the same diameter as the PS template particles were formed in the skeleton of MOF membranes, indicating the successful replication of the template structure.[117] Similarly, Jing et al. prepared a hierarchically porous ZIF-8 (HZIF-8) with additional macropores by using carboxylic acid terminated PS templates (Figure 7a). Thermogravimetric analysis (TGA) showed that a small part of PS still remained in HZIF-8, even after repeating the template removal step twice. They demonstrated that the remaining PS should adhere to the crystal surface of ZIF-8 as the result of the coordination between Zn^{2+} ions and the carboxylic acid. As a result, in addition to the function as the template to construct the macropores, the residual PS modified

https://doi.org/10.1021/acs.chemrev.1c00243
Chem. Rev. 2021, 121, 12278−12326

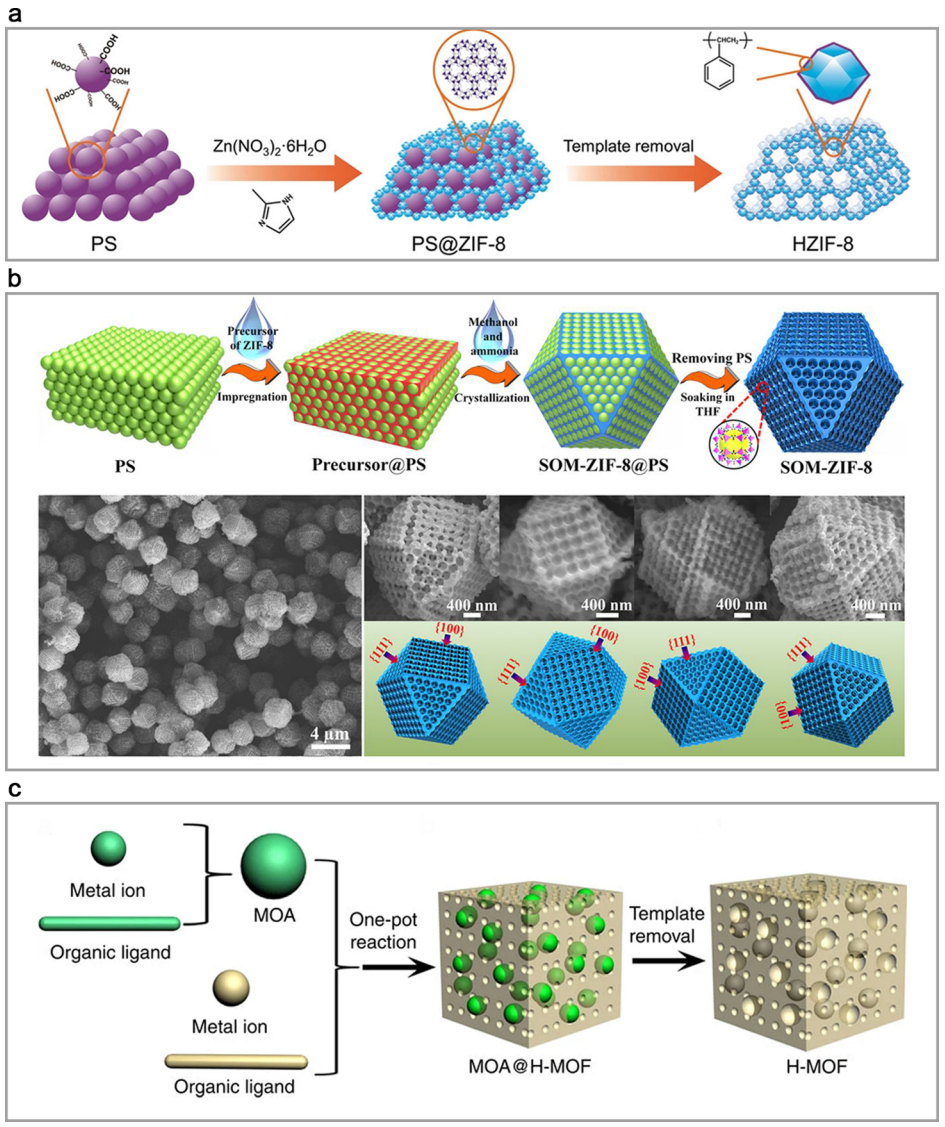

Figure 7. (a) Illustration showing the construction of HZIF-8 based on polystyrene (PS) latex with a carboxylic acid terminated surface. Reproduced with permission from ref 121. Copyright 2018 John Wiley & Sons, Inc. (b) Polystyrene templated methods to introduce highly ordered and oriented macropores into MOF single crystals. Adapted with permission from ref 122. Copyright 2018 The American Association for the Advancement of Science. (c) Schematic construction of HP-MOFs by using metal−organic assemblies (MOAs) as labile templates. Reproduced with permission from ref 123. Copyright 2015 Nature Springer.

the crystal surface of ZIF-8 with enhanced hydrophobicity.[121] It is worth mentioning that Cui et al. presented a spatially confined crystallization in a microfluidic synthesis device to the large-scale synthesis of uniform single-crystalline HP-HKUST-1 particles with PS as templates.[120]

In addition, surfactant bearing a large volume of polar groups can also be employed to induce the growth of MOF crystals on selected hard templates. For example, the Huo group reported a facile strategy of introducing mesopores inside MOF skeletons through the utilization of noble metal nanoparticles (NPs) like Au as the templates, whose surfaces were functionalized with polyvinylpyrrolidone (PVP) to exert an attraction to the MOF precursors. After eliminating Au NPs with KI and I_2 mixed solution in a gentle way, pores mimicking the size and shape of Au NPs were generated in the MOF matrix. The spatial distribution of pores could be finely tuned by varying the addition time of Au NPs templates. With the help of this strategy, various HP-MOFs with shape-, size-, and even space-distribution-controlled porous structures were fabricated by the encapsulation and subsequent removal of metal NPs templates.[118] In order to create single-crystalline macroporous MOF shell embedded with Au NPs, Wang et al. used a core−shell Au@SiO_2 as the templates to produce a micro-/macroporous ZIF-8. After coating the templates with PVP and then immersing them into the solution of MOF precursors, a core−shell−shell Au@silica@ZIF-8 nanostructure was obtained. The silica layer in the composites was selectively etched away by NaOH solution to generate macropores in yolk−shell Au@ZIF-8 macroporous nanoreactors.[119]

The Li and Chen groups prepared a single-crystalline ZIF-8 with highly ordered and oriented macropores based on the incorporation of the strong shaping effects of a monolith template and the double-solvent-induced heterogeneous nucleation approach (Figure 7b). When they attempted to soak highly ordered 3-dimensional (3D) PS (without modified

https://doi.org/10.1021/acs.chemrev.1c00243
Chem. Rev. 2021, 121, 12278−12326

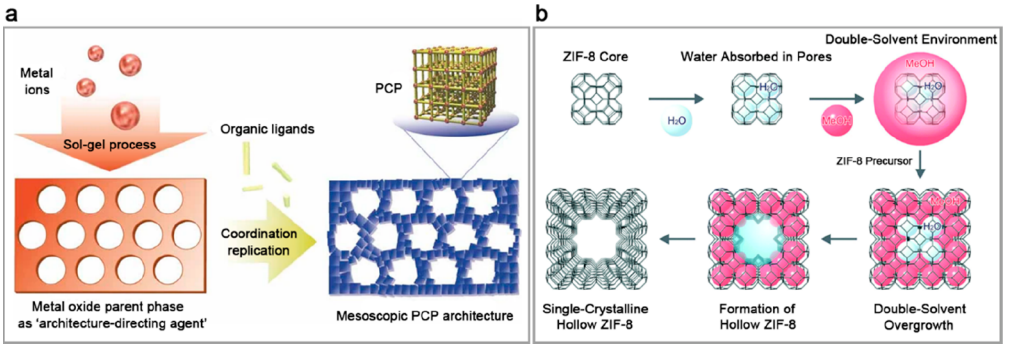

Figure 8. (a) Coordination replication of a metastable metal oxide phase by more stable porous coordination polymer (PCP) crystals. Adapted with permission from ref 126. Copyright 2012 Nature Springer. (b) Schematic showing the double solvent mediated overgrowth of hollow and mesoporous ZIF-8 microcrystals. Adapted with permission from ref 127. Copyright 2015 Royal Society of Chemistry.

groups like carboxylic acid) monoliths into the methanol solution of ZIF-8 precursors, ZIF-8 crystals were all grown outside the monoliths, due to the self-nucleated microporous products. In order to confine the growth of MOFs inside the 3D ordered templates, they developed a double-solvent-assisted method to overcome the energy barrier to homogeneous nucleation, in which ammonium hydroxide induced a rapid crystallization of MOF precursors, while methanol stabilize the precursors and adjusted the balance between nucleation and growth of ZIF-8 crystals. The additional pore diameters and particle sizes could be systematically controlled by adjusting the size of PS and the ratio of ammonium hydroxide/methanol, respectively.[122]

Labile metal−organic hybrid materials are also ideal candidates in the hard-templated synthesis, which exhibit desired interaction with both precursors (metal ions and organic ligands) of MOFs.[123,124] Motivated by this, Huang et al. proposed to use metal−organic assemblies (MOAs) including MOFs as the templates to prepare HP-MOFs through an in situ self-assembly approach, where both the targeted porous materials and the templates belong to coordination complexes, being compatible in structural nature and reaction activity (Figure 7c). Simultaneously, the authors took advantage of their relatively different stabilities to get desired HP-MOFs, that is, the unstable MOAs were etched away with acid treatment while preserving the crystallinity of HP-MOFs.[123]

Additionally, Teng et al. prepared a bimetallic Zn/Co ZIF with a Co-rich core and a Zn-rich shell, based on the dynamic binding competitions between these two metal ions, in which they bonded to 2-methylimidazole (2-MeIM) with distinguishable binding strength (thermodynamics) and binding rate (kinetics). Some mesopores or hollow caves were formed with the assistance of external ultrasonication to deassemble the Co-rich cores.[125]

On the basis of the above examples, hard templates offer a reliable way to introduce meso- and macropores with fixed sizes in conventional microporous MOFs. The close-packed nanostructured templates are especially useful in forming well distributed pores. Unfortunately, in spite of much efforts devoted toward preventing self-nucleation, the hard-template strategy still leads to tiny crystal precipitates in the synthesis mixture because of the weak interaction between MOF precursors and the template. Additionally, harsh processes (e.g., acidic or basic etchants) are often required to remove the templates, during which most MOF structures hardly keep intact.

Self-Sacrificial Template Methods. Self-sacrificial template methods are able to address the self-nucleation issue of the hard template methods, in which the metal ions resource generates by the in situ etching of templates with acidic linker/solvent, thereby directing the nucleation of MOFs on the selected template surface and simultaneously removing the template during the growth of MOF skeletons. Considering the coordination replication technique which allows the direct conversion of preformed three-dimensional macroporous metal oxide/hydroxide/oxyhydroxide monoliths into their corresponding MOF monoliths, using them as the sacrificial templates would release MOF precursors in a controlled manner, thereby allowing the crystallization process close to the template.[123−128] Reboul et al. proved the feasibility of morphological replacement of a shaped sacrificial metal oxide (Al_2O_3), behaving as both the metal source and "architecture-directing agent", by more stable porous coordination polymer (PCP) crystals (Figure 8a).[126] Followed by this, macroporous copper(II) hydroxide-based monoliths were utilized as the self-sacrificial template to produce a macro-meso-microporous monolithic HKUST-1. In the presence of BTC ligands, the coordination replication process enabled the complete preservation of the macroporous features of $Cu(OH)_2$ templates.[128] Recently, a vapor-phase conversion method was reported by Bo et al. for the construction of hierarchically porous MOF films with intrinsic microporosity from ZIF-8 and meso- and macroporosities from interparticle voids. ZnO fractal NP networks were chosen as precursors since the porous network readily underwent complete conversion to ZIF-8 upon exposure to the vapor of 2-methylimidazole.[129]

Not limited to traditional inorganic metal compounds, the same MOFs can be used as themselves' self-sacrificial templates according to an ingenious design. Specifically, Chou et al. generated uniform hollow and mesoporous ZIF-8 microcrystals with a single-crystalline structure via applying double solvent mediated overgrowth method (Figure 8b). First, they synthesized uniform cubic ZIF-8 microcrystals under aqueous conditions, serving as the cores to induce the subsequent overgrowth of ZIF-8 shell in the methanol solution. Attributing to the nanoconfinement effect, water molecules confined in the micropores of ZIF-8 cores delivered a slow exchange rate with methanol during the overgrowth process. The authors proposed that the deprotonation of 2-MeIM gave rise to a pH decrease in aqueous environment, which destabilizes the cubic ZIF-8 core. This local double solvent environment of internal solvent in the core and external

https://doi.org/10.1021/acs.chemrev.1c00243
Chem. Rev. 2021, 121, 12278−12326

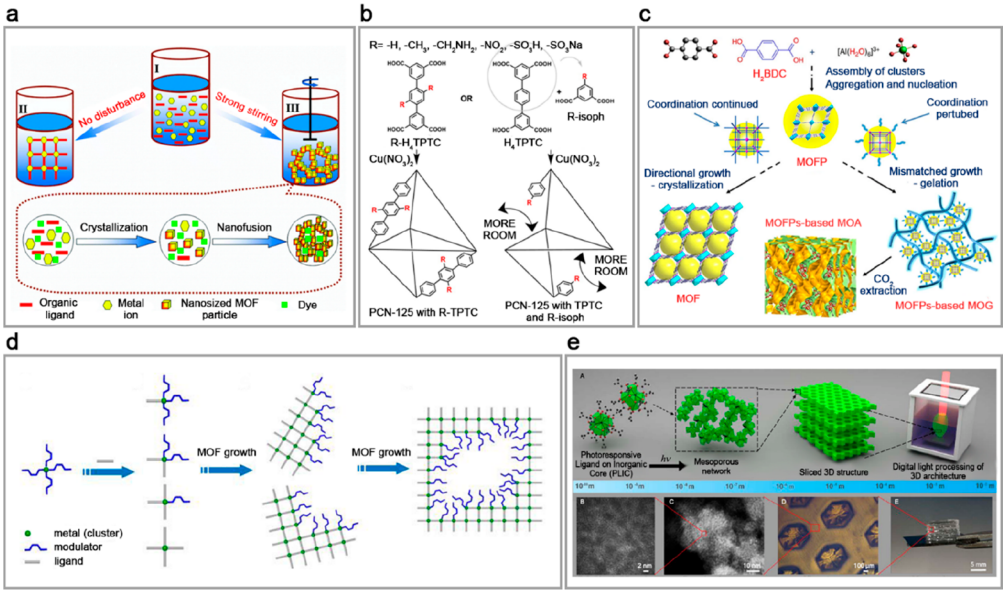

Figure 9. (a) Conceptual illustrations of perturbation-assisted nanofusion mechanism for the formation of HP-MOFs. Adapted with permission from ref 135. Copyright 2014 Royal Society of Chemistry. (b) Schematic illustration of the introduction of defective mesopores in MOFs by using the selected ligand fragments. Adapted with permission from ref 139. Copyright 2012 American Chemical Society. (c) Schematic representation of two-step gelation of MOF nanoparticles for the synthesis of hierarchically porous metal−organic aerogels. Adapted with permission from ref 140. Copyright 2013 Nature Springer. (d) Conceptual illustrations of modulator-induced defect-formation strategy for the formation of mesopores in MOFs. Adapted with permission from ref 141. Copyright 2017 John Wiley & Sons, Inc. (e) Schematic showing the 3D printing technology for the fabrication of HP-MOFs. Adapted with permission from ref 142. Copyright 2019 American Chemical Society.

overgrowth solvent promise the ZIF-8 core to serve as a self-sacrificial template.[127]

Template-Free Methods. Although the above template-directed strategy allows for the introduction of additional larger pores into some MOFs, the intrinsic need for special interaction between templates and MOFs to induce the heterogenous nucleation of the latter and/or the selective template removal steps pose great challenge for the fabrication of various HP-MOFs. Therefore, a facile approach without the assistance of templates would be of great interest to facilitate the practical applications of HP-MOF materials. For the template-free strategy, to create additional larger pores in the originally microporous MOFs, diverse strategies, such as a diluting precursor solution, vigorous stirring, change of precursors, or high-pressure gas extended solution, etc., have been frequently employed to regulate the diffusion process of precursors during the nucleation and growth of MOF crystals. Based on the above strategies, the balances between nucleation and growth process of MOF crystals are precisely controlled to prohibit the assembly of building units into a bulk crystal, thereafter leading to the formation of polycrystal agglomerated mesopores and even macropores.[130−138]

Bai and co-workers prepared a mesoporous nanocube of MOF-5 (MNMOF-5) by diluting the concentration of reactants by 400 times compared with the literature method.[130] In the same year, they also fabricated hierarchical supra-nanostructures of Cu-BDC and Cr-BDC (BDC = 1,4-benzenedicarboxylate) employing a diffusion method, in which mesopores were formed by the assembly of MOF NPs in a random fashion. Concretely, the hexane solution of triethylamine (TEA) was dropped to the N,N-dimethylmethanamide (DMF) solution of MOF precursors. TEA promoted the fast precipitation of MOF nanocrystals at the interface of hexane and DMF, which were agglomerated into hierarchically porous polycrystals.[131] After that, they synthesized a hierarchical supra-nanostructure of HKUST-1 by directly mixing solutions of copper acetate and H_3BTC (H_3BTC = 1,3,5-benzenetricarboxylic acid) under vigorous stirring under ambient conditions.[132] Applying a template-free strategy, Yue et al. also prepared a hierarchically microporous-mesoporous Zn-MOF-74 utilizing a unique stirring process. It was interesting that hierarchical Zn-MOF-74/t (t = reaction time in hours) materials could be obtained within 15 min of stirring at room temperature. According to the calculated pore-size distribution (PSD), the mesopore width was as large as 9 nm in Zn-MOF-74/0.25 and the maximum of pore size was nearly 15 nm in the case of Zn-MOF-74/240 together with 1.1 nm micropores. The possible mechanism for the formation of hierarchically porous Zn-MOF-74 relies on the rational control of the formation and aggregation of nanosized MOF crystals.[133] Subsequently, Yue et al. demonstrated the perturbation-assisted nanofusion strategy (Figure 9a), integrating the vigorous stirring and nanofusion technique, to prepare a series of MOF materials with hierarchical superstructures, including IRMOF-3, Cu-BDC, and Cu-BTEC.[135]

Using a gas to replace the solid templates for the construction of larger pores would be an alternative choice to avoid the additional template removal steps. Peng et al. demonstrated a template-free assembly of mesoporous $Cu_3(BTC)_2$ (HKUST-1) by using CO_2-expanded liquids as switchable solvents. They proposed that the as-synthesized MOF building blocks in the CO_2-expanded solvent were smaller than those formed in CO_2-free condition, due to the reduced solvency and viscosity of the solvent saturated with CO_2. A higher pressure is expected to favor the formation of smaller building blocks. Subsequently, the above nanosized crystals with high surface energy are prone to agglomerate into a network skeleton. Since the greater expansion of the solvent, the assembly of nanocrystal networks is looser at higher CO_2 pressure. Therefore, the mesopore diameters (13−23 nm) of

https://doi.org/10.1021/acs.chemrev.1c00243
Chem. Rev. 2021, 121, 12278−12326

mesocellular MOFs can be systematically adjusted by controlling the CO_2 pressure.[134]

Modulator-Induced Defect-Formation Strategy. To obtain high-quality MOF crystals, the modulators, that is, monodentate ligands with similar coordinate functionality as the organic ligands, are commonly applied during the synthesis process to adjust the kinetics of nucleation and crystal growth, thereby modulating defects, crystal size, and morphology. Inspired by the competitive coordination functions of modulators, Choi et al. introduced heterogeneously arranged pores into a microporous MOF crystal without losing their crystalline nature. After partially replacing BDC with the modulator 4-(dodecyloxy)benzoic acid (DBA) during the synthesis process, MOF-5 with a sponge (spng-MOF-5) and pomegranate-like hierarchical pores (pmg-MOF-5) can be obtained.[143] Later, He et al. synthesized HP-MOF-5 with 2D nanosheet and nanocube morphologies by taking advantage of a synergistic effect of lauric acid and PVP, the former as the modulator to introduce larger pores and the latter directing the morphology.[144]

Zhou and coauthors developed a metal−ligand−fragment coassembly strategy to create functionalized mesopores in microporous MOFs (Figure 9b). The degree of mesoporosity and the amount of additional functionalized groups could be tuned by judiciously adjusting the feed ratio of primitive and fragment ligands.[139] To further understand the electronic and steric properties at the coordinatively unsaturated metal sites (CUS) formed by the defective ligands, Fang et al. reported a defect-engineering strategy by systematically doping defective linkers into HKUST-1, which realized the simultaneous and controllable modification of CUS and introduction of functionalized mesopores.[145] Later, this mixed-ligand approach was further extended to construct HP-HKUST-1 by using a more simple defective linker (benzoic acid).[146]

It should be noted that the monodentate linkers (conventional modulators) and fragment ligands are all classified into the field of modulators, considering both them belong to defective ligands and share some similar purposes/results for the construction of defective mesopores in MOF skeletons. However, the monodentate modulator generally does not take part in the construction of final MOF skeletons. On the contrary, the fragment ligand-typed modulators derived from primitive linkers will be the structural component of MOFs, although they possess less coordinated groups but still inherit partial structure from its primary linkers and even retain the bridging functions.

Generally, the linkers with higher pK_a than their modulators result in the elimination of modulator in the final materials, especially for stable MOFs where the binding between metal nodes and linker is robust. In order to guarantee the competitive coordination process, the linkers with weak coordination interaction with metal ion/clusters were preferable. This actually limits this strategy to some unstable MOFs like MOF-5, which suffers from framework collapse toward water/moisture.[143,144,147] To realize both the pore size enlargement and structural stability in a single MOF material, Jiang and Cai developed a versatile modulator-induced defect-formation strategy (Figure 9d). They proposed the discrete modulator-capped metal-oxo clusters were preformed by using an excess of modulators. Different from the conventional synthetic protocol, the insufficient amounts of linkers were added to ensure an incomplete exchange between modulators and linkers during the 3D assembly of MOF building units. The presence of residual modulators induces defective mesopores with missing linkers, because the elongated alkyl chain in the modulator occupies a large space and also causes steric hindrance that hampers the coordination between metal nodes and organic linkers around the long modulator. Therefore, the sizes of defective mesopores can be controlled by changing the amount and chain lengths of selected modulator. In this report, various HP-MOFs (e.g., HP-UiO-67, HP-MIL-53, HP-MOF-808, HP-DUT-5, HP-UiO-66) with both tailored pore features and high stability can be facilely fabricated.[141] Similarly, Liang and Gu et al. reported a monocarboxylic acid (MA) and organic base comodulation strategy to synthesize the HP-UiO-66 with both adjustable particle size and mesopores.[148] Not limited to monocarboxylic acid, urea modulator was also used as the competitive reagent to produce a hierarchically porous defective MIL-53.[148,149]

Sol−Gel Strategy. The gelation of NPs in the aerosol phase has been used for the fabrication of highly porous monoliths with large empty spaces. If the growth of MOF NPs can be suppressed by a gelation process during the synthesis, it can be expected to achieve the construction of metal−organic gels (MOGs) based on the agglomeration of MOF NPs.[140,150−156] Kaskel and co-workers reported an amorphous MOF aerogel with high micro- and macroporosity. In their synthesis, a MOF gel was formed by mixing the ethanolic solutions of trimesic acid and $Fe(NO_3)_3$ under vigorous stirring. After washing the gel with ethanol, supercritical CO_2 was adopted to exchange the extra solvent to produce the final MOF aerogels. The obtained aerogel exhibited total pore volume as high as 5.6 cm^3/g according to N_2 sorption results.[150] Subsequently, Li et al. developed a two-step gelation route for the synthesis of micro/mesoporous metal−organic aerogels (Figure 9c). In the early stage, the mixture of MOF precursors formed clusters and assembled into tiny MOF NPs. To avoid them growing into bulk crystals in the conventional fashion, a mild heating method was used to perturb the consistent epitaxial growth while increasing the chance of mismatched growth for a gelation. As a result, hierarchically porous MOG monoliths formed by the cross-linking of MOF NPs.[140] To disrupt the crystal growth and enhance gelation over crystallization, Zou and co-workers synthesized MOF-based porous MOGs by utilizing a Fe/Al mixed metal source at properly elevated temperatures. Due to the weaker reactivity of Al^{3+} than Fe^{3+} with BTC ligands, the room temperature coordination process led to noncrystallographic supramolecular Fe-BTC structures. The gelation was completed upon raising temperature to allow for the coordination between Al^{3+} and BTC.[154] In addition, Zhang and co-workers reported a powder-packing synthesis approach to induce a gelation by dropping limited solvent into the solid mixtures of MOF precursors. The resultant HKUST-1 monoliths exhibit intrinsic MOF micropores and interconnected macropores.[152]

3D Printing Method. With the development of 3D printing technology, it can be expected to create sophisticated hierarchical geometries with programmable macroscopic shape and nanoscale details.[142,157,158] Hanrath and co-workers demonstrated a convenient, efficient and fast route to produce HP-MOF geometries in a 3D printer (Figure 9e). Specifically, Zr-oxo clusters were capped with 12 photoresponsive methacrylic acid (MAA) ligands, used as the essential component of 3D printing inks. Ultraviolet exposure induced C═C bond free radical polymerization cross-linked the capped clusters into a mesoporous monolithic superstructure.

https://doi.org/10.1021/acs.chemrev.1c00243
Chem. Rev. 2021, 121, 12278−12326

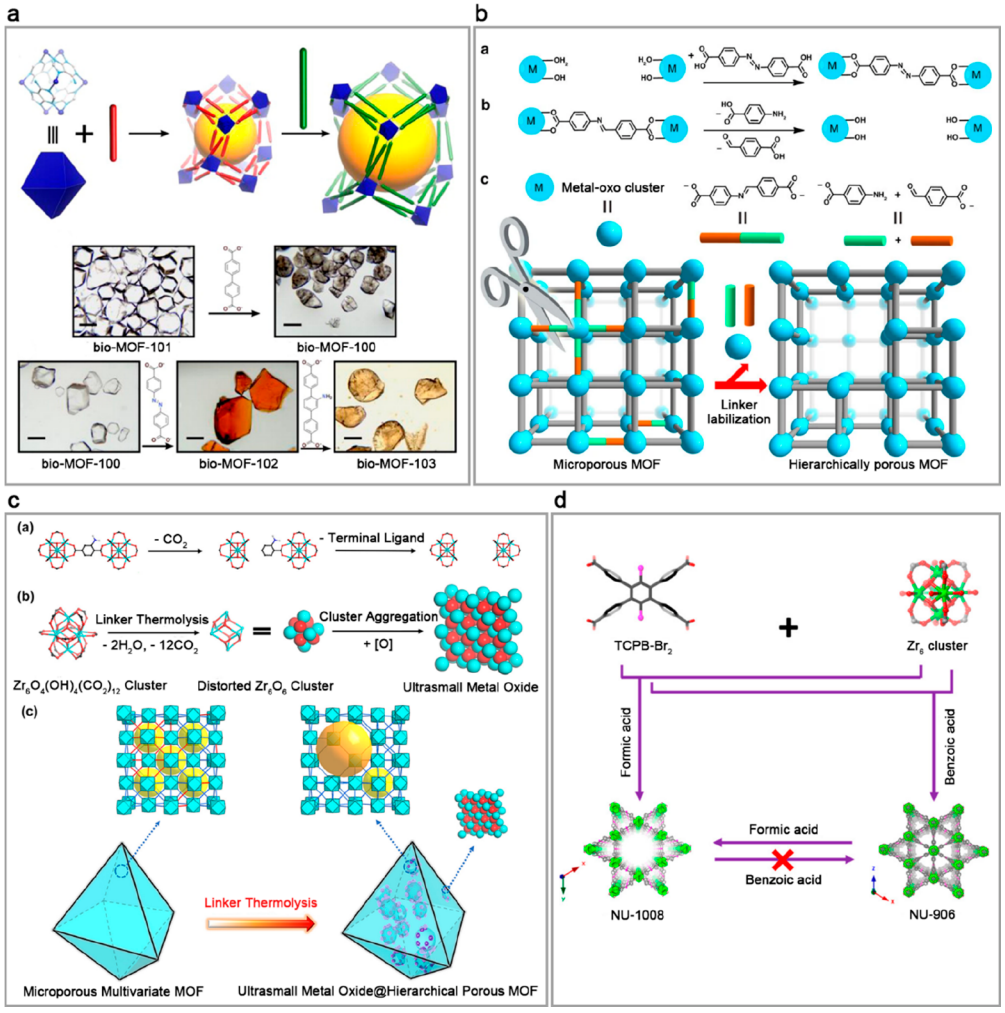

Figure 10. (a) Schematic showing the stepwise ligand exchange method for the expansion of pore sizes of preformed MOFs. Adapted with permission from ref 159. Copyright 2013 American Chemical Society. (b) Schematic illustration of the introduction of mesopores in MOFs by the selective removal of chemically labile linkers. Adapted with permission from ref 161. Copyright 2017 Nature Springer. (c) Scheme showing the formation of mesopores in MOFs based on selective removal of thermally labile linkers. Adapted with permission from ref 162. Copyright 2018 American Chemical Society. (d) Scheme to show the formation and phase transformation of NU-906 and NU-1008. Adapted with permission from ref 163. Copyright 2020 American Chemical Society.

With the control of experiment conditions, the present 3D printing technique integrated the merits of programmable macroscale structures and nanoscale porosity. Interestingly, a 3D hierarchical mesoporous leaf was printed in order to further prove the feasibility of this method, which enabled traditional powder-like porous solids to be constructed into complex geometries with multilevel porous networks that are unattainable by conventional fabrication approaches.[142]

2.1.2.2. Postsynthetic Strategies. Postsynthetic tailoring is emerging as a powerful strategy for imparting desired chemical functionalities/properties into MOFs that otherwise could not be achieved during the de novo synthesis. Currently, the related techniques have also been successfully adopted for the introduction of mesoporosity in MOF structures, including stepwise ligand exchange, chemical etching, thermal decomposition, phase transformation, etc.

Stepwise Ligand Exchange Strategy. Though MOFs with short linkers can be readily prepared, their analogues with longer linkers are usually hard to be obtained, as this is sometimes a thermodynamically unfavorable process or readily causes structural interpenetration. To break the bottleneck, Rosi and co-workers demonstrated that pore dimensions of MOF materials can be systematically extended via the stepwise ligand exchange of a noninterpenetrated MOF (Figure 10a). Starting from bio-MOF-101, three isoreticular analogues with increasingly larger pores, namely, bio-MOF-100, bio-MOF-102, and bio-MOF-103, were respectively prepared by the replacement of shorter NDC (2,6-naphthalenedicarboxylate) ligands with longer BPDC (4,4′-biphenyldicarboxylate), ABDC (azobenzene-4,4′-dicarboxylate), and NH_2-TPDC (2′-amino-1,1′:4,1′-terphenyl-4,4″-dicarboxylate) linkers in sequence.[159] Later, the same group reported a series of mesoporous MOF materials, bMOF-100 with mono-, di-, and trifunctionalization realized by sequential postsynthetic ligand exchange reactions.[160] This ligand exchange method is a powerful approach especially for exploring new meso-MOFs that cannot be directly prepared using traditional synthetic methods.

Metal Ion Metathesis Strategy. In some special cases, the metal ion exchange method can be an alternative strategy to prepare HP-MOFs that are hard to be directly fabricated. Similar to the above postsynthetic ligand exchange strategies,

https://doi.org/10.1021/acs.chemrev.1c00243
Chem. Rev. 2021, 121, 12278−12326

the metal ion metathesis can also be conducted in a series of isoreticular MOFs analogues without sacrificing crystallinity or changing their crystal structures. For example, the Zhou group successfully fabricated a Cr-based PCN-333 through presynthesis of the Fe-based PCN-333 and subsequent metal metathesis using Cr^{3+} to exchange the Fe^{3+}.[164] Possibly easier than a complete metal ion exchange process, the same group reported a partial exchange of metal ions in isoreticular MOFs to prepare some new Ti-based bimetallic MOFs which are highly desired for photocatalysis.[165]

Chemical Etching Strategy. Different from other porous materials, such as zeolites, carbons, porous silica and so on, MOFs are composed of organic ligands and metal ions (clusters) connected by relatively weak coordination bonds. Therefore, the processability of MOFs is limited by the stability of their own structures. For some unstable MOFs, water molecules are easy to attack the coordination bond, causing the collapse of MOF structures. Improving the stability of MOFs in humid environment has become a research hotspot.[166−168] On the other hand, the instability of MOF structure poses a chance to create hierarchical pores if the organic ligands or clusters could be partially removed in a controlled manner, while the overall crystal structure is maintained.[161,169−186] Inspired by this, the Kim group introduced mesopores into a microporous POST-66(Y) MOF by using water as the etchant. The mesoporosity was verified by a change of N_2 sorption isotherm from type I to type IV as a result of water treatment.[174] After that, the chemical etching strategy was widely used and various etchants were also investigated extensively, for example, cyanuric chloride, NaCl solution, hydroquinone, guanidinium surfactants, hydrogen peroxide, O_2 plasma, ozone, methanol, etc.[161,169−186] It should be highlighted that acid treatment has become one of the most popular postsynthetic methods for introducing larger pores especially in the field of Zr-MOFs. Commonly used acids include hydrochloric acid, phosphoric acid, citric acid, fatty acid, and so on.[169−171,175,178,180,184] Recently, the Zhou group developed hierarchically porous PCN-160 through linker labilization. First, stable Zr-MOFs were selected as a platform for the implementation of the linker labilization strategy (Figure 10b), integrating the stepwise ligand exchange strategy and chemical etching strategy in an exquisite design. Subsequently, AZDC (azobenzene-4,4′-dicarboxylate) ligands was partially substituted by CBAB (4-carboxybenzylidene-4-aminobenzate) to give rise to mixed linker MOFs. The key to success is based on the very similar lengths and connectivity/coordination mode between AZDC and CBAB. Finally, acid-labile CBAB linkers were removed by acetic acid etching to produce hierarchically porous PCN-160. N_2 sorption measurements revealed the formation of the hierarchically structured MOF materials with both micropores and mesopores. The optimized mesopore diameter of the missing linker PCN-160 can reach up to 13.6 nm.[161]

Thermal Decomposition Strategy. In addition to the difference in chemical stability, the gradient of thermal stability in a MOF crystal could be utilized to realize the selective removal of partial MOF domain.[187,188] To create local domain with different decomposition temperatures, a multivariate MOF with ordinary linker and thermally labile linker (amino functionalized linker) was judiciously prepared by the Zhou group (Figure 10c). Under a properly elevated temperature, the mix-linker MOF will decompose via a decarboxylation process. HP-MOFs with adjustable mesopores were created by tuning the content of thermal-sensitive linkers without losing the stability and crystallinity of the pristine MOF.[162] Later, Chen et al. transformed a microporous MIL-121 to HP-MOF via thermally triggered decarboxylation of carboxylate linker.[189] To promote the decarboxylation in various stable MOFs, silver catalyst was employed by Jeong et al. to create hierarchical pores in MOF patterns and membranes.[190] In addition, inspired by the thermal instability of inherent defects, various metal NPs@MOFs were transferred into metal NPs@HP-MOFs. The additional mesopores are prone to form around the metal NPs because of the heterogeneous nucleation inducing defects (thermally labile domains) around the extraneous metal NPs during MOF growth.[191]

Phase Transformation Strategy. Because of the structural complexity, various topologies and porous structures can be obtained from the same precursors, generally leading to the difficulty to fabricate pure phase MOFs.[192] On the contrary, taking advantage of the evolution of their structures, Wee et al. reported a thermo-induced 1D-2D-3D transformation strategy to prepare a new MOF COK-18 with 3D interconnected hierarchical pores. The formation mechanism is proposed as a transformation of ribbon-like 1D building units into 2D layers and finally into a 3D network. Compared with conventional HKUST-1, the new phase includes excess copper capped by systematic hydroxyl groups to compensate the charge, which renders open microporous frameworks with defective mesopores.[193] Later, inspired by the modulator-directed topological diversity, Lyu et al. demonstrated a phase transition from a microporous NU-906 with scu topology to a mesoporous NU-1008 with csq topology through a dissolution-reprecipitation mechanism (Figure 10d). In the presence of formic acid, scu-NU-906 (kinetic product) was completely dissolved to yield a clear solution followed by the formation of the new phase of NU-1008 (thermodynamic product).[163]

2.1.3. Hollow HP-MOFs. As an important branch of MOFs, hollow MOFs have attracted wide research interests in recent years, attributed to the combination of both merits of MOFs and hollow nanostructures. To distinguish from classical HP-MOFs, hollow HP-MOFs contain one center mesopore or macropore only within one MOF particle. It is noteworthy that there have been several excellent reviews summarizing state-of-the-art development of hollow MOF micro/nanostructures.[194−200] For example, Liu et al. focused on the synthetic strategies and applications of hollow MOFs and their derivatives.[194] In this Review, we summarized them in the viewpoint of the design and synthesis of hollow HP-MOFs, in which their hierarchical pores were mainly fabricated by introducing additional hollow spaces into conventional microporous MOFs. Depending on the morphology characters of introduced hollow spaces, hollow HP-MOFs were further divided into two parts: 3D hollow HP-MOFs nanospheres/nanocubes and 1D hollow HP-MOFs nanotubes.

2.1.3.1. 3D Hollow HP-MOFs. To create a large cavity in microporous MOFs, various methods have been developed, which can be mainly divided into template-involved methods, biphasic interface strategies, and postsynthetic etching methods.

Template-Involved Methods. In a template-involved route, it is critical to avoid the self-nucleation of MOFs in solution, while promoting the heterogeneous nucleation and directed shell growth of MOFs on the selected template surface. For instance, the Oh group demonstrated a stepwise solvothermal

https://doi.org/10.1021/acs.chemrev.1c00243
Chem. Rev. 2021, 121, 12278−12326

reaction for the construction of hollow HP-MOF spheres (Figure 11a). They preprepared a thin ZIF-8 (also named as

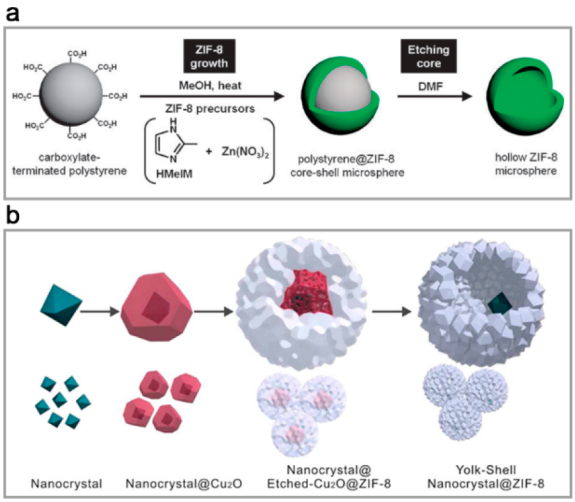

Figure 11. (a) Schematic illustration for the fabrication of hollow HP-MOFs with PS spheres as hard templates. Reproduced with permission from ref 201. Copyright 2012 Royal Society of Chemistry. (b) Schematic illustration for the fabrication of hollow HP-MOFs based on Cu_2O as self-sacrificial templates. Reproduced with permission from ref 204. Copyright 2012 American Chemical Society.

MAF-4) shell on PS spheres, followed by a second growth process to improve the thickness of the MOF shell. After dissolving the template in DMF solution, hollow ZIF-8 nanospheres were obtained.[201] Similarly, Zhang et al. utilized a carboxylate-terminated PS sphere as a core to achieve a hollow ZIF-8 NP.[202] Different from the growth of MOFs in a mixed precursor solution, Wan et al. developed a layer-by-layer technique to induce directed growth of MOF layer on PS spheres, in which two separated solution of metal salts and ligands were used to immerse the template in sequence.[203]

If the cavities of hollow HP-MOF particles were partially filled with another material (e.g., metal/metal oxide nanoparticles), a yolk−shell structure could be generated. In pursuit of the fabrication method of yolk−shell composite materials, some template-involved methods are developed, which exhibit referential value for the synthesis of hollow structures. Tsung and co-workers coated noble-metal NPs with Cu_2O as a hard template. The simultaneous nucleation of ZIF-8 on the template released protons, which corroded Cu_2O to form a hollow space containing a metal NP (Figure 11b).[204] Later, the Huo group synthesized metal NPs@HKUST-1 yolk−shell structure in a similar manner. In their attempt, the Cu_2O coating layer acted as a self-sacrificial template, which not only accounted for the generation of hollow spaces, but also provided Cu^{2+} ions for the nucleation of HKUST-1.[205]

In addition, metal−organic polyhedral (MOPs) were also used as the sacrificial templates for the construction of hollow HP-MOFs.[207] For instance, Choe and co-workers demonstrated a single-crystal to single-crystal transformation from a solid MOP to hollow MOF with controlled layers of shells (Figure 12). First, solid UMOM-1 (MOP) was immersed into the solution of 1,4-diazabicyclo[2.2.2]octane (DABCO, as a linker) to produce a core−shell structure. The coordination between MOPs and linkers started at the external surface of the MOP crystals, so the center of the MOP remained unchanged if the reaction was halted halfway. Owing to their

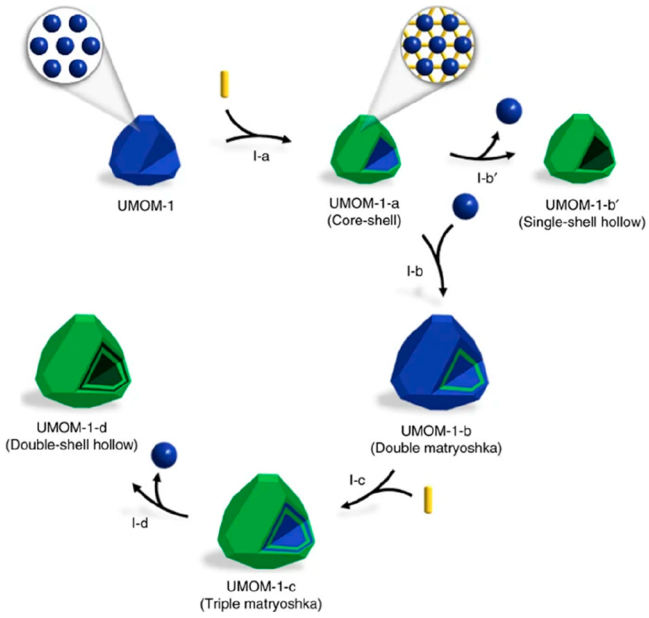

Figure 12. Schematic showing the synthetic process of single-crystal hollow MOFs with multishell via an etching-epitaxial growth strategy. Reproduced with permission from ref 206. Copyright 2017 Nature Springer.

different solubility in methanol, the core was selectively dissolved to form a single-crystal hollow MOF with single-shell. After the epitaxial growth of MOP and then repeating the postsynthetic linker insertion and dissolution processes, a single-crystal hollow MOF with multishell can be achieved.[206]

It is worthy to mention that the Zeng group reported a self-template method to produce hollow ZIF-67. They proposed that $[Co\text{-complex}]^-$ intermediates were preformed and concentrated on positively charged surfactant (CTAB) assembled vesicles, which acted as the nucleation sites during the following heterogeneous growth of ZIF-67 shells.[208] More interestingly, different from conventional capsules with enclosed shell structures, the Wang group reported a bowl-liked MOF microcapsule with open-mouthed shell structures, based on a competitive coordination method via the introduction of polyoxometalates (POMs) into MOF precursor solution. The presence of POM anions would partially break the infinite structures and finally promote the formation of hollow cavity during the growth of MOFs, due to the competitive coordination of POMs and organic linkers with metal nodes.[209]

Not limited to exogenous species (e.g., metal oxides, MOPs) as the templates, MOF itself (generally bimetallic or core−shell MOFs) can also work for this purpose.[210] For instance, the Wang group prepared a hollow HP-MOF nanocube via the structural transformation from Zn/Ni-MOF-5 nanocube to Zn/Ni-MOF-2 nanosheet. They proposed that structurally unstable MOF-5 nanocubes were preformed owing to favorable reaction kinetics at initial state with high concentration of precursors, followed by a structural transformation into thermodynamically favored Zn/Ni-MOF-2 crystal phase. During the conversion, the kinetic intermediates function as an additional supporting template and the evolution process is analogous to the dissolution and recrystallization of inorganic nanocrystals.[211] Later, Yang et al. reported a hollow Zn/Co ZIF based on the phase transformation of a core−shell ZIF-67@ZIF-8. They found that methanol affected the coordina-

https://doi.org/10.1021/acs.chemrev.1c00243
Chem. Rev. 2021, 121, 12278−12326

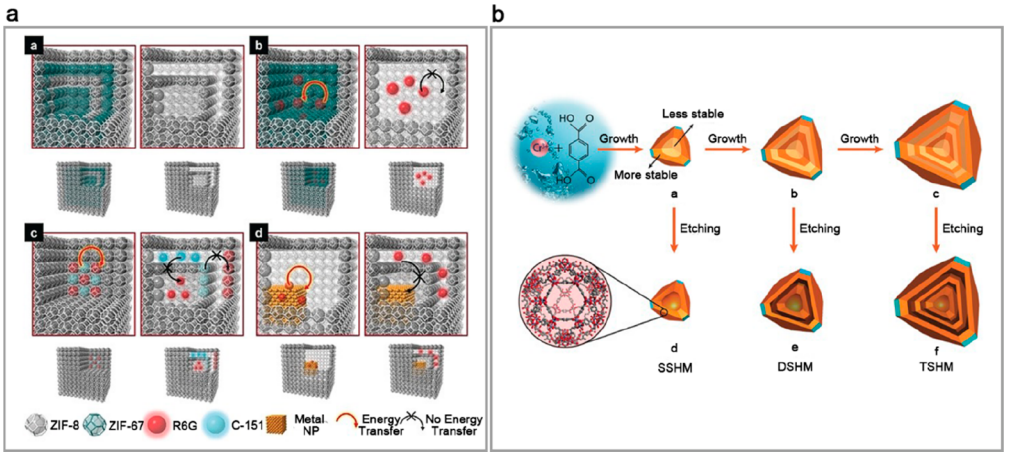

Figure 13. (a) Schematic illustration for the fabrication of hollow HP-MOFs by using labile MOFs as hard templates. Adapted with permission from ref 213. Copyright 2018 John Wiley & Sons, Inc. (b) Schematic showing the fabrication of hollow MIL-101 with multishells based on step-by-step crystal growth and subsequent etching processes. Adapted with permission from ref 214. Copyright 2017 John Wiley & Sons, Inc.

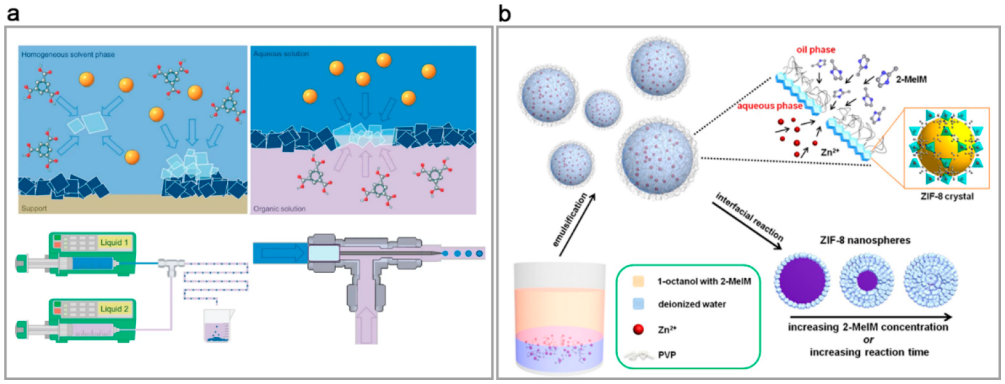

Figure 14. (a) Schematic showing the biphasic interface strategy to realize the large-scale preparation of hollow HP-MOFs. Reproduced with permission from ref 215. Copyright 2011 Nature Springer. (b) Schematic showing the emulsion-based interfacial synthesis method for the large-scale preparation of hollow ZIF-8. Reproduced with permission from ref 216. Copyright 2014 American Chemical Society.

tion mode of cobalt ions in ZIF-67 and thus caused a mild phase transformation of the core under solvothermal conditions.[212] Similarly, Liu et al. prepared a multishelled hollow ZIF-8 after selectively dissociating ZIF-67 from the multilayered ZIF-67@ZIF-8 microcrystals (Figure 13a). The number of shells in hollow ZIF-8 can be tuned by controlling the epitaxial layer-by-layer overgrowth of ZIF-8 and ZIF-67, thanks to their same sodalite (SOD) topology.[213]

It was worth mentioning that Liu et al. showed a rational strategy to fabricate multishelled hollow MIL-101(Cr) with single crystalline shells through step-by-step crystal growth following by subsequent etching processes (Figure 13b). This strategy relies on a surface-energy-driven mechanism to induce uneven local stability in a crystal during the stepwise growth of MIL-101 layers. In each newly grown MOF shell, its interior layer can be selectively removed by acetic acid due to the weaker chemically stability than the exterior layer. Furthermore, the cavity size and shell thickness in each layer can be precisely controlled by tuning the etching time and other reaction conditions.[214]

Biphasic Interface Strategies. Although template-involved strategies are straightforward for the construction of hollow structures in conventional microporous MOFs, additional template removal and special requirements (e.g., different dissolution or chemical stability properties) for the core−shell structures pose challenges for their practical execution. In contrast, biphasic interface strategies offer a facile and alternative way to realize the large-scale preparation of hollow HP-MOFs (Figure 14a). Spherical gas bubbles or liquid droplets are typically selected as temporal soft templates for the formation of hollow spaces, which are easily removed during the subsequent solvent washing process without any etchant, and the MOFs were directed grown between the interface of two immiscible gas−liquid or liquid−liquid.[215−222]

Generally, MOF crystals are formed via a homogeneous nucleation of precursor mixture. Despite additional functional groups were grafted to induce a heterogeneous nucleation on selected substrates, it is hard to grow perfect MOF layers due to unavoidable self-nucleation in homogeneous mixture. Considering the formation of MOF crystals relies on the reaction of metal ions and ligands which present markedly different solubility characteristics, it is straightforward to separate them into immiscible solvents, thereby confining their contact, mixing, and reaction only at the biphasic interfaces. Inspired by this, De Vos and co-workers reported a continuous-flow preparation of hollow MOF capsules. First, metal-ion-containing aqueous solution and ligand-containing organic solution were separately filled into two syringe needles. A biphasic synthesis mixture was then generated by breaking off in a coflowing stream where aqueous droplets were

https://doi.org/10.1021/acs.chemrev.1c00243
Chem. Rev. 2021, 121, 12278−12326

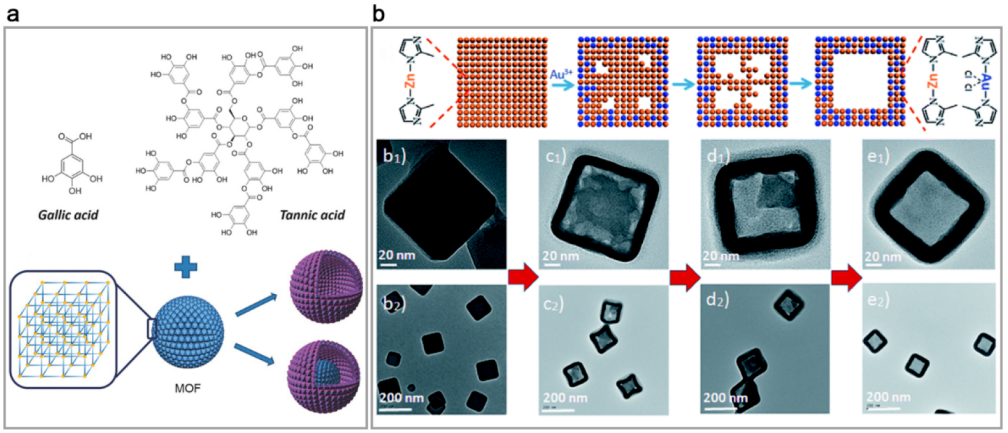

Figure 15. (a) Schematic showing the etching of microporous MOFs into hollow MOFs by using phenolic acids as the etching reagent. Reproduced with permission from ref 225. Copyright 2016 John Wiley & Sons, Inc. (b) Schematic showing the cation exchange strategy to create hollow voids in ZIF-8. Reproduced with permission from ref 226. Copyright 2018 The Royal Society of Chemistry.

dispersed in the flowing and continuous organic phase (Figure 14a).[215] In addition, the Jiang and Xu groups developed an emulsion-based interfacial synthesis method for the large-scale synthesis of hollow ZIF-8 nanospheres (Figure 14b). A water-in-oil nanoemulsion was prepared by using PVP as a stabilizer and 1-octanol as the oil phase. The Zn^{2+} in aqueous phase was directed coordinated with 2-MeIM in the oil phase on the interfaces of emulsion droplets. The resulting shell thickness could be facilely controlled by tuning the concentration of precursors or reaction time.[216] Later, Jeong et al. developed a droplet microfluidic system for the fast and continuous-flow preparation of hollow MOF nanospheres. For the fast crystallization of MIL-88A on the emulsion interfaces, tributylamine (TBA) was added to promote the deprotonation of ligands and thus enhanced the kinetics of the MOF growth. Poly(vinyl alcohol) (PVA) was also used to stabilize the emulsion droplets during the MOF synthesis.[217]

In addition to in situ interfacial growth, bottom-up interfacial assembly of preformed MOF particles into hollow superstructures was also developed to prepare hollow HP-MOFs. For instance, the Huo and Bradshaw groups prepared an oil-in-water (o/w) Pickering emulsion by exerting high shear forces to biphasic mixtures of dodecane and aqueous solution. In their attempt, preformed ZIF-8 NPs were dispersed in the aqueous phase, while the organic phase contained polymer monomers and free radical initiators. The cross-linkage of monomers started upon heating the emulsion to 65 °C, creating an insoluble polymer network at the biphasic interface. The ZIF-8 NPs were embedded in the polymer matrix to form a hollow MOF capsule.[218] Subsequently, the same groups reported a hollow HP-MOF by using a Pickering-stabilized hydrogel strategy. The hydrogel droplets dispersed among the emulsion were primarily covered with preprepared UiO-66 particles, followed by a two-step growth procedure to construct a robust ZIF-8 shell.[219] Different from the above two-step approaches, Pang et al. demonstrated a single-step emulsion-based approach to form hollow MOF superstructures. The formation of monodisperse MOF (FesocMOF) NPs and subsequent assembly took place consecutively in the one-pot synthesis.[220]

Postsynthetic Etching Methods. Similar to the postsynthetic techniques for the introduction of mesoporosity in MOF structures, they are also powerful for the conversion of preformed microporous MOFs into hollow HP-MOFs. Because of the high stability demand toward MOFs, the development of these technologies is still in the initial stage. Currently, two strategies, including surface-protected acid etching and metal ion exchange, are mainly involved.[223−227]

The Yamauchi group developed a general strategy to controlled etching of the interior of Prussian blue (PB) and their analogues into hollow forms with the assistance of PVP. Because of the poor stability of PB in acidic solution, PB will dissolve upon soaking in a HCl solution. With the protection of a proper amount of PVP on the surface, the etching rate on the surface is relatively slow. The H^+ ion diffuses through the particle surface and concentrate in the central parts of PB. The local high-concertation of H^+ causes a selective etching and thus renders a hollow PB.[223] This acid-etching method can be readily extended to other common MOF systems, as exemplified by the work of Cai et al. Using HCl as the etchant and PVP as the protective reagent, they successfully created hollow cavities in Ga-soc-MOF.[224] Recently, Hu et al. reported a general strategy to create hollow space inside MOFs, while simultaneously realizing the surface modification (Figure 15a). The weak phenolic acids were used as the etching reagent, which released free H^+ ion to destroy the structures of MOFs. However, the corresponding anions failed to penetrate into MOFs due to relatively large molecular sizes compared with the pores of microporous MOFs. On the other hand, phenolic acids were able to coordinate with dissolved metal ions to form metal−phenolic networks (MPNs) on the MOF surface. The MPNs functioned as a protective coating during the etching process and also functionalized the surface of the resulting hollow MOFs.[225]

Not limited to the acid etching methods, the Wu and Jiang groups reported a cation exchange strategy to create hollow voids in ZIF-8 particles based on a nonequilibrium interdiffusion during cation exchange reactions (Figure 15b). After the addition of $NaAuCl_4$, the Au^{3+} would partly replace Zn^{2+} in the frameworks of ZIF-8. Kirkendall voids were generated and finally formed a hollow void, because the out-diffusion rate of Zn^{2+} was faster than the in-diffusion rate of Au^{3+}. Accordingly, various hollow structures with different shell thickness, shape and size can be rationally controlled by changing the concentration of Au^{3+} ions and ZIF-8 particles.[226]

2.1.3.2. 1D Hollow HP-MOFs. Currently, several methods including template-involved and template-free methods have been developed for the fabrication of 1D hollow HP-MOFs, in

https://doi.org/10.1021/acs.chemrev.1c00243
Chem. Rev. 2021, 121, 12278−12326

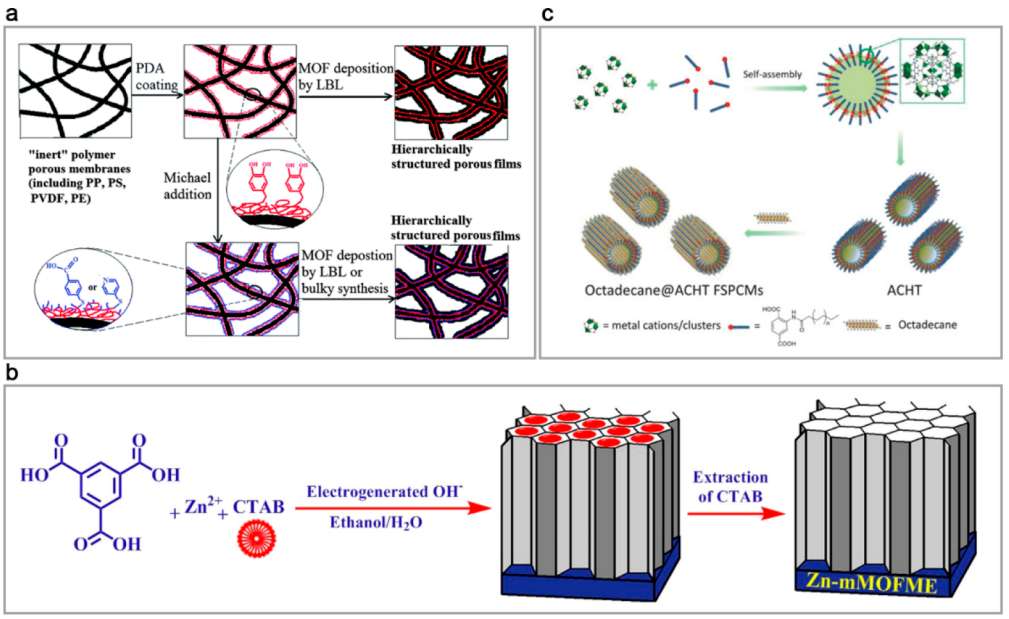

Figure 16. (a) Schematic showing the polydopamine (PDA) coating strategy for the growth of MOFs on "inert" polymer nanowire-based hierarchically porous networks. Reproduced with permission from ref 228. Copyright 2015 The Royal Society of Chemistry. (b) Schematic showing the fabrication of mesoporous MOF thin films (mMOFTF) by the electrochemically assisted self-assembly (EASA) technique. Reproduced with permission from ref 230. Copyright 2017 American Chemistry Society. (c) Schematic showing the formation of hollow MOF tubes by using alkylated bridged ligands. Reproduced with permission from ref 232. Copyright 2018 John Wiley & Sons, Inc.

which nanotube-like 1D voids are enclosed by porous MOF shells.[228−232]

For the template-involved methods, wire or tube-like nanomaterials are preferred templates for creating 1D hollow spaces. To realize the heterogeneous nucleation of MOFs on "inert" polymer nanowire-based materials, Zhou et al. developed a general and facile polydopamine (PDA) coating strategy (Figure 16a), attributing to the self-polymerization and tightly adhesive ability of PDA. To prove its general applicability, various polymeric substrates (e.g., polyprolene (PP), polystyrene (PS), polyethylene (PE), and poly-(vinylidene fluoride) (PVDF)) were used for the growth of various microporous MOFs (e.g., HKUST-1, MOF-5, ZIF-8, and MIL-100). After the dissolution of polymers by THF, corresponding hollow MOF tubes were achieved.[228] In addition, a self-sacrificial template method was developed by the Lou group for the formation of 1D HP-ZIF-67 prism with a hollow structure. The 1D nanoprisms were preformed by the assembly of cobalt acetate hydroxide. After soaking it into the ethanol solution of 2-MeIM, a fast ion-exchange occurred. Because of the faster out-diffusion rate of Co^{2+} ions, ZIF-67 was prone to grow on the surface parts in an interconnected way and thus form 1D hollow voids.[229]

It is worth mentioning that the Nematollahi group demonstrated an electrochemically assisted self-assembly (EASA) technique for the fabrication of mesoporous MOF thin films (mMOFTF) with hollow 3D hexagonally packed crystals. In the EASA, OH^- ions were in situ generated at the cathode surface (Figure 16b). The local high alkalinity at the electrode double layer boosted the deprotonation of ligands, which were concentrated around CTAB micelles because of the electrostatic attraction. The spatially uneven distribution of anionic ligands led to the formation of mesoporous MOFs with 1D hexagonal passes. EASA strategy released OH^- in a relatively mild way, thus preventing the uncontrolled precipitation of MOF microcrystals. The hollow mMOFTF was simultaneously grown and deposited onto the selected conductive substrates/electrodes via this method.[230]

In the template-free synthesis, some competitive or structure-directing reagents were used to modulate the growth behaviors of conventional MOFs. For instance, the Wang group reported the synthesis of hierarchical MOF nanotubes by using polyoxometalates (POMs) as structural modulators. They proposed the addition of POMs altered the equilibrium between the metal cations and the organic ligands and thus regulated the growth behaviors of the MOF crystals. In the early state, $Fe(acac)_3$ released $acac^-$ because of the competition coordination of POMs. The alkaline $acac^-$ rapidly deprotonated water to give OH^-. Thereafter, organic linkers were deprotonated and coordinated with metal ions to form the kinetic intermediates of POM-coated coordination polymer, followed by the growth of MOF shell with less amounts of POM. The core was thermodynamically unstable and subsequently dissolved to form a hollow void in the final hierarchical MOF nanotubes.[231] In addition, Wang and co-workers constructed alkylated MIL-101 hollow tubes with both mesopores and macropores, using a series of alkylated ligands instead of BDC to coordinate with Cr^{3+} (Figure 16c). During their synthesis, the alkylated linker working as the structure-directing reagent formed cylindrical assemblies, which induced the formation of hollow MOF tubes.[232]

2.2. MOF-Based Hierarchically Porous Composites (HP-Composites)

The integration of microporous MOFs with conventional porous materials, especially mesopore and macropore-containing materials, have been proven a promising approach for the construction of hierarchically porous structures. Such MOF-based hierarchically porous composites combine structural strengths of different materials into a single composite, expanding the practical applications of MOF-based hierarchically porous materials.[233−240]

https://doi.org/10.1021/acs.chemrev.1c00243
Chem. Rev. 2021, 121, 12278−12326

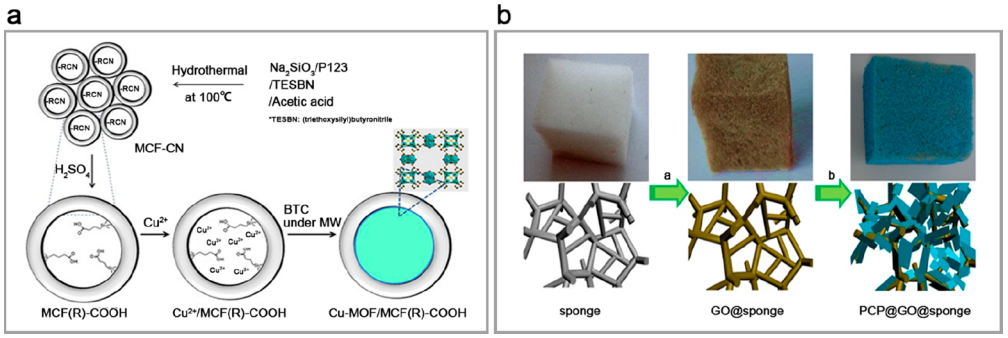

Figure 17. (a) Schematic showing the in situ formation of HKUST-1 in COOH-modified mesostructured cellular silica foams (MCF). Adapted with permission from ref 242. Copyright 2012 Elsevier. (b) Schematic showing the in situ growth of USTC-6 in commercial 3D foam-like porous monoliths. Adapted with permission from ref 249. Copyright 2016 Nature Springer.

2.2.1. MOF-Based HP-Composites Involving Meso-/Macroporous Materials. For the integration of microporous MOFs with meso-/macroporous materials (e.g., mesoporous silica, macroporous polymers, 3D foam materials, etc.), many novel strategies including de novo synthesis or postsynthetic hybridization were developed to combine the merits of both types of materials.[241−253] For instance, Jaroniec and co-workers reported a synthetic approach for the construction of MOF-based HP-composites through the simultaneous formation of MOFs and mesoporous supports (mesoporous silica or alumina) in one-pot reactions. The precursors of MOFs and mesoporous supports were mixed together and underwent a microwave-assisted hydrothermal synthesis, in which the formed MOF crystals deposited on the in situ generated mesoporous supports.[241] Additionally, Seo et al. demonstrated a stepwise synthetic approach for the hybridization of microporous MOFs and mesopore silica foam by the in situ growth of nanosized HKUST-1 in the mesopores of preformed mesostructured cellular silica foam (MCF). To create MOF nucleation sites in the mesopores of MCF, −CN groups modified MCF (MCF-CN) were fabricated by the co-condensation of 3-cyanopropyltriethoxysilane and sodium silicate, followed by a hydrolysis reaction to produce the −COOH group-modified MCF (MCF-COOH). After immersing the MCF-COOH in the Cu^{2+} containing solution, their terminal −COOH groups coordinated with Cu^{2+} for inducing the selective growth of HKUST-1 nanocrystals in the mesopores. Comparing with single microporous MOFs and mesoporous MCF, their composites exhibited both high microporosity and mesoporosity (Figure 17a).[242] Later, Cirujano et al. reported a solid-state crystallization strategy for the selective confinement of MOF nanocrystals within mesoporous materials (MPM). Different from conventional synthetic procedures, MOF precursors were introduced into the pores of MPM by a multistep incipient wetness impregnation (IWI), followed by a solid-state conversion for the confined growth of tiny MOF crystals in mesoporous cavities. The MPM confined tiny MOF composites exhibited more defective active sites and robust stability than common bulk MOFs.[243]

Apart from implanting MOF nanocrystals in the pores of mesoporous materials, the latter can also grow on the surface of MOFs. For instance, the Zeng group presented a general strategy to coat enforcing shell of mesoporous SiO_2 shell on MOFs (UiO-66, ZIF-7, ZIF-8, and HKUST-1). The shells with large channel-typed pores enhanced the mechanical stability of MOFs without sacrificing the accessibility of interior MOFs.[254] Similarly, the Yu and Jia groups reported a hierarchically porous MIL-101@SiO_2 yolk−shell nanoreactor by integrating the above SiO_2 coating method and a subsequent selective water-etching process. They proposed that the interaction of open Cr (electrophilic) sites on the surface of MOFs and nucleophilic oxygen of water molecules induced the selective removal of MOFs from outside.[255]

3D foam-like porous monoliths have been recognized as excellent supports for the generation of micro- and macroporous MOF composites. For instance, Pinto et al. reported a MOF composite foam through the direct growth of UiO-66 on an open cell polyurethane foam (PUF). This approach endows the final MOF foam with macroporous monolith structure and intrinsic microporosity of MOFs.[246] Similarly, macroporous polyacrylamide (PAM) and polymerized high internal phase emulsions (polyHIPEs) have also been used as the supports for the construction of MOF-based HP-composite monoliths.[244,245,247,248] Wang et al. put forward a photoinduced copolymerization method for preparing a UiO-66-NH_2/polymer composite. The pristine MOF was functionalized with methacrylamide groups before UV light irradiation to induce polymerization. This postsynthetic modification offers a strategy to increase the compatibility between MOFs and polymers with low polarity.[256]

Specially, commercial foam/sponge materials are readily available supports for MOF-based HP-composites. For example, Jiang and co-workers fabricated a macroscopic USTC-6@GO@sponge composite (GO is short for graphene oxide). In order to induce the deposition of MOF crystals on commercial sponge materials, a GO layer was coated on the latter before subsequent solvothermal synthesis of USTC-6 (Figure 17b). The final materials featured the excellent hydrophobicity of MOFs and structural properties of macroporous monoliths.[249] Later, the Zhou group reported a one-pot strategy to integrate PCN-224 and melamine foam (MF) into a hierarchical composite. The MOF/MF composite was prepared under a straightforward solvothermal condition. First, the monolithic melamine foam was totally submerged in an *N*,*N*-dimethylmethanamide (DMF) solution of MOF precursors, followed by a solvothermal synthesis process. The resulting PCN-224/MF hierarchical composite inherited the flexibility and elasticity of the parent melamine foam.[250]

2.2.2. MOF-Based HP-Composites Involving Biotemplates. The assembly of MOFs into microcapsules has attracted great interest because of their unique properties. Despite some defect-free hollow MOFs have demonstrated the feasibility of MOF microcapsules with size-selective perme-

https://doi.org/10.1021/acs.chemrev.1c00243
Chem. Rev. 2021, 121, 12278−12326

ability, the mechanical brittleness of MOFs poses potential challenge for the application of free-standing microcapsules. Alternatively, some biotemplates with huge hollow structures and large volumes of polar groups for the nucleation of MOFs have been recognized as promising templates for the construction of hollow MOF-based composites. The Zhang group showed that cell wall with excellent rigidity and strength could be used as mechanically stable support for the construction of MOF microcapsules with large voids and size-selective permeability of targeted molecules.[257] On the other hand, Liang et al. demonstrated that the growth of MOFs on the surface of biomaterials can improve the stability of living cells/organisms.[253]

2.2.3. MOF-Based HP-Composites Involving the Assembly of 1D or 2D Nanostructures. In addition to the hybridization of microporous MOFs with traditional porous materials, additional large pores can be formed from the interparticle voids during the assembly of MOFs on 1D nanotubes, 2D nanosheets, and so on.[238,258−265] For example, Wisser et al. prepared biological chitin/MOF composites with hierarchically porous structures. MOF crystals were dominantly formed inside the 1D hollow channels, owing to the presence of proteins inside the hollow chitin nanofibers.[259] Similarly, Cao and co-workers reported hierarchical densified MOFs/carbon nanotube (CNT) hybrid materials, based on an in situ growth ZIF-8 on CNT and a subsequent drying process to compact the composite monoliths (Figure 18). The

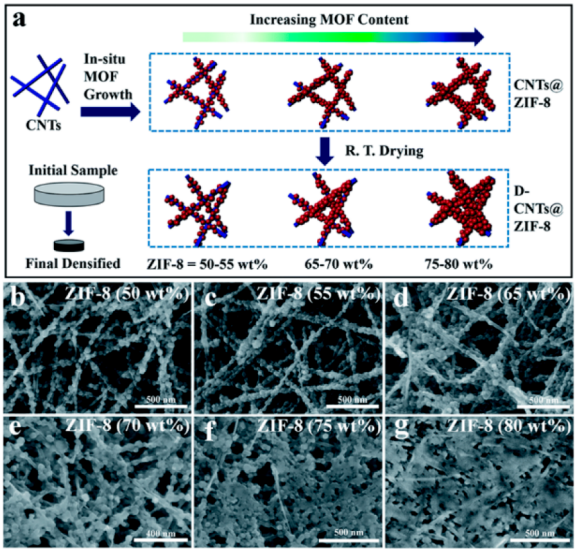

Figure 18. Schematic showing the formation, growth, and volume shrinkage of ZIF-8 on carbon nanotubes (CNTs). Reproduced with permission from ref 260. Copyright 2019 The Royal Society of Chemistry.

microstructure and density of final monoliths can be controlled by adjusting the content of MOFs.[260] Additionally, Coskun and coauthors reported graphene/MOF composites with interconnected micropores and mesopores through the growth of ZIF-8 crystals on 3D mesoporous graphene templates.[261] Jayaramulu et al. reported a bottom-up solution-assisted self-assembly approach for the hybridization of fluorinated GO (FGO) and ZIF-8.[262] Later, Fischer and co-workers fabricated a hierarchically porous metal−organic nanofibrous gel composite via the hybridization of metal−organic porous gels (MOG) with FGO, in which oxygen functionalities (e.g., hydroxyl, epoxy, carboxylate) of FGO directed the growth of MOF nanocrystals.[263]

2.2.4. MOF-Based HP-Composites Involving 2D Meshy Materials. In addition to the tiny pore size, MOF crystals are fragile and easily broken into fine powders although they can form monoliths. To address these issues, MOFs were integrated with flexible network materials to form a MOF-based hierarchically porous film.[266−270] For example, the Wang group reported a versatile approach to process MOFs into nanofibrous filters (MOFilter). A mixture solution of polymer binder (e.g., polyacrylonitrile (PAN), polyvinylpyrrolidone (PVP), polystyrene (PS)) and MOF particles (e.g., ZIF-8, UiO-66-NH_2, MOF-199, MOF-74) were spin-coated onto fiber meshy martials by an electrospinning technique (Figure 19).[266] To realize fast and large-scale preparation of flexible MOF-based mixed matrix membranes (MMMs), the same group developed a thermally induced phase separation-hot pressing (TIPS-HoP) method based on a roll-to-roll approach. To demonstrate the versatility, some common MOFs were hot-pressed with various substrates (e.g., nonwoven fabric, plastic mesh, metal mesh, glass cloth, melamine foam). These final MOF-based MMMs contain large volumes of macrosized channels between microporous MOF NPs, which is highly desirable for practical applications, especially mass-transport-involved processes.[267]

2.2.5. MOF-Based HP-Composites Involving 3D Array Materials. Array materials with oriented arrangement and unique hierarchically porous structures have been used as the supports for the construction of MOF-based HP-composites.[271−275] Zhan et al. demonstrated a self-template strategy for the generation of ZnO@ZIF-8 core−shell heterostructures assembled in the form of oriented arrays. The preprepared ZnO arrays were etched to release Zn^{2+} ions in the presence of 2-MeIM. By controlling the rate between the dissolution of ZnO and nucleation of ZIF-8, ZIF-8 were heterogeneously grown on the surface of ZnO nanorods.[271] Similarly, Xu and co-workers fabricated a bimetallic ZIF-based nanorod array (ZnO@ZIF-CoZn) through coating a layer of ZIF-CoZn thin film on a ZnO nanowire array (Figure 20a). Different from the formation of ZnO@ZIF-8, foreign Co^{2+} ions were introduced during the self-sacrificing process. The competitive coordination between Co^{2+} and Zn^{2+} ions with 2-MeIM results in the formation of a bimetallic ZIF-CoZn layer on ZnO array templates.[272] Later, Deng et al. prepared a bimetallic CoNi-MOF nanosheet array. During their synthesis, $Co(OH)_2$ array was electrodeposited onto carbon fiber papers (CFP) and then immersed in the solution containing of Ni^{2+} ions and organic linkers. The oriented $Co(OH)_2$ array acted as both the template and the source of Co^{2+} ions to induce the formation of vertically oriented MOF-based hierarchically porous structures.[273] It was worth mentioning that the Zhao group reported a universal method for the direct growth of ultrathin MOF nanosheet arrays on various substrates, in which the MOF nanosheet were in situ generated on corresponding supports through a one-step chemical bath reaction of the aqueous solution of MOF precursors in the presence of the substrate (Figure 20b).[274]

2.3. MOF-Based Hierarchically Porous Derivatives (HP-Derivatives)

Given the periodic porous structures and tailored compositions as well as very high surface area, MOFs have been demonstrated to be ideal sacrificial templates/precursors for

https://doi.org/10.1021/acs.chemrev.1c00243
Chem. Rev. 2021, 121, 12278−12326

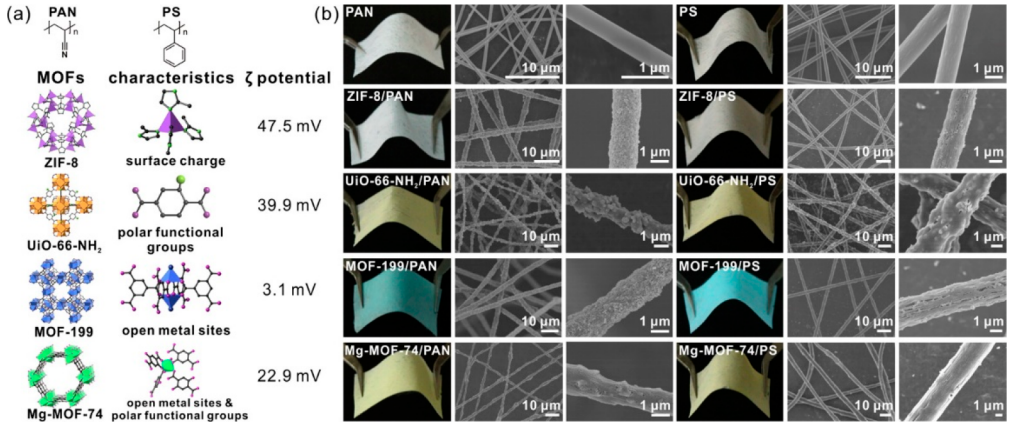

Figure 19. Schematic showing the composite of MOFs with various 2D meshy materials. Reproduced with permission from ref 266. Copyright 2016 American Chemical Society.

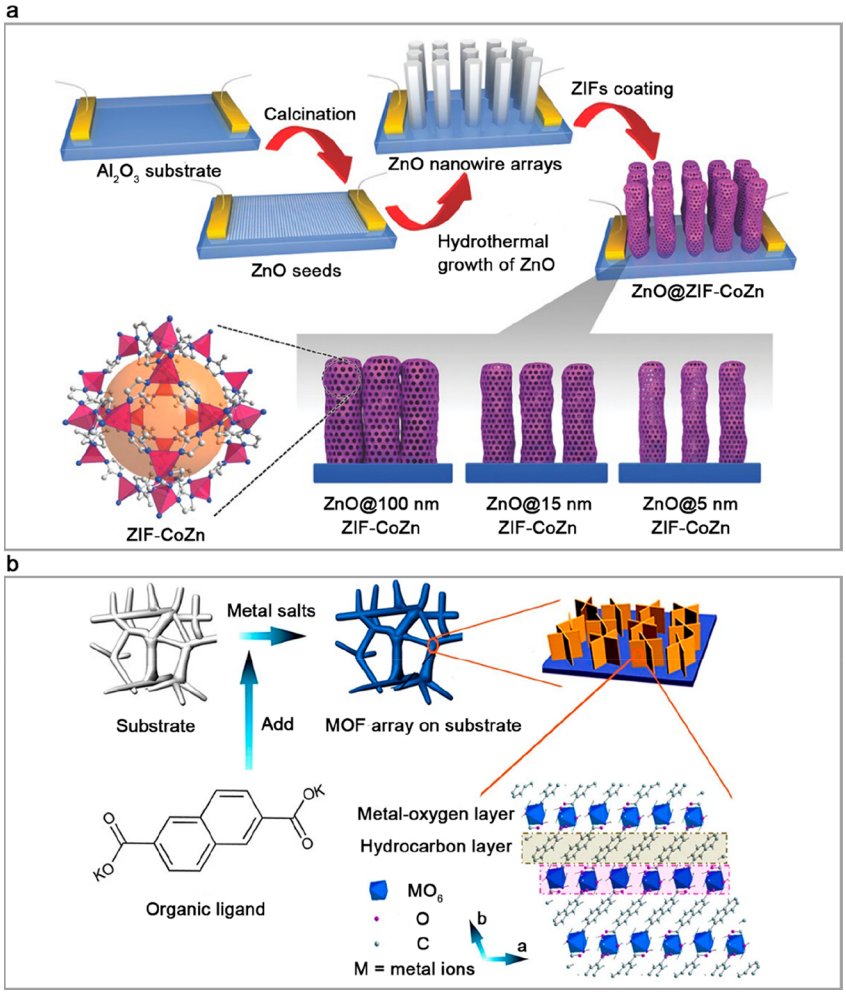

Figure 20. (a) Schematic showing the synthesis strategy of ZnO@ZIF-CoZn nanoarrays. Adapted with permission from ref 272. Copyright 2016 John Wiley & Sons, Inc. (b) Schematic showing the formation of hierarchically porous MOF nanosheets on various substrates. Adapted with permission from ref 274. Copyright 2017 Nature Springer.

the fabrication of diverse porous materials, affording high porosity and evenly dispersed active components in their derivatives. Furthermore, in contrast to the parent MOFs, the resulting MOF-based HP-derivatives generally present enhanced stability, conductivity, mesoporosity, and even macroporosity, which are of great importance toward applications, particularly energy-related electrocatalysis.[35,40,42,276−290]

2.3.1. MOF-Derived Hierarchically Porous Quasi-MOFs. The quasi-MOFs can be obtained via an elaborate transformation to afford a transition-state structure between pristine MOFs and fully converted materials by MOF pyrolysis. Upon partially removing the organic ligands by thermal transformation, the obtained metal-oxo nodes are more exposed in the interrupted framework. In addition,

https://doi.org/10.1021/acs.chemrev.1c00243
Chem. Rev. 2021, 121, 12278−12326

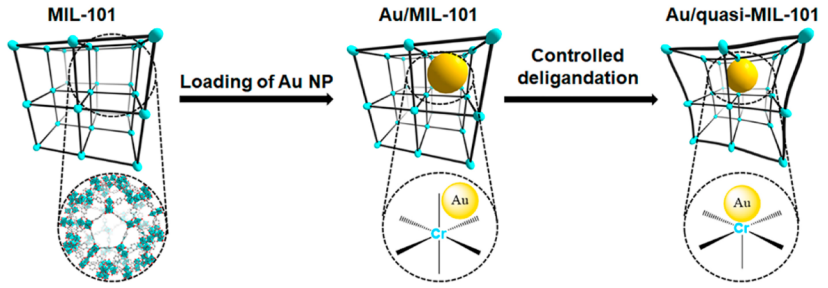

Figure 21. Schematic showing the elaborate transformation of MIL-101 into hierarchically porous quasi-MIL-101. Reproduced with permission from ref 292. Copyright 2018 Elsevier.

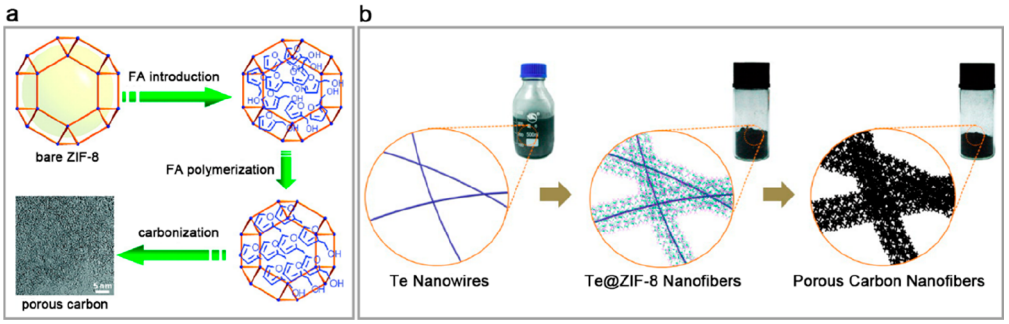

Figure 22. (a) Schematic showing the complete transformation of ZIF-8 into N-doped hierarchically porous carbons. Adapted with permission from ref 306. Copyright 2011 American Chemical Society. (b) Schematic showing the template-directed formation and complete transformation of ZIF-8 into hollow porous carbon nanofibers. Adapted with permission from ref 309. Copyright 2014 American Chemical Society.

partial collapse/removal of MOFs results in large voids in microporous MOFs.[291] As a proof of the concept, the Xu group for the first time prepared Au/quasi-MIL-101 composites through a controlled deligandation approach (Figure 21). The final quasi-MOF with reduced number of linkers capped on metal clusters led to stronger interaction between guest NPs and MOFs while retaining overall crystalline skeletons of pristine MOFs.[292] Similarly, various metal NPs/MOF composites were converted into metal NPs/quasi-MOFs, for example, M/quasi-Ce-BTC nanorods (M = Au, Cu, Au−Cu), CeO_2/Quasi-MIL-101(Cr), etc.[291,293] According to these reports, the pyrolysis temperature and atmosphere should be strictly controlled to avoid fully decomposed carbon/metal oxide products.

Different from the derivatives from MOF composites, pristine MOFs can be directly converted into metal (oxides)/quasi-MOF composites, in which metal (oxide) NPs were in situ produced during the partial removal of linkers and the following agglomeration of tiny metal (oxide) clusters in MOFs. For examples, MIL-101 (Cr), ZIF-67 (Co), MIL-125 (Ti), and MIL-100 (Fe) were converted to Cr_2O_3/quasi-MIL-101, Co/quasi-ZIF-67, TiO_2/quasi-MIL-125, and Fe_3O_4/quasi-MIL-100, respectively.[294−297] Specifically, a novel transformation was realized when expanding this strategy to bimetallic MOFs. Generally, different metal ions possess different coordination abilities with the same organic linker. During the thermal degradation of bimetallic MOFs, the metal ion binding to ligands weakly tended to dissociate first and converts to corresponding metal (oxide) NPs, while the other robust metal−ligand binding held the framework structures of the parent MOFs to some extent. Inspired by this, Hu and co-workers achieved a quasi-MOF confined Cu nanowire through partial thermolysis of bimetallic CuCo-MOFs. The Co^{2+} ions exhibited stronger coordination with ligands, thus contributing to the preservation of the overall MOF structure. The in situ formed mesoporous skeleton during pyrolysis induced Cu clusters to aggregate into a nanowire morphology.[298] Later, the same group reported the synthesis of quasi-CoMn-MOF-74 encapsulated $CoMnO_x$ NPs based on the controlled deligandation of bimetallic CoMn-MOF-74.[299] In addition to the formation of more defective sites, the Huo and Zhang groups reported a thermal-induced shrinkage behavior of MOFs at a medium annealing temperature (200−280 °C). On the basis of this mechanism, they selected MOFs with relatively high shrinkage ability as the core to produce core−shell MOFs@MOFs, subsequently converting then into corresponding yolk−shell MOFs@MOFs with hierarchically porous structures by controlled thermal treatment.[300]

2.3.2. MOF-Derived Hierarchically Porous Carbons, Metal-Based Compounds, and Their Composites. The MOF-derived hierarchically porous materials can be produced by complete conversion of MOFs into the corresponding porous carbons, metal-based compounds (metal NPs, metal oxides/sulfides/phosphides, etc.), and their composites depending on the reaction conditions. These derivatives not only inherit the structural merits (e.g., high porosity, tunable porous structures, compositions, and morphologies) of parent MOFs to some extent but also endow the final materials with additional features, such as robust chemical stability, high electrical conductivity, additional mesoporosity, and even macroporosity. It is worthy to mention that there have been several excellent reviews summarizing state-of-the-art development of MOF-derived porous materials.[35,40,42,276−289,301−304] In this Review, we would discuss several typical reports only to demonstrate the rational construction of hierarchically porous structures based on complete conversion of MOFs into their derivatives. The hierarchical pores are mainly generated by partially inheriting the microporosity of MOFs and the

https://doi.org/10.1021/acs.chemrev.1c00243
Chem. Rev. 2021, 121, 12278−12326

introduction of additional porous structures during the conversion of MOFs.

2.3.2.1. MOF-Derived Hierarchically Porous Carbons. MOF-derived hierarchically porous carbons are generally prepared by the pyrolysis of MOF precursors under the atmosphere of inert gas (Ar or N_2) and subsequent removal of metal species by a leaching process (in situ evaporation during the conversion, or acid etching, etc.). For the first time, the Xu group achieved porous carbon materials with high porosity and hierarchically porous structures by the pyrolysis of MOF-5 as templates and furfuryl alcohol (FA) as an additional carbon source. During the heat-treatment process, ZnO NPs were formed temporally and subsequently reduced to Zn metal when the temperature raised up to 800 °C, followed by in situ Zn evaporation upon reaching its boiling point (908 °C) to create additional mesoporosity.[305] Later, the same group revealed the importance of stability of MOF precursors for the final porosity of MOF-derived porous carbons, for the first time, selecting a chemically and thermally stable MOF (ZIF-8) as both templates and precursors of nitrogen-doped carbon (Figure 22a). They achieved hierarchically porous carbons with even higher microporosity than the parent MOF. The surface area of the resulting carbon can be further increased after adding FA as the second carbon source.[306] Furthermore, the Yamauchi group directly pyrolyzed Al-MOFs into porous carbons without any additional carbon sources, in which the in situ formed Al NPs were removed by HF etching. The resultant fibrous carbon showed extremely high surface area and contained large cracks/voids.[307,308]

Given the microporous nature of MOF templates, the above hierarchically porous carbon materials are usually dominated by micropores. To further optimize the content of mesopores, macropores and even hollow caves in MOF-derived carbon materials, the Liang and Chen groups developed an in situ confinement pyrolysis approach for the conversion of PVP-modified MOFs (ZIF-8) into nitrogen-enriched meso-microporous carbon (NEMC). On the contrary, disorder-aggregated and micropore-dominated porous carbon NPs were produced by the directly pyrolysis of ZIF-8. According to control experiment results, PVP coating played an important role in promoting the mesoporous carbon structure. Because of the strong interaction between the Zn^{2+} ions of ZIF-8 and carbonyl groups of PVP, the ZIF-8 crystal shrank from the inside to the outside while heating to create additional hollow spaces.[310] Furthermore, external species as self-sacrificial templates were combined with MOFs to introduce more mesoporosity in the derived porous carbons. The Yu and Jiang groups reported a nanowire-directed templating synthesis approach for the preparation of hollow porous carbon nanofibers (Figure 22b). In addition to meso−microporous structures derived from ZIF-8 shells, the thick Te nanofiber templates were in situ evaporated during the pyrolysis to create 1D hollow tubes, of which the hollow size can be increased by using thicker Te nanofibers as templates.[309,311] Sun et al. put forward a double-template approach for the fabrication of MOF-derived porous carbons with hierarchical pore structures. In their attempt, Al-MIL-101-NH_2 was loaded with Cu^{2+} ions prior to calcination. During the calcination process, Al metal nodes and grafted Cu^{2+} ions were transformed into Al_2O_3 and Cu NPs, respectively. After HF etching, hierarchically porous carbons with controlled mesopores mimicking the sizes of these particles were generated.[312]

2.3.2.2. MOF-Derived Hierarchically Porous Metal-Based Compounds. Owing to the abundant metal nodes (e.g., Zn, Co, Cu, Mg, Ni, Mn, Fe, Ti, etc.), MOFs have been recognized as suitable candidates for the construction of porous metal-based compounds. MOF-derived hierarchically porous metal-based compounds (e.g., oxides, hydroxides, sulfides, phosphides, etc.) are generally prepared by annealing or chemical treatment to remove the organic parts of MOFs. Driven by different kinetics of metal node conversion and organic linker decomposition, hierarchically porous metal-based compounds with a hollow structure can be deliberately fabricated. For example, the Lou group achieved hierarchical Fe_2O_3 microboxes with hollow structures after annealing of Prussian blue (PB) microcubes under air atmosphere.[313] Differently, the Jiao and Chen groups prepared layered double hydroxides (LDHs) assembled hollow nanocages through a solvothermal treatment of ZIF-67. By refluxing ZIF-67 in ethanol solution of different metal salts, the corresponding hollow LDHs with related metals (Co^{2+}−Co^{3+}, Mg^{2+}−Co^{3+}, Ni^{2+}−Co^{3+}) can be formed. In detail, the instability to acid rendered ZIF-67 to dissolve in the metal salt solution, leaving behind a hollow core in the precipitated LDH shell.[314] Similarly, Lou and co-workers achieved hollow Co−Ni LDHs by using ZIF-67 as the template and precursor. They demonstrated a hollow metal phosphide nanobox by thermal treatment of the resulting hollow LDHs with NaH_2PO_2 (Figure 23a).[315] In the same year, the Fan group reported a hollow metal selenide produced by thermally induced selenylation of a Co-MOF.[316] Typically, a hierarchically porous $MoSe_2$ nanosphere with a hollow structure was achieved after annealing Co-MOF nanocrystals with commercial selenium powder at 450 °C (Figure 23b).

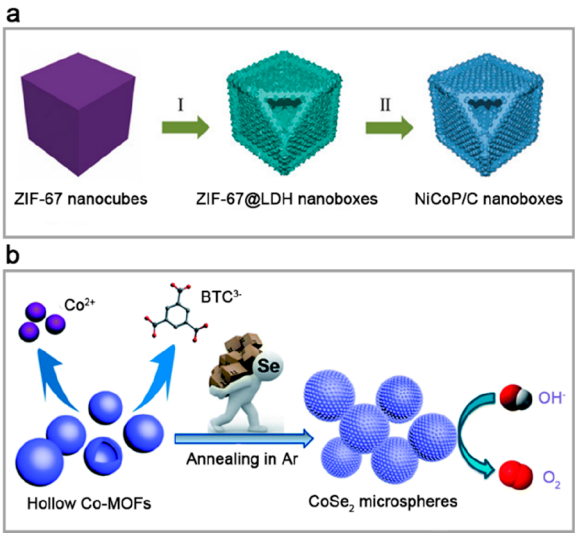

Figure 23. (a) Schematic showing the transformation of ZIF-67 nanocubes into NiCoP/C nanoboxes. Adapted with permission from ref 315. Copyright 2017 John Wiley & Sons, Inc. (b) Schematic showing the thermal transformation of hollow Co-MOF into hollow $CoSe_2$ microspheres. Adapted with permission from ref 316. Copyright 2017 The Royal Society of Chemistry.

2.3.2.3. MOF-Derived Composites of Metal-Based Compounds and Hierarchically Porous Carbons. Considering the coexistence of organic and metal species in MOFs, as well as their periodic arrangement, MOFs are promising as precursors for the hierarchically porous carbons incorporating metal-

https://doi.org/10.1021/acs.chemrev.1c00243
Chem. Rev. 2021, 121, 12278−12326

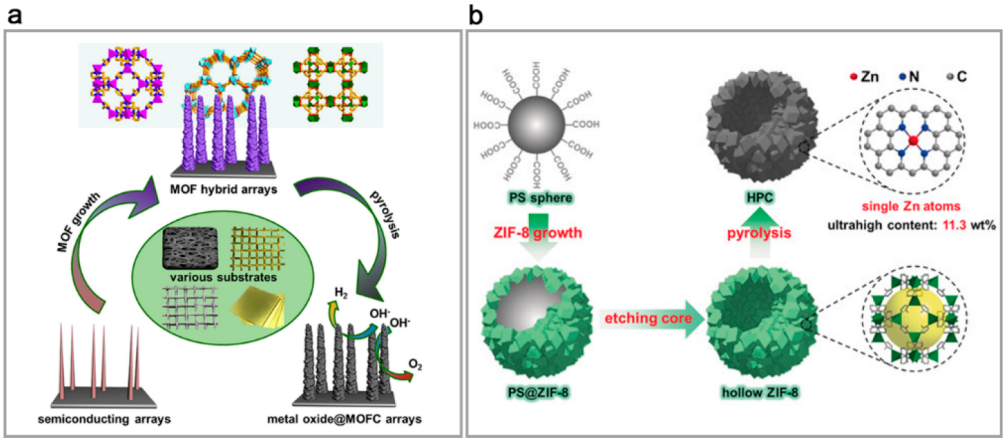

Figure 24. (a) Schematic showing the template-directing growth of various MOF arrays on different substrates and corresponding MOF-derived hierarchical composites. Reproduced with permission from ref 324. Copyright 2017 Elsevier. (b) Schematic showing the formation and conversion of hollow MOFs into corresponding hollow MOF-based HP-composites. Reproduced with permission from ref 325. Copyright 2019 John Wiley & Sons, Inc.

based compounds. By judicious selection of MOFs with desired metal species, corresponding metal-based compound/porous carbon composites can be fabricated by facile pyrolysis. For example, metal oxides embedded in porous carbons were obtained by direct thermal-treatment of ZIF-67 (Co), MIL-88A (Fe), Mn-BTC, MIL-125 (Ti), and so on, under inert atmosphere.[317−321] Similarly, metal sulfides, metal phosphides, metal selenides can be incorporated into MOF-derived hierarchically porous carbons by controlling the conversion conditions. The Jiang group reported hierarchically porous CoP/reduced graphene oxide (rGO) composites. The ZIF-67/GO composites were pyrolyzed into Co_3O_4/rGO and subsequently underwent a phosphating process using NaH_2PO_2.[322]

It was worthy to mention that the derivatives from MOF-based array materials present promising potentials for practical application, due to unique self-supporting and hierarchical structures. The well-aligned arrangement of MOF crystals and large open space between them make the active metal-based compounds in MOF-derived composites more accessible. For example, the Qiao group directly grew a unique Co-MOF on copper foil, followed by pyrolysis into hybrid Co_3O_4-carbon porous nanowire arrays.[323] To realize the conversion of various MOF nanocrystals into well-aligned array structures, Jiang and co-workers developed a versatile template-directed strategy for the construction of MOF-based arrays. By using well-aligned semiconducting nanostructures (e.g., CoO, NiO, and Cu-$(OH)_2$) as self-sacrificial templates, different MOFs were grown on various conductive substrates. The MOF-derived hierarchical composites with well-aligned and self-supporting structure were formed after a facile thermal-treatment process (Figure 24a).[324]

Particularly, MOFs are promising precursors for the formation of metal single-atoms (SAs) supported by heteroatom-doped porous carbon.[301] The agglomerated metal NPs were readily generated during harsh calcination conditions. To avoid this, the Li and Wu groups employed a bimetallic ZnCo-ZIF as precursor. During the annealing process, Zn^{2+} ions acted like a "fence" to separate Co ions and thus prohibited the agglomeration of Co atoms, while the organic ligands were pyrolyzed into N-doped carbons to fix the Co SAs. When the temperature reached over 800 °C, the Zn atoms would in situ evaporate to produce the composites of Co SAs dispersed in the N-doped carbon with high porosity.[326] To enlarge the pore sizes of MOF derived composites, the Jiang group employed a hollow ZIF-8 nanospheres as the pyrolysis precursors (Figure 24b). By a facile annealing approach, a hierarchically porous carbon with a hollow structure and high content (11.3 wt %) of single Zn atom was obtained.[325]

2.4. Comparison of Different Types of MOF-Based Hierarchically Porous Materials

The intrinsic HP-MOFs possess well-defined hierarchically porous structures, which is highly desirable for understanding structure−property relationships. Moreover, most of them can be synthesized via one-step solvothermal methods, which do not involve troublesome postsynthetic treatment processes. Unfortunately, despite the numerous choices of metal nodes and organic linkers, their structural types and pore sizes are limited, which is hard to satisfy the different demands for various practical applications. The length and size of linkers cannot be extended at will because the very long linkers readily bring about severe interpenetration or stability issues.

The construction of defective HP-MOFs by introducing additional mesopores into conventional microporous MOFs has been proven to be an excellent solution. This strategy allows for the conversion of extraordinarily stable MOFs (e.g., ZIF series, UiO series, MIL series, etc.) into corresponding hierarchical structures, thus making it possible for diverse ends. However, it is still hard to generate very large pores for the applications involving large species. Moreover, chemical etching strategy or modulator-induced-defect-formation strategy must be conducted in an appropriate manner. Excess amounts of etching reagents or modulators will be detrimental to the crystallinity of MOF structure instead of creating large pores.

Hollow MOFs represent another type of hierarchically porous structure, posing excellent promise for nanoreactors and some special applications, such as the storage of huge size (even micron) and large volume of species. The size of the hollow cavity and thickness of MOF shells are both tailorable by varying the parameters of templates and growth conditions. Stepwise growth procedures can even lead to exquisite multishell structures. In spite of diverse strategies developed

https://doi.org/10.1021/acs.chemrev.1c00243
Chem. Rev. 2021, 121, 12278−12326

to embed additional pores in different regimes of various popular MOFs, the introduced pores in defective and hollow MOFs are generally amorphous, although the surrounding microporous skeleton is able to maintain its initial crystallinity. It is still challenging to introduce mesopores, macropores, and hollow cavities with an ordered structure into the parent microporous materials.

In addition to the extension of pore size, MOF materials face great challenges during the molding process to form targeted monolith for the real-life applications, due to the poor processability of MOF powders. Integrating MOFs with additional materials bearing flexible mechanical properties has been recognized as a promising solution to improve the processability of MOF-based materials. Additionally, MOF-based HP-composites endow synergistic properties from different materials into a single composite, superior to their individual components and physical mixtures, thereby further expanding the application fields of conventional MOF materials. However, the spacing among them is hard to be controlled and the resulting composites usually fail to provide a long-range order—the challenge to achieve the heterogeneity within order in the composite structures. How to realize a synergistic performance improvement by integrating MOFs with another functional material is also challenging because of the lack of precise control of the microstructure and lack of knowledge on the microscopic mechanism lying behind.

On the other hand, MOF-based HP-derivatives possess some enhanced properties (e.g., stability and conductivity) in comparison to their parent MOFs. Unfortunately, some structural advantages will unavoidably lose during the transformation process, such as the crystalline structure and well-defined pore size distribution. On the whole, different types of MOF-based hierarchically porous materials show their unique structural strengths and weaknesses.

3. ENHANCED APPLICATIONS OF MOF-BASED HIERARCHICALLY POROUS MATERIALS

The extension of pore diameters of MOFs to cover micropores, mesopores, and even macropores has been one of the most important targets to meet various demands toward the practical applications. Recently, many applications, such as catalysis, sensing, biomedicine, sewage treatment, energy storage, and air filtration, etc., are being developed by taking advantage of hierarchical pores and unique structural strengths of MOFs, in which different types of MOF-based hierarchically porous materials exhibit unique structural merits toward targeted applications.

3.1. Heterogeneous Catalysis

Although homogeneous catalysts possess important strengths of high tunability, activity, and selectivity, they usually suffer from poor stability and recoverability.[327,328] By contrast, their heterogeneous counterparts offer high stability and improved recyclability, but they always encounter reduced activity and selectivity, as well as increased difficulty to modulate the quantity and spatial location of active sites, attributed to their amorphous or solid nature.[329−338] Because of the well-defined and tunable structures at molecular level, MOFs are able to integrate respective advantages of these two kinds of catalysts.[233,320−326] The crystalline nature endows MOFs definite structure and uniformly dispersed active sites; their high porosity facilitates the mass transport and ensures the accessibility of active sites. Moreover, MOFs provide permanent pore space to encapsulate active guests for synergistically enhanced catalysis; their adjustable structures endow great opportunities to modulate the physical/chemical microenvironment around catalytic sites (e.g., chiral, hydrophilic/hydrophobic, and electron-deficient/rich microenvironment).

Despite the above structural advantages of MOFs for heterogeneous catalysis, their pore sizes are mainly tunable in the microporous regime, which is actually unfavorable as the small micropores slow down the diffusion and restricts large-species-involved reactions. To address these issues, HP-MOFs, integrating micropores with mesopores and even macropores, can improve the accessibility of inner active sites and reduce the resistance of mass transfer involving large-size species. Their micropores ensure the high surface area while mesopores/macropores across the microporous matrix contribute to the transport and required space for large-size species. In this way, HP-MOFs not only integrate both advantages of homogeneous and heterogeneous catalysts, but also combine the strengths of porous materials that fall in different pore regimes. Therefore, the development of HP-MOFs as heterogeneous catalysts is particularly interesting.[18,22,23,25,43,339] To summarize their structural strengths and structure−performance relationships, the reported HP-MOF catalysts are divided into five categories based on the type and origin of hierarchical pores: heterogeneous catalysis based on intrinsic HP-MOFs, defective HP-MOFs, hollow HP-MOFs, MOF-based HP-composites, and MOF-based HP-derivatives, respectively.

3.1.1. Heterogeneous Catalysis Based on Intrinsic HP-MOFs. The active sites of heterogeneous catalysts based on intrinsic HP-MOF basically originate from three places: the coordinatively unsaturated metal sites (CUSs) on metal nodes, the dangling functional groups on the organic linkers, and guest active species in pore spaces.[340] Metal ions/clusters in MOFs are usually coordinated with organic linkers and solvent molecules (as well as modulators, hydroxide, or halide ions to balance the charge of MOF structures), the latter of which can be readily removed through heating in vacuum to produce CUSs while the overall framework structure retains intact. The resultant CUSs (Lewis acidic sites) interact with and activate the substrates, thereby promoting their conversion to target products. For example, unsaturated Cr(III) centers in MIL-101(Cr) are extraordinarily efficient for acid-catalyzed cyanosilylation of benzaldehyde;[77] open Fe(III) sites in MIL-100(Fe) are able to catalyze Friedel−Crafts benzylation;[341] and Lewis-acidic Zr(IV) ions in NU-1000 exhibit excellent catalytic performance for the degradation of nerve agents and their simulants.[342]

The functional groups on organic ligands of intrinsic HP-MOFs can also be tailored for heterogeneous catalysis. Typically, partially protonated $-SO_3Na$ was introduced into MIL-101(Cr) using monosodium 2-sulfoterephthalate acid as the linker in the presence of hydrochloric acid.[343] The resulting MOFs showed high activity toward the catalytic cellulose hydrolysis, ascribed to the presence of strong Brønsted acid sites on their mesopore surfaces. To further increase the number of active sites, Jiang and co-workers demonstrated a postsynthetic acid treatment strategy for the construction of almost completely sulfonic acid functionalized MOFs. The resulting MIL-101-SO_3H exhibited excellent catalytic performance in the alcoholysis of epoxides under ambient conditions.[344] Apart from the dangling functional groups on

https://doi.org/10.1021/acs.chemrev.1c00243
Chem. Rev. 2021, 121, 12278−12326

pore surfaces, active sites can also be involved in the main skeleton of MOFs. This can be exemplified by PCN-222(Fe), constructed by using functional metalloporphyrin as organic linkers, which exhibited excellent peroxidase-like catalytic activity owing to the high density of cytochrome P450 enzyme-like metalloporphyrin centers.[63]

The catalytic scenarios of intrinsic HP-MOFs are restricted by the active sites provided by CUSs and linkers. An effective method to expand the scope of catalytic reactions is to modify the metal nodes or linkers through postsynthetic modification. After tethering different amine groups to open Cr sites in MIL-101(Cr), Hwang et al. prepared a series of base catalysts for Knoevenagel condensation reactions.[345] Similarly, Banerjee et al. introduced catalytically active chiral molecules into MIL-101 by postsynthetic modification. Such chiral MIL-101 exhibited excellent performance for asymmetric aldol reactions between various aromatic aldehydes and ketones.[346] Besides the modification of CUSs with organic molecules, grafting a metal complex onto M-oxo nodes endows MOFs the potential for heterogeneous single-site catalysis. For example, Noh et al. demonstrated a solvothermal deposition strategy for the deposition of catalytically active molybdenum(VI) oxides on the node of NU-1000, which were extraordinarily effective for cyclohexene epoxidation reaction.[347] Similarly, Li et al. presented an atomic layer deposition (ALD) method for uniformly and precisely installing Ni ions onto metal clusters of NU-1000. The isolated Ni ions ensured excellent catalytic performance for gas-phase hydrogenation reactions.[348]

In addition to the above approaches introducing active sites, as porous materials, HP-MOFs with high porosity and large pore volume are able to accommodate various guest species (e.g., metal complexes, enzymes, and metal NPs) into their pore spaces by noncovalent interaction.[349] The resulting guest/MOFs can serve as a multifunctional platform for their synergistic effect in catalytic reactions, largely extending the application of MOFs in catalysis. For example, Farrusseng and co-workers installed metal phthalocyanine complexes into mesopores of MIL-101(Cr) through a wet infiltration method. The resultant catalyst was able to catalyze selective oxidation of tetralin into 1-tetralone.[350] To guarantee that metal NPs were selectively incorporated inside the pores of MOFs, Aijaz et al. developed a double-solvent approach (DSA) to encapsulate tiny Pt NPs into MIL-101 (Pt@MIL-101).[351] In contrast to the traditional impregnation method, such DSA minimized the chances of MNPs deposition on the surface of MOFs. As a result, Pt@MIL-101 exhibited high activity for reactions in different phases, such as gas-phase CO oxidation, liquid-phase $NH_3{\cdot}BH_3$ hydrolysis, and solid-phase $NH_3{\cdot}BH_3$ thermal dehydrogenation. In addition to monometallic NPs, bimetallic PdAg alloy NPs were successfully introduced into mesoporous cavities of MIL-101 via a similar DSA by the Jiang group.[352] This catalyst reveals the potential of HP-MOFs to integrate host−guest cooperation and bimetallic synergy in a single material, in which MOF host contributes to Lewis acidity, Pd offers hydrogenation activity, and Ag ensures high selectivity. As a result, PdAg@MIL-101 exhibited both excellent catalytic activity and selectivity toward one-pot cascade reactions. Not limited to bimetallic alloy NPs, the same group successfully prepared Pd@Co core−shell and PdCo alloy NPs inside the pore of MIL-101 via selecting different reduction agents.[353] In contrast to the PdCo alloy, the MIL-101 encapsulated Pd@Co core−shell presented superior catalytic activity and especially excellent cyclic stability in hydrolytic dehydrogenation of NH_3BH_3. The location of guest metal NPs relative to MOFs can be well demonstrated by combined characterization techniques, including electron tomography, ^{129}Xe NMR, and positron annihilation spectroscopy (PAS).[354]

3.1.2. Heterogeneous Catalysis Based on Defective HP-MOFs. Although intrinsic HP-MOFs have shown obvious strengths for heterogeneous catalysis, limited types of intrinsic HP-MOFs undoubtedly restrict their application scenarios toward various reactions. Incorporating additional mesopores or macropores into the structure of microporous MOFs extends pore sizes, introduces defective active sites, and thus solves the issues caused by narrow pore sizes. Actually, different microporous MOFs (e.g., HKUST-1, ZIF-8, ZIF-67, MIL-125, UiO-66, MIL-53, and MOF-5) have been converted into the corresponding hierarchically porous structures with improved catalytic performances.[18,22,23,25,43]

Highly ordered macropores were introduced into ZIF-8 by using polystyrene sphere (PS) matrices as hard templates. The resulting microporous-macroporous ZIF-8 showed higher activity than all control catalysts for Knoevenagel reactions between benzaldehydes and malononitriles with bulky groups. The ordered macropores made the active sites inside ZIF-8 matrix accessible, greatly enhancing the conversion rate of substrates. However, polycrystalline porous ZIF-8 and disordered macroporous ZIF-8 with similar pore sizes contained closed pores which blocked the active sites, thus lowering their catalytic performance.[122] In addition, Wee et al. synthesized a microporous ZIF-8 for catalytic esterification of oleic acid with glycerol. They discovered that the in situ etching of ZIF-8 with oleic acid created additional mesopores in the MOF matrix, contributing to the conversion of substrates.[171] HKUST-1 represents an ideal candidate for a variety of copper-based catalytic reactions. Peng et al. reported a template-free assembly of micromesoporous HKUST-1 by using CO_2-expanded liquids as switchable solvents. The as-synthesized HP-HKUST-1 was highly active in catalyzing the aerobic oxidation of benzylic alcohols under mild temperature and atmospheric pressure.[134] Later, Zhan and Zeng reported a macro-meso-microporous HKUST-1 via a "domain growth" mechanism, which showed improved Lewis acid activity for quinoxaline synthesis via oxidative cyclization between 2-hydroxy-acetophenone and phenylenediamine, in contrast to pristine bulk HKUST-1.[136] Similarly, Cui et al. utilized single-crystalline HKUST-1 particles with a hierarchically porous structure to accelerate the Friedländer reaction between 2-aminobenzophenones and acetylacetone. The experiment results revealed the catalytic reaction were promoted by the hierarchically porous HKUST-1, which ensured fast mass diffusion/transfer in contrast to the routine microporous HKUST-1.[120] Additionally, microporous/mesoporous MIL-125(Ti) were prepared by a vapor-assisted crystallization method. For the oxidation reaction of dibenzothiophene with *tert*-butyl hydroperoxide, the hierarchically porous MIL-125 outperformed the counterpart with the sole micropores. This was attributed to the facile access of the substrate to internal active sites of MOF with large mesopores, while micropores in the pristine MIL-125 were inadequate to accommodate dibenzothiophene. Furthermore, thiophene adsorption studies revealed that the former contained more unsaturated metal sites.[103]

Generally, the impregnation of catalytically active moieties into MOFs is an effective solution to facilitate their dispersion and protect them from aggregation. The in situ incorporation

https://doi.org/10.1021/acs.chemrev.1c00243
Chem. Rev. 2021, 121, 12278−12326

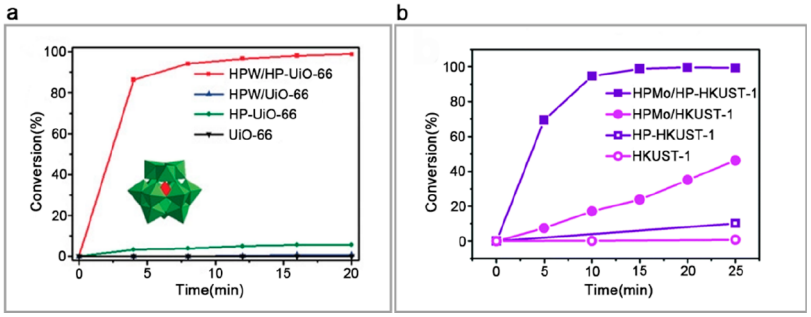

Figure 25. (a) Ring opening of styrene oxide with methanol over HPW/HP-UiO-66. Adapted with permission from ref 141. Copyright 2017 John Wiley & Sons, Inc. (b) Ring opening of styrene oxide with methanol over HPMo/HP-HKUST-1. Adapted with permission from ref 180. Copyright 2018 The Royal Society of Chemistry.

of foreign species sometimes impedes the MOF growth. On the other hand, the in situ growth of MOFs around the active guests causes transfer impedance and covers partial active sites on their surface. In these cases, postsynthetic incorporation methods provide an alternative solution to bypass the above issues. However, this strategy poses highly demand for large pore sizes to implant large guest species. In these cases, HP-MOFs offer a straightforward approach for the incorporation of large-size active species into their mesopores. Particularly, the introduction of additional mesopores or macropores by creating defects in HP-MOFs to produce guests/HP-MOFs can optimize the catalytic performance of active guests/MOF hosts, attributing to the improved mass transfer and easy exposure of active sites.[355] For example, Zhang et al. reported Pt/UiO-66 with hierarchical pores using Au nanoparticles as the hard template.[118] Such HP-MOFs could not only retain a continuous and well-defined crystal structure, but also possessed mesopores with controlled size, shape, and spatial distribution through adjusting the encapsulation conditions. As a result, the obtained Pt/HP-MOF hybrid materials displayed excellent catalytic activity (attributing to facilitated mass transfer in the internal mesopores) and good selectivity (because of the size-selective permeability of external microporous frameworks) in catalytic hydrogenation reactions. Similarly, Meng et al. constructed a series of metal@MOFs (Pt@UiO-66-NH_2, Pt@UiO-66, Pt@ZIF-8, and Au@ZIF-8) with hierarchical pores by a heat-treatment approach to selectively decompose the MOF structures around the encapsulated metal NPs, taking advantage of the heterogeneous nucleation induced relatively week stability on the interfacial structures.[191] The resulting Pt@UiO-66-NH_2 exhibited an increased catalytic rate and selectivity in the olefin selective hydrogenation, attributed to more interfacial defective sites and large pore spaces. He et al. demonstrated a competitive coordination strategy for the construction of Pd/HP-MOF-5.[144] This could integrate the advantages of HP-MOFs and surfactant-free Pd NPs and, thus, showed an improved activity toward the reduction of nitroarene. Wang et al. presented an Au@ZIF-8 nanoreactor which possesses a single-crystalline MOF shell with intrinsic well-defined micropores and introduced defective macropores in the interior of MOF particles.[119] These structural features of the Au@ZIF-8 nanoreactor ensured the size selectivity of reactants, the accessibility of encapsulated Au NPs to reactants, and the mass diffusion of reacting substrates and products. As a result, the Au@ZIF-8 nanoreactor delivered excellent size-selectivity, enhanced conversion, and good cycling stability when used to catalyze the aerobic oxidation of alcohols with different molecular sizes. Later, Teng et al. reported bimetallic HP-ZIFs encapsulated Pt NPs (Pt@HP-Co/Zn-ZIF), which showed excellent molecular-size selectivity and cycling stability toward the hydrogenation of alkenes.[125]

Besides metal NPs, Cai et al. utilized defective HP-UiO-66 for the heterogenization of polyoxometalates (Figure 25a). The resultant phosphotungstic acid (HPW, $H_3PW_{12}O_{40}{\cdot}nH_2O$)-impregnated HP-UiO-66 (HPW/HP-UiO-66) led to significantly higher activity than the microporous counterpart, due to a higher content of active species that can be installed into the former.[141] Similarly, Liu et al. constructed a hierarchically porous HKUST-1 (HP-HKUST-1) via citric acid modulator for the encapsulation of phosphomolybdic acid hydrate (HPMo).[180] As a result, HPMo/HP-HKUST-1 possessed higher activity toward methanolysis of styrene oxide than HPMo/HKUST-1, attributing to the higher uptake of active HPMo and larger pores that facilitate the diffusions of reactants to active sites inside MOF pores (Figure 25b). Later, Feng et al. reported HP-UiO-66 encapsulated ZrO_2 NPs via controlling the linker thermolysis in multivariate MOFs.[162] The resulting ZrO_2@HP-UiO-66 produced an excellent catalytic performance for Meerwein−Ponndorf−Verley (MPV) reaction, which could be ascribed to tiny ZrO_2 and more Lewis acidic sites exposed on the Zr−O clusters.

3.1.3. Heterogeneous Catalysis Based on Hollow HP-MOFs. Although the introduction of large pores (e.g., mesopores and macropores) into the common microporous MOF can solve the problem of mass transfer, in some special cases, it is difficult to meet the needs to encapsulate very large size and load high-content guests. Actually, the presence of additional mesopores sometimes affects the ordering or integrity of their original microporous structures, and thus destroys the size-selective behavior. On the other hand, downsizing the MOF particles can reduce mass transfer resistance by shortening the mass transfer path of reactants and products, without disturbing the integrity of the MOF interior structure. However, as the particle size of MOFs becomes smaller, their chemical stability often becomes worse due to the presence of large amounts of defective sites on their surface. The higher surface energy of tiny MOF particles also pushes them to agglomerate into a large particle.[356] Assembling nanolevel MOF particles into a dense shell to construct a hollow structure would be an intelligent solution to the problems faced by the above two strategies. The large cavity provides sufficient space to store more and even larger functional guest species like proteins. The shell composed of compacted and continuous MOF layer endows the size selectivity and substrate enrichment functions of intrinsic

https://doi.org/10.1021/acs.chemrev.1c00243
Chem. Rev. 2021, 121, 12278−12326

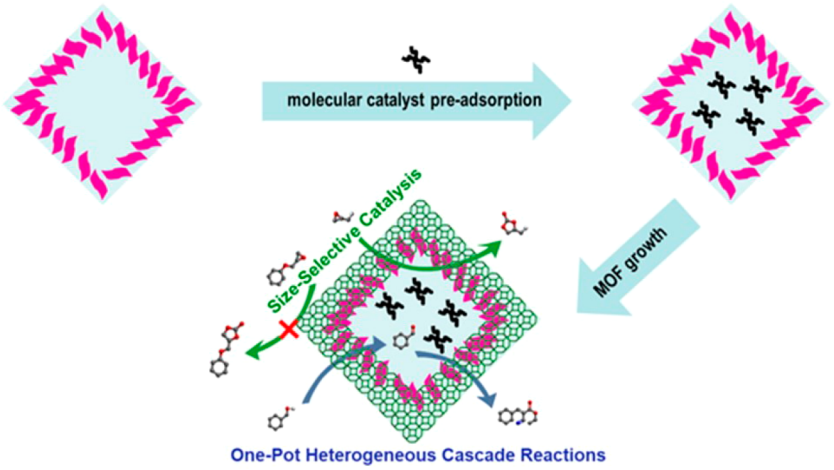

Figure 26. Encapsulation of molecular catalysts in hollow HP-MOFs for size-selective and one-pot heterogeneous cascade reactions. Reproduced with permission from ref 359. Copyright 2020 Oxford University Press.

MOF structures. Therefore, these HP-MOFs with hollow capsule and microporous shell have been employed as nanoreactors for heterogeneous reactions, as the yolk−shell catalysts provide a strategy to perform selective catalysis without changing the kinetics or generating a diffusional barrier.[194,356,357]

For the heterogeneous catalysis based on the pristine MOFs, the introduction of hollow caves can not only shorten the diffusion path and promote the exposure of their intrinsic active sites but also generate additional defective sites, which is highly desired for the Lewis-acid promoted reactions. For example, Zhang et al. used a hollow structured ZIF-8 nanosphere (hollow ZIF-8) as an efficient heterogeneous catalyst for [3 + 3] cycloaddition reactions of diones and α,β-unsaturated aldehydes to produce synthetically valuable pyranyl heterocycles.[202] The synergistic catalytic effects of acidic Zn(II) ions and basic imidazolate linkers, the flexible shell with the presence of surface mesopores, and hollow structure worked together to enable higher catalytic efficiency than homogeneous precursors and solid bulk and tiny ZIF-8 NPs. To further explore the synergistic effect of intrinsic pores of MOFs with additional hollow structures, Liu et al. fabricated multishelled hollow MIL-101(Cr) with single-crystalline shells.[214] The resultant multishelled hollow MIL-101 crystals showed significantly enhanced catalytic activity during styrene oxidation, in which active sites in each layer could be used more efficiently. In addition to hollow MOF nanospheres, Xu et al. reported a hierarchical Fe/Co-BTC nanotube.[231] These nanotubes showed an excellent catalytic performance for the detoxification of sulfur compounds with O_2, owing to the open hollow channels and the synergistic effect between the two metal centers.

Additionally, hollow HP-MOFs are ideal platforms for the encapsulation of active guests, in which the thin and dense MOF shells shorten the transfer path and exhibit the intrinsic functions of MOF (e.g., substrate enrichment, size-selective catalysis), while the presence of additional hollow microcapsule accommodates active guests. For example, Kuo et al. utilized yolk−shell Pd@ZIF-8 catalysts for hydrogenations of different sized alkenes (e.g., ethylene, cyclohexene, cyclooctene).[204] Due to molecular-size selectivity of ZIF-8 layers, only ethylene and cyclohexene can be coverted by encapsulated catalysts. Similarly, Yang et al. encapsulated Pd NPs into hollow ZIF-8 nanospheres through a facile emulsion-based interfacial reaction method.[216] The well-defined porous structure of ZIF-8 shells enabled the encapsulated Pd NPs size-selective hydrogenation behavior. Liu et al. installed presynthesized PtAu dual NPs into hollow HKUST-1.[205] The resulted yolk−shell PtAu@HKUST-1 were employed as catalysts for the liquid-phase hydrogenation of olefins. While the catalysis of *n*-hexene by PtAu@HKUST-1 showed high conversion, the larger molecular size of *cis*-stilbene than the opening of HKUST-1 made it difficult to diffuse through MOF shells and access interior catalytic sites. Zhang et al. demonstrated bimetallic MOF (Zn/Ni-MOF-2) nanosheet assembled hollow nanocubes (NAHNs) for the immobilization of Pd clusters.[211] The immobilized Pd clusters exhibited an enhanced catalytic activity toward alkoxycarbonylation reaction of aryl iodides, ascribed to the unique structure (hierarchical, hollow, and bimetallic nanostructures) and gas adsorption property of hierarchical Zn/Ni-MOF-2 NAHNs. Similarly, Yang et al. reported a Pd@bimetallic Zn/Co-ZIFs yolk−shell composite.[212] The enhanced gas storage and porous confinement effect, originating from the hollow capsule and the shell of Zn/Co-ZIFs shell, conferred this unique catalyst with superior selectivity and activity toward the semihydrogenation of acetylene. Wang et al. encapsulated surfactant-free Pd NPs into the ZIF-8 hollow nanospheres.[358] In the liquid-phase hydrogenation of olefins, the encapsulated surfactant-free Pd NPs gave much better performance than polyvinylpyrrolidone-protected Pd NPs. Wan et al. reported a hollow nanostructure featured double MOF shells with Pd NPs for size-selectivity toward the liquid-phase hydrogenation reaction, in which the hollow cavity facilitated mass transfer of chemical species and created a microenvironment as a nanoreactor. The inner HKUST-1 shell close to the void acted as porous matrix to disperse and immobilize metal NPs, and the outer ZIF-8 shell functioned as a protective layer to prohibit leaching of metal NPs and also as a molecular sieve coating to guarantee molecular-size selectivity.[203]

It is highly desirable to encapsulate soluble species into hollow MOFs to combine both merits of homogeneous catalyst and MOF hosts, although it poses even higher demand for the integrity of MOF shells than trapping heterogeneous species. Jiang and co-workers demonstrated a versatile strategy for the construction of yolk (soluble)−shell (crystalline)

https://doi.org/10.1021/acs.chemrev.1c00243
Chem. Rev. 2021, 121, 12278−12326

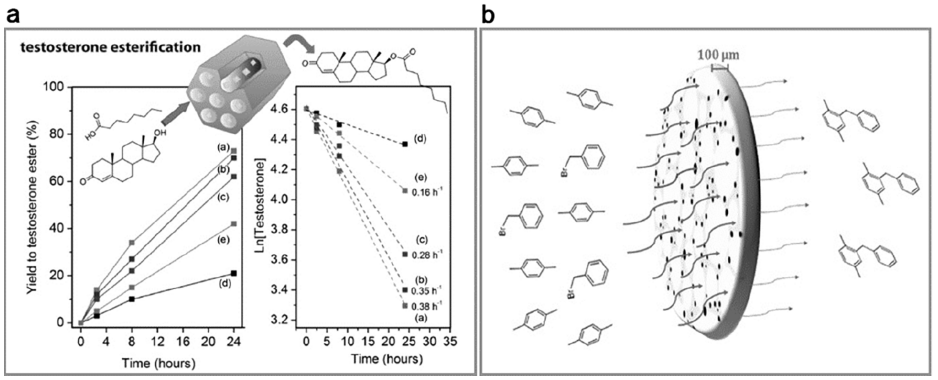

Figure 27. (a) Testosterone esterification with caprylic acid over UiO-66-NH_2/SiO_2 hybrid materials. Reproduced with permission from ref 243. Copyright 2017 John Wiley & Sons, Inc. (b) Batch- and flow-through Friedel−Crafts alkylation of *p*-xylene with benzyl bromide catalyzed by MOF−polymer-based hybrid membranes. Reproduced with permission from ref 247. Copyright 2015 John Wiley & Sons, Inc.

capsules (Figure 26).[359] The hollow LDHs with large opening were elaborately used to preadsorb metalloporphyrins into the hollow cavities. Subsequently MOF shells were grown on the LDH templates to close the opening. In this way, the soluble catalysts could be readily positioned and confined into the interior cavity of MOF-based capsules. Additionally, the synthetic approach allows to change the MOFs and active species, thereby making this method very powerful and extendable. As a result, the soluble active species incorporated in the MOF capsules not only realized the heterogenization of the molecular catalyst without the compromise of the strengths of individual components, but also endowed the homogeneous catalysts with additional functions, including substrate enrichment, multifunctional cascade and size-selective catalysis.

3.1.4. Heterogeneous Catalysis Based on MOF-Based HP-Composites. Despite different forms of HP-MOFs exhibit great performance toward diverse catalytic reactions in the laboratory scale, the related research reports are mostly focusing on the design and application of MOF-based catalyst powders, which are difficult to be directly used for industrial applications. The tedious molding process always brings about a lot of issues. For example, some active sites are buried, MOFs are easy to agglomerate or detach, mechanical stability is deteriorated, and mass transfer resistance is increased. In these cases, integrating MOFs with other stable and easy molding porous materials could be an effective strategy, in which mesoporous or macroporous bulk hosts serve as protective shells to improve the mechanical stability of encapsulated MOFs and enable processability/moldability. In addition, their large pore channels ensure the accessibility of interior active sites.[34,36,233−238,240,360]

For example, UiO-66-NH_2/SiO_2 hybrid materials, constructed by solid-state crystallization of UiO-66-NH_2 nanocrystals within mesoporous silica, exhibited enhanced catalytic activity compared to the bulk-MOFs for the synthesis of steroid derivatives (Figure 27a). The confinement effect of mesoporous silica made the active sites from tiny MOF NPs more accessible, and also gave rise to enhanced chemical and mechanical stability of MOF nanocrystals.[243] Additionally, macroporous melamine foam (MF) was employed as host materials to integrate MOFs (e.g., PCN-224), generating a series of MOF/MF composite materials with preserved MOF crystallinity, hierarchical porosity, and increased stability endowed by melamine foam.[250] The resulting MOF/MF composite materials exhibited excellent catalytic performance for the epoxidation of cholesteryl esters, thanks to the interpenetrative mesoporous and macroporous structures which ensured the MOF/melamine foam composite high dispersibility and accessibility of interior catalytic sites. Similarly, various MOFs including ZIF-8, UiO-66, MIL-101, and HKUST-1 were encapsulated into the macroporous polymer composites.[248] The resulted MOF composites exhibited excellent mechanical stability even after pressing or long-term mechanical stirring. As a catalyst for the Knoevenagel reaction, the macroporous matrix encapsulated ZIF-8 showed a high conversion rate compared with bulk ZIF-8 NPs and microparticles.

To further promote the applications of MOFs for batch-through reactions, a MOF−polymer-based hybrid membrane with fully opened hierarchical pores were constructed through embedding MIL-100(Fe) NPs into dicyclopentadiene based macroporous polymer scaffold (Figure 27b).[247] The facile accessibility of the catalytic sites from the MOFs as well as the robustness of the hybrid membranes were confirmed by a batch- and flow-through Friedel−Crafts alkylation of *p*-xylene with benzyl bromide. In the membranes, the catalytic activity of MOFs and the convective mass transfer of the microporous polymer matrix are synergized, which is highly desired for flow-through chemistry.

3.1.5. Heterogeneous Catalysis Based on MOF-Based HP-Derivatives. MOFs derived hierarchically porous carbon, metal-based compounds and their composites find broad prospects in various kinds of catalytic processes,[42,277,361,362] especially energy-related applications, including thermal catalysis,[288] photocatalysis,[363] and electrocatalysis.[364−368] Though the crystalline features can be destroyed more or less during the transformation, MOF-based HP-derivatives are equipped with better stability, hierarchical pores, conductivity, light-harvesting ability, etc.

During the pyrolysis processes, new phases such as metal and metal oxides are commonly generated among the MOF matrix, which bring about additional catalytic active sites. Metal and metal oxide performed well in accelerating various kinds of thermal catalytic reactions, such as oxidations, reductions, cross-couplings and acid−base catalyzed reactions.[288] The Li group synthesized a N-doped porous carbon embedded with Co NPs by pyrolyzing a nonporous Co-MOF. The obtained catalyst exhibited high performance in the oxidative amidation reactions of aromatic aldehydes. Control experiments proved that the synergy between Co NPs and the

https://doi.org/10.1021/acs.chemrev.1c00243
Chem. Rev. 2021, 121, 12278−12326

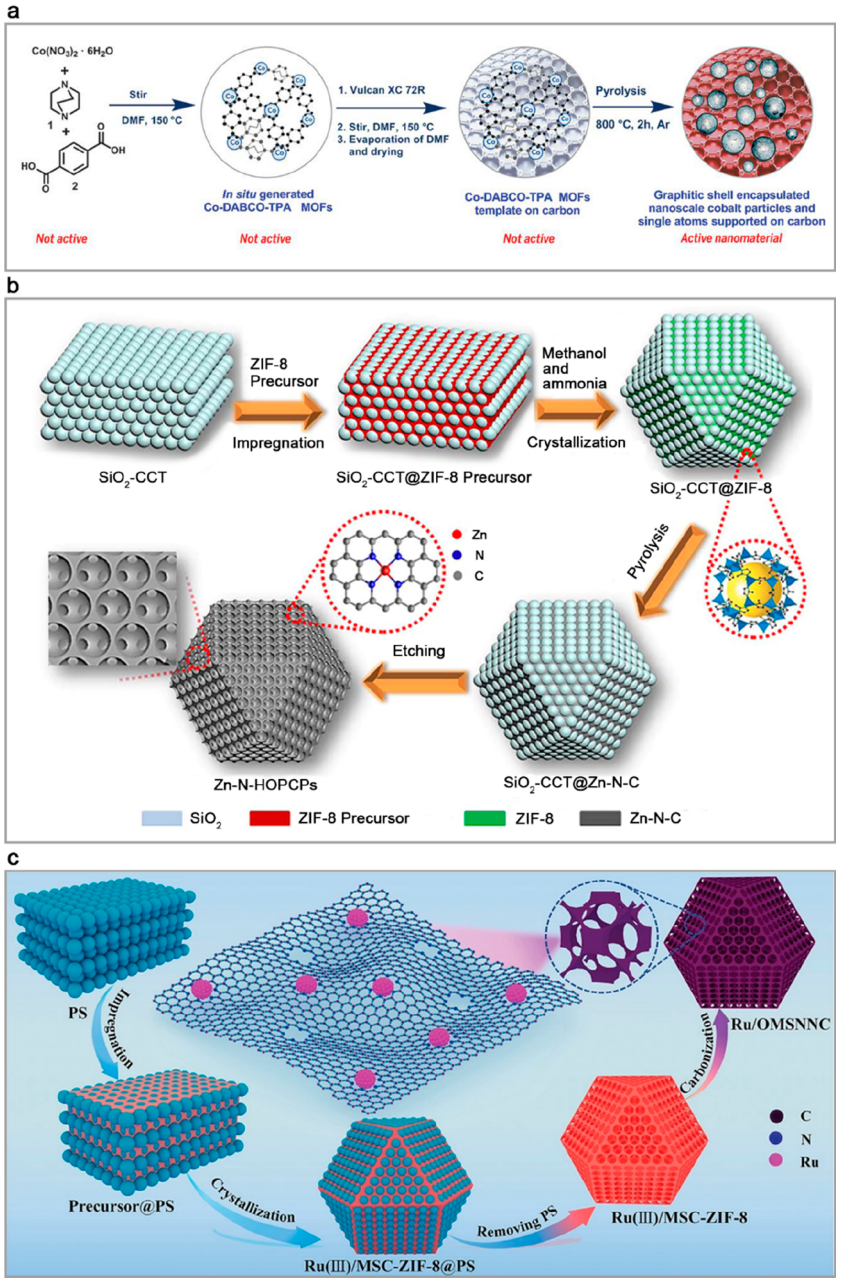

Figure 28. (a) Schematic showing the strategy to fabricate Co@C reductive amination catalyst by pyrolyzing a Co-MOF. Reproduced with permission from ref 370. Copyright 2017 American Association for the Advancement of Science. (b) Illustration for the synthesis of Zn−N-doped porous carbon with ZIF-8 as a precursor and SiO_2 crystal as a template. Adapted with permission from ref 372. Copyright 2020 Elsevier. (c) Illustration for the synthesis of porous N-doped carbon embedded with electrocatalytic active Ru nanoparticles. Reproduced with permission from ref 376. Copyright 2021 John Wiley & Sons, Inc.

carbonaceous substrate was responsible for the efficient catalysis. Moreover, the heat treatment improved the porosity of the original MOF, which might solve mass transfer issues.[369] Jagadeesh et al. pyrolyzed Co-DABCO-TPA MOF with Vulcan XC 72R to fabricate Co NPs encapsulated by graphitic shells. The Co@C composite catalyst demonstrated its universality in catalyzing the reductive amination of aldehydes (Figure 28a).[370] A hierarchically porous nickel oxide was synthesized by pyrolyzing a Ni-MOF with $ZnCl_2$ as a pore former by Gao et al. The porous oxide was further furnished with enzymes (e.g., horseradish peroxidase or cytochrome C) to give a bionanoreactor. The mesopores sufficiently confined the enzymes to improve their resistance to denaturation upon heating, while the micropores enriched substrate molecules for enhanced catalysis.[371]

The carbonaceous substrate and metallic components of MOF-based HP-derivatives both show better photo response than the pristine MOF. The porous carbon and metal nanoparticles display relatively broad light absorption spectrum, which are promising candidates for photothermal catalysis. Some semiconducting metal oxides, sulfides and phosphides with specific band gaps absorb incident light to generate excitons, which can be utilized for photoredox conversions. Jiang and co-workers demonstrated a hollow Zn single-atom/N-doped porous carbon by calcinating preformed hollow ZIF-8 NPs. Compared to bulk ZIF-8 derived porous

https://doi.org/10.1021/acs.chemrev.1c00243
Chem. Rev. 2021, 121, 12278−12326

carbon, this hollow material exhibited a superior performance in photothermal catalytic CO_2 cycloaddition with epoxides. The hollow structures utilized solar energy more efficiently by multiple reflections, which was beneficial for the endothermic CO_2 fixation reaction.[325] Similarly, Guo et al. pyrolyzed ordered SiO_2 crystal templated ZIF-8 into a Zn−N-doped porous carbon with spheric macropores for the same catalytic purpose. The presence of macropores made the inside active $Zn-N_4$ sites accessible, as well as improving the light harvesting ability of the carbon material (Figure 28b).[372] Xiao and Jiang synthesized hierarchically porous CdS by using MOFs as templates. According to photoluminescence spectroscopy and electrochemical measurements, the photoelectron−hole recombination in HP-CdS was more efficiently suppressed than bulk and nano CdS. The HP-CdS experienced a satisfactory photocatalytic hydrogen evolution reaction performance because of the accessibility of photogenerated excitons by aqueous protons.[373]

MOF-based HP-derivatives show great potential for energy-related electrochemical conversions, such as electrocatalytic hydrogen evolution reaction (HER), oxygen reduction reaction (ORR), CO_2 reduction reaction (CO_2RR), etc. Converting MOFs into hierarchically porous graphitic carbon will significantly enhance the conductivity, which is a prerequisite for electrocatalysis. By finely tuning the structure and component of MOFs, the derived porous carbon can be further doped with various kinds of elements. Jiang and co-workers pyrolyzed a mesoporous porphyrin MOF, PCN-222(Fe), into Fe single-atom/N-doped porous carbons. The catalysts exhibited high ORR performance in both acidic and alkaline solutions.[374] Li and co-workers chose 2D layered MOFs as precursors to fabricate MO_x (M = Co, Ni or Cu)/porous carbon nanosheet composite by pyrolysis. Taking Co_3O_4/C_{BTC} (derived from 2D Co-BTC) as an example, when tested with electrocatalytic oxygen evolution reaction (OER), it displayed both a low electrode overpotential and small Tafel slope compared to control catalysts. The porous arrayed structure of carbon brought about many mass transfer advantages, such as the more exposed active sites and faster release of gas bubbles. The short interlayer distance also prevented the metal oxide particles from agglomeration.[375] Very recently, the Xu and Zhu groups reported a macroporous N-doped carbon embedded with Ru nanoparticles. This catalyst displayed better HER catalytic activity than commercial Pt/C, which was attributed to the homogeneous distribution and sufficient exposure of Ru nanoparticles (Figure 28c).[376]

3.1.6. Relationship between Hierarchical Pores and Catalysis. Intrinsic HP-MOFs with periodic structures and ordered pores are suitable as ideal models to study the structure−activity relationship for catalysis, especially large-molecule-involved catalysis. However, their limited structural types cannot meet various needs. The introduction of defective mesopores into the common microporous MOF structures can further enrich the types of HP-MOFs. Such defective HP-MOFs possess well-defined micropores and additional amorphous mesopores. In addition to increasing the pore size of MOFs, the abundant defect sites on the surface of introduced mesopores not only further enrich the types/number of active sites of routine microporous MOFs, but also serve as trapping sites to stabilize the guest species and thus suppress their leaching. Therefore, defective HP-MOFs have unique advantages in encapsulating large-size guest species. However, the introduction of defective mesopores destroys the continuous microporous structure of the original MOFs, thereby influencing the size-selective catalytic function. Besides, the introduction of mesopores into MOF particles is still difficult to meet the requirements of a high loading and encapsulation of very large guest species. In these cases, hollow HP-MOFs with dense microporous MOF shells and large (even micron size) cavities can meet the above needs, while retaining the particular functions of the original microporous materials. Therefore, hollow HP-MOFs are ideal platforms as microreactors. Although the above HP-MOFs with different structural forms can meet diverse catalytic function demands, the poor mechanical stability and processability are unfavorable to their industrial applications. Combining the common MOFs with other meso-/macroporous host materials can integrate the advantages of porous materials in different pore size regimes, in which MOFs endow rich active sites and the latter ensures high mechanical properties and convective mass transfer. Therefore, the resulting MOF-based HP-composites present great potential toward reactions in batch- and flow-through mode. To take a step further, MOFs can be converted to hierarchically porous carbons and metal-based compounds. By rational control of synthetic conditions (e.g., pyrolysis temperature, pyrolysis time, cofeeding substrates), the obtained MOF derivatives with different catalytic functions and enhanced stability can be achieved. In these materials, hierarchically porous structures also play important roles in accumulating substrates and promoting electrical conductivity and light-harvesting ability.

3.2. Gas Storage and Separation

Hierarchical structures, a wide range of pore sizes and variations of the constructing units (metals and organic linkers) enable HP-MOFs an outstanding platform for the adsorption/separation of gas molecules.[377] Generally, gas storage ability is investigated based on the adsorption of pure gas. Actually, gas sorption and separation toward practical applications require MOFs to selectively adsorb specific gas from a gas mixture. Taking carbon capture as an example, the selective adsorption of carbon dioxide is particularly important for selective CO_2 capture from H_2, CH_4, and flue gas.[44,378−380]

For the intrinsic HP-MOFs, CUSs produce a polar microenvironment for the capture of CO_2 via a dipole−dipole interaction. This can be exemplified by MIL-100(V).[381] Their coordinatively unsaturated V sites strengthened the interaction between CO_2 molecules and MOFs, making the CO_2 sorption capacity larger than methane sorption capacity. As a result, they realized a CO_2 uptake four times higher than CH_4 uptake in MIL-100(V). Furthermore, the introduction of defective mesopores or hollow spaces in the common microporous MOF structures endow additional adsorption sites and allow access and diffusion of large molecules. For example, a metal−ligand-fragment coassembly strategy was studied to introduce functionalized mesopores in MOFs ((N)-PCN-125).[139] The lack of high connectivity between organic linkers and metal nodes in defective (N)-PCN-125 rendered additional favorable CO_2 adsorption sites. Considering the coexistence of additional defective sites on the metal clusters and uncoordinated carboxylate groups in the functionalized linker, the defective (N)-PCN-125 was better adsorbents for CO_2 capture than the structurally perfect PCN-125. To satisfy needs toward practical applications, MOFs have been extensively reported to fabricate hierarchically porous composites with other components for

https://doi.org/10.1021/acs.chemrev.1c00243
Chem. Rev. 2021, 121, 12278−12326

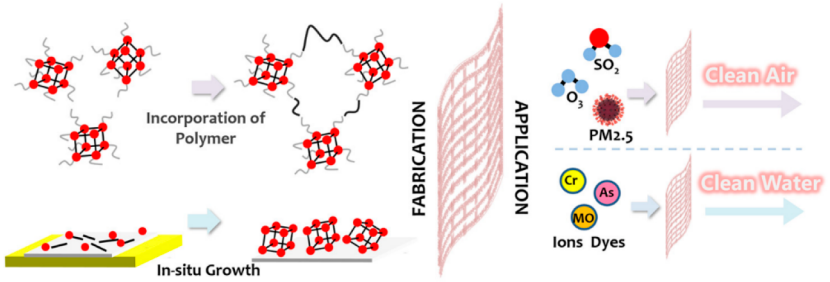

Figure 29. Schematic showing the air filtration by the MOF/chitin composite materials. Reproduced with permission from ref 238. Copyright 2019 American Chemical Society.

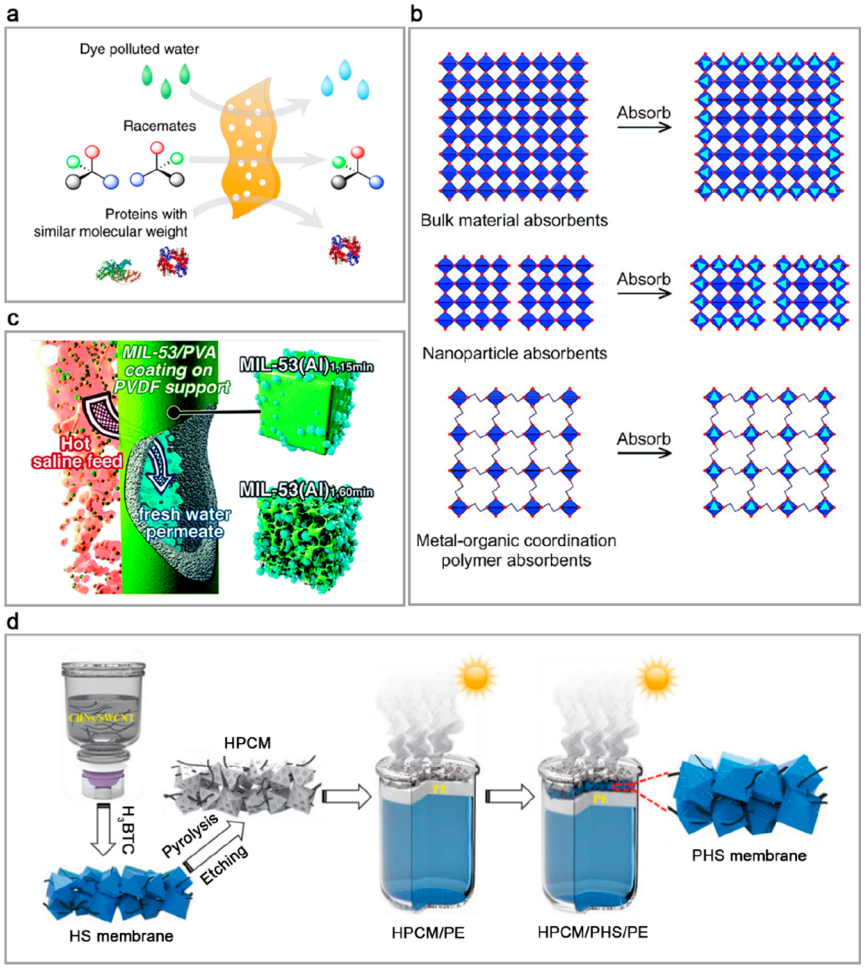

Figure 30. (a) Schematic showing MOF-based hierarchically porous membranes for dye, racemates, and protein separations. Reproduced with permission from ref 270. Copyright 2019 Nature Springer. (b) Schematic showing the origin of high adsorption capacity of porous MIL-100(Fe). Reproduced with permission from ref 390. Copyright 2012 American Chemical Society. (c) Schematic showing of the MOF-based nanocomposite pervaporation membrane for brine treatment. Reproduced with permission from ref 149. Copyright 2018 The Royal Society of Chemistry. (d) Illustration of the double-layered structure for water purification. Adapted with permission from ref 265. Copyright 2019 John Wiley & Sons, Inc.

various gas-phase adsorptions. For example, ZIF-8 as a functional component was composed with mesoporous graphene oxide (GO) to ensure a strong interaction of CO_2 with the adsorbent in micropores, while the presence of mesopores was important to facilitate the fast gas diffusion into densely packed adsorbents.[261] These are vital for practical applications like pressure-swing adsorption, which require relatively high pressure for CO_2 capture and storage.

3.3. Air Filtration

Air pollution (e.g., particulate matter (PM), bioaerosols, and toxic gases) has become one of the most severe threats toward the environment and human health. Purifying air through air purifiers or fresh air ventilators is a popular way to regulate indoor air quality and protect people from health hazards.[382] However, the commonly used fibrous filters in the above-mentioned air-purification equipment suffer significant disadvantages including high air resistance and limited inhibition ability against harmful microorganisms. Because of the large

https://doi.org/10.1021/acs.chemrev.1c00243
Chem. Rev. 2021, 121, 12278−12326

surface area and wide pore distribution, HP-MOFs hold great potential for the application of harmful gas capture.[383] On the other hand, MOFs are commonly fine powders. Since shaped materials are necessary for their practical applications, the poor processability of MOFs hinders the development of MOF-based filters. As noted above, the integration of MOFs with other porous materials is a very promising way to endow MOF-based HP-composites with considerable flexibility and processability (Figure 29).[238] For example, Wisser et al. used nontoxic, biodegradable, and low-weight chitin-based networks, obtained from a marine sponge, as a host material for MOF deposition inside their hollow channels, in which the MOF was effectively protected from mechanical stress and abrasion.[259] The high accessibility of encapsulated MOFs for gas adsorption was ensured by the macroporous host materials. As a result, the obtained hierarchically porous composites were promising as effective and robust adsorption material for both polluted gas and water.

SO_2 is one of the main gas pollutants that is harmful to both human health and the biological system. Zhang et al. fabricated nanofibrous MOF filters by compositing of MOFs with polyacrylonitrile (PAN) polymer for SO_2 capture.[266] The MOF-199/PAN filter and UiO-66-NH_2/PAN filter showed a much stronger adsorption effect to SO_2 compared with the pure PAN filter, ascribing to the abundant binding sites (e.g., open metal sites and amino groups) within MOFs. In addition, the hierarchical pores enabled a small pressure drop (not exceeding 20 Pa at a flow rate of 50 mL/min) in the MOF filter.

PM is also one of the main gas pollutants, especially in developing countries. HP-MOFs with abundant unsaturated metal sites and functional groups are potential sorbents for removing highly polar PM based on electrostatic interactions, while mesopores and even macropores ensure the high air permeability.[384] Wang and co-workers revealed the possibilities of MOF-based filters (MOFilters) for efficient PM removal.[266] Nanofibrous PAN was selected as the polymer matrix to integrate MOF-199, UiO-66-NH_2, Mg-MOF-74, or ZIF-8. In a real hazy weather condition, the above MOFilters exhibited superior PM removal efficiency compared with the PAN counterpart. The relatively positive zeta potential of MOFs enabled MOFilter to polarize the polar particulate matter, thereby exerting a strong electrostatic attraction. Later, the same group developed a roll-to-roll hot-pressing strategy for the mass production of MOF filters.[267] This strategy was successfully applied in different MOF systems (e.g., ZIF-8, ZIF-67, and Ni-ZIF-8) and on various substrates (e.g., plastic mesh, glass cloth, metal mesh, nonwoven fabric, and melamine foam). Five kinds of MOFilters show different structural advantages toward different working conditions, depending on the composition of MOFs and macroporous matrix substrates. For example, ZIF-8@Melamine foam achieved long-term durability with a high PM removal efficiency (>95.4% over 12 h). After simple washing and drying processes, it could be reused without significant performance loss. The ZIF-8@Glass cloth and ZIF-8@Metal mesh with high endurable temperatures were available for the PM filtration at 200 °C. The ZIF-8@Plastic mesh with a high light transmittance and good air permeability presented a quadruple increase in PM removal efficiency in contrast to the bare plastic mesh.

3.4. Sewage Treatment

Clean water resources are depleting rapidly due to contamination with various pollutants (e.g., aromatics, dyes, heavy metals, pesticides, crude oils, etc.). One of the most attractive methods to remove these pollutions from water is adsorption because it is a simple and low-cost process with mild operating conditions. HP-MOFs with high porosity and large pore sizes have been extensively studied for the field of sewage treatment, such as oil−water separation, drinking water purification, and the removal of various organic contaminants, dyes, hazardous metal species, pesticides, and microcystins (Figure 30a).[270,385−389]

3.4.1. Removal of Organic Contaminants. Organic compounds containing sulfur/nitrogen are naturally existing species in fossil fuels and oils (e.g., crude oil, gasoline, diesel, jet fuel, and heating oil). Considering catalyst poisoning and environmental pollution issues, it is necessary remove these harmful compounds from crude oils before commercial use.[385] Nuzhdin et al. used MIL-101(Cr) as a porous sorbent to remove various nitrogen-containing compounds (NCCs) from light cycle oil.[391] An excellent adsorption capacity of 19.6 mg N g^{-1} was reached, attributing to large mesoporous spaces and the strong Lewis acid−base interaction between the nitrogen of NCCs and open Cr^{3+} sites in MIL-101(Cr). Similarly, Qi et al. utilized hierarchically porous Cu-MOFs to selectively capture aromatic sulfides. Due to the introduction of Cu(I) and hierarchical porosity, the saturated adsorption capacity reached 0.406 mmol g^{-1}, which was 6-fold higher than that of the original Cu-MOFs (0.069 mmol g^{-1}).[185]

3.4.2. Removal of Heavy Metals. Some metals, such as lead (Pb), arsenic (As), copper (Cu), mercury (Hg), antimony (Sb), chromium (Cr), manganese (Mn), cadmium (Cd), etc., are toxic to ecological systems and human beings. The recovery of these harmful metal ions from the environment has been a global concern over the last few decades. Zhu et al. reported the removal of arsenic (As^{5+}) from aqueous solutions over MIL-100(Fe) (Figure 30b).[390] According to that report, the adsorption capacity of As^{5+} with MIL-100(Fe) was around 6 and 36 times higher than that of iron oxide NPs and commercial iron oxide powders, respectively. Combined IR, XPS, and TEM element mapping experiments demonstrated that the porous MOF structure made the interior adsorption sites available. Wu et al. reported hierarchical ZIF-8 absorbent containing interconnected micropores and mesopores.[104] Attributing to the hierarchically porous structure, an excellent arsenate adsorption performance was produced compared to commercial porous materials (e.g., active carbon and zeolite).

In spite of the above advantages, the flexibility and processability of crystalline MOF powders should be improved for future industrial applications. To avoid the aggregation of MOF NPs and remedy the poor compatibility between MOFs and polymers during their combination, Zhang et al. developed a photoinduced postsynthetic polymerization (PSP) strategy for the covalent cross-link of MOF nanocrystals with flexible polymer chains.[256] The resulting free-standing MOF-based membranes with crack-free and elastic structures were able to effectively remove toxic Cr(VI) ions in water, which were superior to the corresponding MOF/polymer blend membrane. The MOF−polymer composite tubular structures were investigated by Chen et al., in which the hollow tube enabled a low pressure drop.[384] Typically, ZIF-8/sodium alginate hollow tubes were effective for removing AsO_4^{3-} ions from *N*,*N*-dimethylformamide (DMF). Furthermore, a multilayer coaxial

https://doi.org/10.1021/acs.chemrev.1c00243
Chem. Rev. 2021, 121, 12278−12326

hollow tube with double-layer MOFs (ZIF-8 and MIL-101-NH_2) was able to trap mixed inorganic−organic pollutions (e.g., AsO_4^{3-} and methyl orange dyes) in DMF solution at the same time.

3.4.3. Drinking Water Purification. Agricultural pesticides and herbicides are frequently detected in groundwater. It has been reported that phenoxy acids (one component of pesticides) could cause liver tumors. As such, the permitted concentrations of pesticides in drinking water and groundwater should not exceed 0.1 μg/L for a single compound or 0.5 μg/L for the sum of all pesticides based on the European standard.[392] Methylchlorophenoxypropionic acid (MCPP), one type of phenoxy acids, has been widely used as a herbicide in spite of its high toxicity. MCPP has been frequently detected in groundwater with the concentrations usually exceeding the limitation in groundwater abstraction wells. Fu et al. used hierarchically porous chitosan/UiO-66 composite as the adsorbent of MCPP, which possessed good mechanical stability to offer ideal adsorption capacity while retaining the advantage of easy recycling.[251] In addition, microcystins (MCs), produced by cyanobacteria in water, have caused severe environmental problems throughout the world. The conventional treatment by chemical methods such as chlorination or potassium permanganate oxidation unavoidably produces unfavorable byproducts. Xia et al. facilely synthesized two HP-MIL-100-based gels for the high-efficiency removal of MC-LR, the most toxic member of the MC family.[151] The resultant MIL-100(Al) xerogel and aerogel can remove over 96.3 wt % of the MC-LR in water, and their adsorption capacities were as high as 6861 and 9007 μg/g at an initial MC-LR concentration of 10000 ppb, respectively. Unprecedentedly, the lowest residual MC-LR concentration reached 0.093 μg/L, which was much lower than the standard concentration for drinking water of 1 μg/L, proposed by the World Health Organization.

The treatment of highly concentrated brine is technically challenging and energy demanding, as conventional pressure-driven filtration membrane is not a viable option, for which the high osmotic pressure must be overcome. The concentrated brine can also lead to rapid scaling and pore-blocking for the membrane distillation process. Alternatively, membrane pervaporation is a promising technique. The dense pervaporation membranes can effectively mitigate the scaling problem, but they still suffer from low desalination productivity and poor operational stability with brine feeds. Liang et al. reported a hierarchically porous pervaporation membrane through incorporating defective MOFs into poly(vinyl alcohol) membranes, which can effectively promote the fresh water productivity in concentrated brine treatment, with the salt rejection of >99.999% (Figure 30c).[149] In addition, among diverse strategies to alleviate the freshwater shortage, solar vapor generation is considered to be a sustainable and ecofriendly technology with no consumption of fossil fuels and no pollution. Ma et al. developed a special double-layer structure, which contained a MOF-derived hierarchically porous carbon membrane (HPCM) for solar absorption and a polystyrenesulfonate@HKUST-1/single-walled carbon nanotube membrane (PHS) for water supply and salt blocking (Figure 30d).[265] The converted heat was utilized efficiently in situ to drive the evaporation of water-trapped HPCM. The PHS membrane with polystyrenesulfonate-modified channels successfully prevented the deposition of salt. Because of the synergistic combination of the HPCM and PHS membranes, the device exhibited a remarkably high water evaporation rate of 1.38 kg m^{-2} h^{-1} and solar-vapor generation efficiency of 90.8% under 1 sun.

3.4.4. Oil−Water Separation. Oil spills in oceans and rivers are seriously dangerous to marine species and human beings, leading to a long-term threat to public health and the environment. The separation of oil from water without causing environmental pollution is a challenging task.[393−397] Nature-inspired superhydrophobic materials (lotus leaf, butterfly wings) have gained much importance for applications in oil-spill cleaning. Recently, many hydrophobic MOFs based on long-chain alkyl substituent groups or fluorine-containing linkers have been reported. Jiang et al. synthesized a highly stable porous MOF (USTC-6) with a corrugated $-CF_3$ surface that featured high hydrophobicity.[249] The uniform growth of USTC-6 throughout a graphene oxide (GO)-modified sponge was achieved and yielded a macroscopic USTC-6@GO@ sponge sorbent with hierarchical pores, which repelled water and exhibited a superior adsorption capacity for diverse oils and organic solvents. Similarly, the Fischer and Zboril groups reported a sponge@highly fluorinated graphene oxide@ZIF-8 composites for oil−water separation.[262] The synergistic properties of the surface modification of C−F groups, the alkyl-substituted imidazole groups, nanoscale roughness, and micromesoporous nanoarchitecture yielded an excellent capability for the selective absorption of polar and nonpolar organic solvents from water. Later, the Fischer group reported fibrous hierarchically porous hybrid FGO@MOGs composed of MOF Gels (MOGs) with fluorinated graphene oxide (FGO), which displayed quick oil-uptake, chemical inertness, good reusability, and strong adsorption capacity for various organic solvents and oils.[263] Jing et al. used hydrophobic HP-ZIF-8/polystyrene composites for enhanced oil adsorption performance while maintaining very low water uptake.[121]

3.4.5. Hierarchical Pore-Sewage Treatment Relationship. MOFs are superior to other porous sorbents in adsorptive removal of various toxic components because of their high surface area, various pore geometries, facile functionalization, and tunable porosities. Intrinsic HP-MOFs with well-defined structures and high surface area are suitable for the selective capture of various hazardous species in water. The variety of metal centers and organic linkers in the framework provides great opportunities toward the adsorption of various hazardous compounds in wastewater. The open metal sites in intrinsic HP-MOFs play a dominant role in binding various polarizable toxic compounds. Moreover, the acid/base properties of HP-MOFs are also utilized to coordinate hazardous contaminants with opposite base/acid properties.

For efficient adsorptive removal of various toxic components, specific adsorption sites, high porosity, and suitable pore geometry are required. Although some intrinsic HP-MOFs has been recognized as excellent promise sorbents and ideal porous models for the study of structures and gas sorption interactions, the limited number of intrinsic HP-MOFs is hard to satisfy various demand for practical applications. Defective HP-MOFs with additional defective sites, adjustable pore structure, and large amounts of structure types can further expand the application of HP-MOFs toward sewage treatment. In addition to adsorptive removal of hazardous species from wastewater, purifying the sewage by pervaporation membranes or solar vapor generation is an emerging alternative to regenerate freshwater.

https://doi.org/10.1021/acs.chemrev.1c00243
Chem. Rev. 2021, 121, 12278−12326

Although HP-MOFs have high porosity and abundant functional sites for the capture or separation of contaminants, they are hard to effectively utilize the clean and inexhaustible solar energy. MOF-based HP-composites constructed by integrating MOF with materials like carbon nanotubes with full solar spectrum absorption and excellent thermal transfer properties can solve the above issues. In addition, MOF-based HP-composites constructed by the combination of MOFs with macroporous bulk materials present the strengths for the batch- and flow-through sewage treatment, which would be highly important for practical applications.

3.5. Sensing

Because of their well-defined porous structures, MOFs have been utilized as powerful protective layers to enhance the response sensitivity of traditional chemical sensors.[9,398−402] It can be expected that the introduction of hierarchically porous structures in conventional MOF-based sensors will further enrich the functions of final materials. This can be exemplified by metal oxide arrays/MOF composite chemiresistors, in which metal oxides have been developed for many industrial and domestic applications of volatile organic compound (VOC) detection due to their low cost, portability, real-time operability, and ease of use. However, the selectivity is still a major challenge for commercial metal oxide gas sensor devices. For example, water vapor is a typical interference of metal oxide gas sensors for VOC detecting, which commonly exists in the air with high concentration (40−70 RH%, ∼11440−20019 ppm). To solve these issues, Yao et al. proposed a new material design strategy to improve the performance of chemiresistor gas sensor by combining the high sensitivity of nanostructured metal oxides with the high selectivity and catalytic activity of MOFs into a single material (Figure 31).[272]

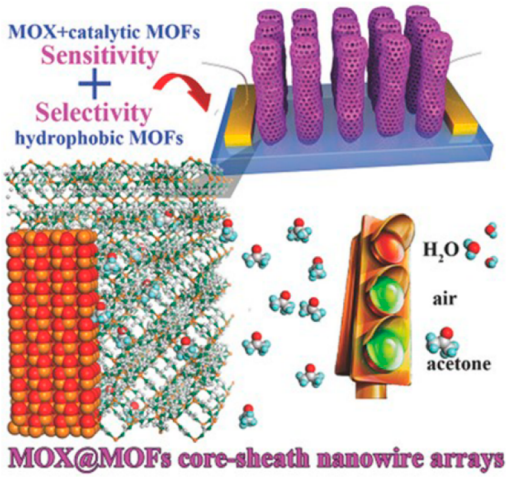

Figure 31. Schematic showing metal oxide@MOF hierarchically porous arrays as chemiresistor of acetone. Reproduced with permission from ref 272. Copyright 2016 John Wiley & Sons, Inc.

In such a core−shell nanostructured material, the hydrophobic porous layer of ZIFs was used to selectively usher desired target species and reject water vapor from passing through to reach metal oxide surface. In this way, the selectivity of the metal oxide gas sensor was greatly improved.

Additionally, the hierarchically porous structures and tunability make it possible to control the interaction between HP-MOFs and the involved guests. Generally, the encapsulated guest molecule often results in the change of luminescence for the HP-MOF hosts or guest molecules. Liu et al. utilized multishell hollow MOF microcrystals as an ideal system to host multiple guests with controlled communication (e.g., energy transfer) between them.[213] A core−shell ZIF-67@ZIF-8 with rhodamine 6G (R6G) fixed in the pores of ZIF-67 emitted a different fluorescence profile from the native R6G, ascribing to the energy transfer from R6G to ZIF-67 in the former. In contrast, the R6G presented its original profile with enhanced intensity after ZIF-67 was dissociated to form a hollow ZIF-8 encapsulated R6G. Because the free R6G molecules were located in the cavities, no obvious energy transfer was detected. Therefore, for the hollow MOF encapsulated guest species, the freedom of active molecules was maximized, while the energy transfer between MOF and the guest molecules was minimized. In this case, hollow structures represented a good solution to trap photoactive species without disturbing their light response abilities.

On the basis of the above structural strengths, HP-MOFs exhibit great potentials in various sensing applications (e.g., pH sensor, determination of pesticide residues, clinical diagnosis of diabetes, and photothermal therapy). For example, Deibert et al. developed a reversible colorimetric fluorescence pH sensor based on highly stable PCN-222.[403] Upon exposure to an aqueous solution with pH 0, the purple PCN-222 turned green, and this colorimetric response was reversible and reproducible. In addition to the application based on the fluorescence effect of HP-MOFs, their catalytic effects ensure an enhanced sensitivity toward the detection of pesticides. Taking glyphosate (one of the most commonly used herbicides) as an example, it is a nonelectroactive pesticide and thus is difficult to be detected with traditional electrochemical methods. By using hierarchically porous Cu-BTC MOF as an electrochemical sensor, the large specific surface area of the material can increase the electrode reaction site and further improve the detection performance of glyphosate in soybean. The coordination between glyphosate and Cu^{2+} centers would generate a sudden change in responsive current.[404] Additionally, HP-MOFs exhibit great advantages in clinical diagnosis. For example, the fast and real-time monitoring of the glucose content in blood is essential for the clinical diagnosis and therapy of diabetes, a common chronic disease in daily life that has become a serious and increasing global health burden. Wang et al. demonstrated a high-performance nonenzymatic glucose sensor by compositing hierarchical flower-like nickel(II)-based MOF with carbon nanotubes, based on the electrochemical activity of HP-MOFs, in which the Ni(II) centers serve as the active sites for the adsorption and oxidation of glucoses while the hierarchical pores ensure facile diffusion of electrolytes and high exposure of active sites in MOFs.[264] Besides clinical diagnosis, HP-MOFs pose great potentials for clinical therapy. Hu et al. constructed a hollow MOF via synergistic etching and surface functionalization with phenolic acid.[225] The modified MOFs were simultaneously coated by metal−phenolic films, which endowed the MOFs responsive to near-infrared irradiation to produce heat for potential photothermal therapy applications. Particularly, the hollow spaces of hollow MOFs provide large volume of spaces to load desirable drugs and the near-infrared irradiation effect of the shells was used to control the release of drugs at selected locations in the organisms.

https://doi.org/10.1021/acs.chemrev.1c00243
Chem. Rev. 2021, 121, 12278−12326

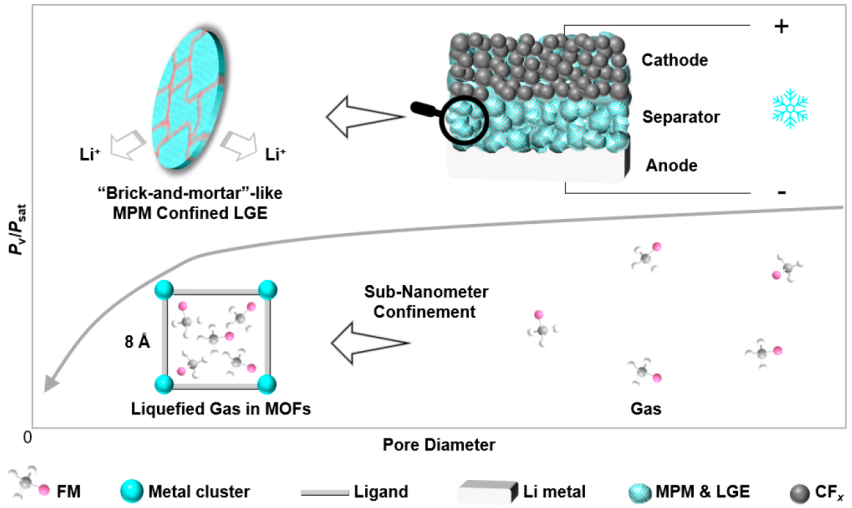

Figure 32. Schematic showing the mechanism of nanoconfinement effects for lowering the equilibrium pressure of liquefied gas and the implementation of MPM-based LGE for Li-battery cells. Reproduced with permission from ref 417. Copyright 2021 Springer Nature.

3.6. Energy Storage

To realize the sustainable development of our society, various clean and renewable energy sources are attracting more attention and developing rapidly in the past few decades. The energy storage devices, such as supercapacitors (SCs) and batteries, play indispensable roles in fabricating sustainable energy conversion and storage systems.[405] MOFs have been demonstrated to be useful for electrochemical energy storage and are considered as one of the most promising electrode material candidates for SCs and batteries because of their remarkable surface area, controllable pore structures and compositions with potential pseudocapacitive redox centers. Recently, HP-MOFs with mesopores or macropores reveal outstanding electrochemical properties, attributing to the synergetic effects of hierarchical pores.[45,405−411] For example, Du et al. demonstrated that the hierarchically porous structure constructed with Ni-MOF nanosheets can supply more active sites for electrochemical reactions to realize the excellent SC performance.[137] As a result, the hierarchically porous Ni-MOF revealed an outstanding specific capacitance of 1057 F/g at a current density of 1 A/g. Meng and co-workers utilized MIL-101 (Fe) with high mesoporosity as the cathodes of lithium-ion batteries (LIBs), which delivered a capacity of 110 mAh g^{-1} by integrating 0.62 Li^+ ions per Fe^{3+} (Li/Fe).[412] On the contrary, microporous MIL-53 (Fe) only reached a capacity to 70 mAh g^{-1}.[413] To further increase the reversible capacity of Li−S batteries, additional redox-active species (anthraquinones) were integrated with the hosts of NU-1000, ascribed to the presence of large pore spaces and abundant open sites on metal nodes of MOFs. Such modified MOFs encapsulated sulfur cathodes provided a superior long-term cycling performance and high capacity compared with those with pristine MOF systems. Similarly, Xu et al. used bimetallic hierarchical Fe/Co-BTC nanotubes as anode materials for LIBs.[231] The hierarchical tubular architecture ensured high porosity, which was beneficial for mass transport, increased the active sites, and provided shorter Li^+-ion diffusion channels, thereby making this architecture a promising candidate for LIBs anode.

However, the random orientations and low conductivity nature of MOFs lead to severely degraded performance. Designing a facile strategy for the oriented growth of MOFs on selected conductive substrates is of significant importance for MOF applications in energy storage. For instance, Deng et al. grew oriented MOFs on carbon fiber paper (CFP). As a consequence, the $Co(OH)_2$ derived oriented MOFs (CoNi-MOF) on CFP delivered an enhanced performance as a hybrid supercapacitor electrode compared to Ni-MOF in the powder form.[273] In addition, densification of MOF-based HP-composites without sacrificing the porosity is important for high volumetric capacity. Taking lithium−sulfur (Li−S) battery electrodes as the example, densification of porous 3D structures to remove most of the large macropores, while keeping the necessary (meso- and microporous) porosity for hosting sulfur and polysulfides, seems to be a promising way to increase the Li−S electrode density. Cao et al. prepared densely packed MOFs and carbon nanotube (CNT) hybrid materials with tailored hierarchically porous structures.[258] The optimized bulk density and porosity by controlling the MOF content lead to simultaneously high areal and volumetric capacities, both of which are critical factors for developing high energy density and compact energy storage devices.

Apart from electrode materials, MOF-based hierarchically porous materials have been excellent candidates as functional battery separators. In particular, some electrode materials and/or their charge/discharge intermediates, such as organic electrodes and polysulfides, are soluble in electrolytes. In this case, the incorporation of ionic sieve function of MOFs to conventional separators proves a direct solution to avoid the leaching of active materials and possible undesirable side-reactions.[414] For instance, a hierarchically porous membrane was fabricated by in situ growth of polystyrenesulfonate threaded HKUST-1 membranes on macroporous Celgard membranes.[415] Integrating the strengths of the high Li^+ ionic conductivity of polystyrenesulfonate, microporous MOF layers, and flexible mechanical property of commercial membrane, the resulting composite membranes successfully blocked polysulfides without noticeable trade-off redox kinetics. Similarly, other MOFs (e.g., UiO-66-SO_3Li, UiO-66-SO_3H) were also subsequently utilized for the construction of functional separators with hierarchically porous structures. Therefore, MOF-based hierarchically porous materials with versatile structural characteristics have presented great promise for various battery materials.[416]

https://doi.org/10.1021/acs.chemrev.1c00243
Chem. Rev. 2021, 121, 12278−12326

In addition to the above functional applications based on size-selective effects, the nanoconfinement effects have also been successfully utilized in the field of battery chemistries. Generally, some dramatic changes of their physical and chemical properties can be expected upon confining molecules in the nanoscale environment, thereby enriching the possibilities for new applications. For example, liquefied gas electrolytes (LGEs) have shown great promise for electrochemical systems operating at extremely cold conditions (especially below −30 °C) because of their unique physicochemical properties (e.g., extremely low melting points, facile ion transport).[418] Unfortunately, a high pressure is needed to condense the gas into liquid state, which unambiguously renders potential safety concerns for practical applications. A large volume of experimental and simulation results demonstrate that the actual pressure required to condense gas molecules (e.g., N_2, CO_2) in porous carbon (slit-shaped pores) reduces by >10 times as the pore diameter decreases from 7 to 1 nm.[419] To apply the nanoconfinement effect (capillary condensation) in the battery chemistries for shifting the critical properties of gas-based electrolytes, Cai et al. developed a novel "brick-and-mortar"-like strategy to construct mechanically flexible MOF−polymer membranes (MPMs) by using the microporous MOFs as the porous "brick" and polymer binder as the mechanically flexible "motor" (Figure 32).[417] However, conventional MOF-based membranes are not suitable for desired ion migration in LGE under reduced pressure, due to the presence of numerous gaps between the binders and MOF particles which inevitably degrade the continuous liquefied gas flux required for Li^+ migration throughout the entire membrane. To produce a dense and continuous microporous network throughout the nanoscale MOFs assembled macroscopic membranes, the MOFs was elaborately in situ grown on a 2D GO nanosheet, in which a large cross-sectional area of MOF nanosheet enlarge the contact of MOF assembled units. By using the MPMs as the battery separators that can uptake a large volume of gaseous electrolyte, lithium batteries can operate with high capacity at extremely low temperatures (−40 °C) and reduced working pressure, which is not possible for the state-of-the-art porous separators.

4. COMPARISON OF HP-MOFS WITH OTHER POROUS MATERIALS

In the past three decades, porous materials have attracted great attention in many fields. Classical porous materials (e.g., zeolites, porous polymer, mesoporous silica and carbons, macroporous foams, etc.) have been explored widely due to their low cost and superior stability. However, they suffer from some problems, ascribing to the nonuniform structure, irregular pores, and lack of clear structure−property relationships. The crystalline nature, structural diversity, organic−inorganic hybridization, and ultrahigh porosity endow HP-MOFs unique advantages compared to the traditional crystalline porous materials (e.g., inorganic zeolites) and amorphous porous materials (e.g., porous organic polymers, mesoporous silica, porous carbons).

One particular advantage of HP-MOFs in comparison to inorganic porous materials like porous zeolites, silica and carbons is the designability (reticular feature) and structural tunability. As the structures of MOFs are determined by the geometry of SBUs as well as the shape and size of the organic ligands, MOFs possesses excellent potential in structural predesign and molecular-level tunability in their structures. In addition to their diverse structures and compositions, intrinsic HP-MOFs possess uniform pore sizes/environments and very high surface areas in contrast to traditional amorphous materials, such as carbons, porous organic polymers and mesoporous SiO_2. Each atom in MOF structures is precisely positioned and most of them are tailorable. The pore sizes of HP-MOFs are continuously tunable and thus bridge the gap between typically microporous zeolite, mesoporous silica, and even macroporous foam materials. This pore structure design is important for the functional properties of HP-MOFs, in which the small pores in HP-MOFs improve host−guest interactions, while the mesopore ensures the accessibility of active sites, fast mass diffusion and space to store guest species. Lastly, the well-defined and tailorable crystalline structures of MOFs make them an ideal platform for the establishment of clear structure−property relationships, which is of great significance for phenomenological understanding and thus providing guidance for the design of new functional materials. In a word, HP-MOFs have shown their great potential to integrate various structural merits of different porous materials into a single material, such as the tunability of organic materials like porous polymer, the well-defined structure of crystalline materials like zeolites, wide pore distribution to cover different regime from micropore (zeolites, activated carbons) to mesopore (silica, carbons) and to macropore (3D foam materials).

5. CONCLUSION AND PERSPECTIVE

We have summarized the main synthetic strategies and recent functional applications of HP-MOFs, MOF-based HP-composites and MOF-based HP-derivatives. The topic of MOF-based hierarchically porous materials has undergone explosive growth, especially in the past two decades, and the situation is still continuing. In the early state, the intrinsic HP-MOFs were developed to extend the micropores of MOFs to mesopore regime by reasonable choice of longer ligands, larger metal clusters, rational design of topological structures, etc. However, the mesopores in this kind of HP-MOFs are generally accessed through much smaller apertures, limiting the size of molecules that can diffuse into the functional mesopores. In addition, the construction of mesopores by elongated linkers easily leads to framework interpenetration, and the resulting mesoporous structures are prone to collapse after removing the templates or guest solvent molecules. As an alternative solution, defective HP-MOFs were fabricated by introducing additional meso/macropores into conventional microporous MOFs. Related technologies can be divided into two subgroups: the in situ synthetic and postsynthetic strategies. The in situ synthetic strategies include soft/hard template methods, template-free methods, modulator-induced defect formationstrategy, sol−gel strategy, 3D print, etc. The postsynthetic strategies are comprised of chemical etching strategy, thermal decomposition strategy, stepwise ligand exchange strategy, phase transformation strategy, etc. Unfortunately, the presence of large volumes of defective mesopores undefinedly destroy the perfect microporous structure to some extent. In these cases, the introduction of a huge hollow cave in a MOF crystal to form a hollow HP-MOF with a well-defined microporous shell presents unique structural strength for the selective release and storage of huge size and large volumes of species. Not limited to the formation of large pores in pristine MOFs, hierarchically porous materials can also be generated by

https://doi.org/10.1021/acs.chemrev.1c00243
Chem. Rev. 2021, 121, 12278−12326

the integration of MOFs with additional meso-/macroporous materials, including mesoporous silica, macroporous polymers, 1D nanotubes, 2D meshy, and 3D foam materials. Lastly, the partial destruction of MOFs to form quasi-MOFs and complete convention of MOFs into corresponding porous carbons, metal-based compounds and their composites can also be powerful strategies for the construction of hierarchically porous materials while only partially inheriting the structural features of pristine MOF materials.

While early targets of HP-MOFs (generally called as mesoporous MOFs) were focused on the extension of the pore diameters of MOFs, recently, more and more new hierarchically porous materials have been developed based on various MOF-based materials (pristine MOFs, MOF composites, and MOF derivatives). On the basis of their specific strengths of hierarchical pores and selected MOFs, their applications have been extended to wider fields, such as catalysis, gas storage and separation, air filtration, sewage treatment, sensing, and energy storage. Owing to well-defined porous structures, the intrinsic HP-MOFs have been widely applied in heterogeneous catalysis, sensing, adsorption, and separation research fields, which not only deliver a superior performance but also pace the way to study the underlying structure−performance interaction, thereby giving guides for the construction of new and excellent materials toward future applications, especially for large-species-involved applications. The defective HP-MOFs exhibit great potential as excellent supports, adsorbents (e.g., removal of toxic gas, sewage treatment) and Lewis acid catalysts for large-species-involved process, in which abundant defective sites around the introduced large pore spaces pose strong interactions between MOFs and guests or reactants, which is of importance for targeted uses. Hollow HP-MOFs with the presence of a huge cavity has the ability to contain large-size guests (even micron size), such as proteins and enzymes. In addition, considering dense microporous MOF shell endow a size-selective penetration function, hollow HP-MOFs create the microenvironment as various nanoreactors. To further widen the application scenarios, MOF-based HP-composites integrating MOFs with other materials' strengths, for example, flexible mechanical properties and easy processability, which are highly desired for practical applications like batch/flow reactors, continuous membrane separation and battery separators. Lastly, the MOF-based HP-derivatives not only partially inherit the structural features of pristine MOF materials but also possess some enhanced properties (e.g., stability and conductivity), which are highly beneficial for photocatalysis, electrochemical catalysis, batteries, etc. Therefore, the organic−inorganic hybrid, crystalline, and porous nature of pristine MOFs, as well as hierarchically porous structures, make MOF-based hierarchically porous materials superior to other porous materials in various fundamental research, such as zeolites, activated carbon, mesoporous silica and carbon, porous polymer, and macroporous foam materials.

Although tremendous advances have been achieved and great potential have been indicated in recent years, MOF-based hierarchically porous materials are still in their infancy, and great challenges still remain: (i) The stability (mainly water, chemical, thermal stability) of MOFs is still not satisfactory. The chemical and thermal stability usually become worse upon the extension of pore sizes. (ii) In spite of the crystalline nature of original MOFs, the structures of additional pores (mesopore, macropore or hollow cavity) are amorphous and defective. This poses challenge to the precise analysis of the spatial pore structure of HP-MOFs. (iii) The pore size distribution of HP-MOFs (to the exclusion of intrinsic HP-MOFs) is uneven. Although many HP-MOFs exhibit a narrow distribution trend in some specific pore ranges, they actually present random size distribution. (iv) The introduction of additional pores into the parent MOF matrix suffers from trade-off effect between the intrinsic structural merits of original MOFs and additional pore structures. Typically, the presence of defective mesopores destroys of the perfect structure of pristine MOFs and, thus, influences the size-sieving function of well-defined micropores. (v) The conductivity of HP-MOFs requires improvement to promote charge transfer toward enhanced photocatalysis, electrocatalysis, and battery chemistry. (vi) While limited reports on the adjustment of mechanical properties, particle sizes and morphology of HP-MOFs, they are of great importance for molding process toward practical applications. (vii) The cost of HP-MOFs is currently not very low because of the complex experiment procedures and their needs toward special reagents/templates (e.g., hard/soft template, modulator, defective ligand, huge clusters, or linkers) depending on the synthetic strategy and compositions. (viii) The strategies for the construction of MOF-based hierarchically porous materials are limited to laboratory-level at this stage, and their large-scale fabrication is rarely reported.

In summary, there are still quite a lot of challenges before realizing their practical applications. We are still on the road to go for low-cost and large-scale application of MOF-based hierarchically porous materials, beyond the proof-of concept examination in lab-level. To achieve this, the processability of HP-MOFs (commonly brittle and hard to handle at large scale) should be considered. In addition, a batch or flux preparation of MOFs is desired for future commercial applications of various MOF-based materials. The combination of experimental and computational approaches can provide more insightful elucidation of structure−activity relationship and thus push the development of hitherto inaccessible MOF-based hierarchically porous materials. It can be expected more innovative applications will continuously emerge based on the extensive collaborative from different research fields, including material science, chemistry, engineering, environment science, energy, etc. With persistent endeavor toward the above challenges, we definitely believe that MOF-based hierarchically porous materials should present a promising future.

AUTHOR INFORMATION

Corresponding Author

Hai-Long Jiang − *Hefei National Laboratory for Physical Sciences at the Microscale, CAS Key Laboratory of Soft Matter Chemistry, Department of Chemistry, University of Science and Technology of China, Hefei, Anhui 230026, P. R. China*; orcid.org/0000-0002-2975-7977; Email: jianglab@ustc.edu.cn

Authors

Guorui Cai − *Hefei National Laboratory for Physical Sciences at the Microscale, CAS Key Laboratory of Soft Matter Chemistry, Department of Chemistry, University of Science and Technology of China, Hefei, Anhui 230026, P. R. China*

Peng Yan − *Hefei National Laboratory for Physical Sciences at the Microscale, CAS Key Laboratory of Soft Matter*

https://doi.org/10.1021/acs.chemrev.1c00243
Chem. Rev. 2021, 121, 12278−12326

Chemistry, Department of Chemistry, University of Science and Technology of China, Hefei, Anhui 230026, P. R. China

Liangliang Zhang − *Hefei National Laboratory for Physical Sciences at the Microscale, CAS Key Laboratory of Soft Matter Chemistry, Department of Chemistry, University of Science and Technology of China, Hefei, Anhui 230026, P. R. China; Frontiers Science Center for Flexible Electronics (FSCFE), Northwestern Polytechnical University (NPU), Xi'an, Shaanxi 710072, P. R. China;* orcid.org/0000-0002-5091-018X

Hong-Cai Zhou − *Department of Chemistry, Texas A&M University, College Station, Texas 77843-3255, United States;* orcid.org/0000-0002-9029-3788

Complete contact information is available at: https://pubs.acs.org/10.1021/acs.chemrev.1c00243

Author Contributions

†G.C. and P.Y. contributed equally to this work.

Notes

The authors declare no competing financial interest.

Biographies

Guorui Cai received his Ph.D. in Inorganic Chemistry from University of Science and Technology of China (USTC) in 2019 under the guidance of Prof. Hai-Long Jiang. He is currently a postdoctoral researcher in Prof. Zheng Chen's group at UC San Diego. His current research is focused on the design of hierarchically porous MOF-based materials for heterogeneous catalysis, electrolyte chemistry, and functional separators for rechargeable batteries at extreme temperatures.

Peng Yan was born in Shandong, China, in 1999. He received his B.S. degree (Materials Chemistry) at University of Science and Technology of China (USTC) in 2021. He did scientific research training in Prof. Hai-Long Jiang's group during his undergraduate, where he will continue his graduate study in inorganic chemistry right away. His research interest lies in the design of MOFs and related materials toward heterogeneous catalysis.

Liangliang Zhang received his Ph.D. in Inorganic Chemistry from Shandong University under the supervision of Prof. Daofeng Sun. In 2013, he joined the faculty of China University of petroleum. He worked in Prof. Hongcai Zhou's group at Texas A&M University as a visiting scholar during 2016−2017; then, he moved to Northwestern Polytechnical University in 2018. He worked with Prof. Hai-Long Jiang at USTC for a while in 2019. His current research interests are centered on construction of high-valence porous MOFs and their catalytic applications.

Hong-Cai Zhou obtained his Ph.D. in 2000 from Texas A&M University under the supervision of F. A. Cotton. After a postdoctoral stint at Harvard University with R. H. Holm, he joined the faculty of Miami University, Oxford, OH in 2002. He moved to Texas A&M University in 2008 and was appointed a Robert A. Welch Chair in Chemistry in 2015. Since 2014, he has been listed as a Highly Cited Researcher annually by Clarivate Analytics (formerly Thomson Reuters). In 2016, he was elected a fellow of the AAAS, ACS, and RSC. In 2017, he won a Distinguished Achievement Award in research by TAMU's Association of Former Students. He is best known for pioneering "kinetic control" and "retrosynthetic design" to form a "toolkit" for "pore engineering" in MOF synthesis, which enables the preparation and functionalization of MOFs for a variety of applications, especially in gas storage, separation, catalysis, and biomedicine.

Hai-Long Jiang earned his Ph.D. (2008) in Inorganic Chemistry from Fujian Institute of Research on the Structure of Matter, Chinese Academy of Sciences. He subsequently worked at the National Institute of Advanced Industrial Science and Technology (AIST, Japan), first as an AIST Fellow and later as a JSPS Fellow during 2008−2011. After a postdoctoral stint at Texas A&M University (USA), he became a full professor at USTC in 2013. He was elected a Fellow of the Royal Society of Chemistry (FRSC) in 2018 and was annually listed as a highly cited researcher (chemistry) by Clarivate Analytics since 2017. His research interest is currently lies in biomimetic microenvironment modulation (MEM) of catalytic centers based on crystalline porous materials (particularly MOFs).

ACKNOWLEDGMENTS

This work was supported by the National Natural Science Foundation of China (21725101, 22161142001, 21871244, and 21521001), Dalian National Laboratory Cooperation Fund, CAS (DNL201911), and Collaborative Innovation Program of Hefei Science Center, CAS (2020HSC-CIP005).

REFERENCES

(1) Chen, L.-H.; Sun, M.-H.; Wang, Z.; Yang, W.; Xie, Z.; Su, B.-L. Hierarchically structured zeolites: from design to application. *Chem. Rev.* **2020**, *120*, 11194−11294.
(2) Li, W.; Liu, J.; Zhao, D. Mesoporous materials for energy conversion and storage devices. *Nat. Rev. Mater.* **2016**, *1*, 16023.
(3) Hartmann, M.; Machoke, A. G.; Schwieger, W. Catalytic test reactions for the evaluation of hierarchical zeolites. *Chem. Soc. Rev.* **2016**, *45*, 3313−3330.
(4) Sun, L.-B.; Liu, X.-Q.; Zhou, H.-C. Design and fabrication of mesoporous heterogeneous basic catalysts. *Chem. Soc. Rev.* **2015**, *44*, 5092−5147.
(5) Wang, J.; Ma, Q.; Wang, Y.; Li, Z.; Li, Z.; Yuan, Q. New insights into the structure−performance relationships of mesoporous materials in analytical science. *Chem. Soc. Rev.* **2018**, *47*, 8766−8803.
(6) Sun, Q.; Dai, Z.; Meng, X.; Xiao, F.-S. Porous polymer catalysts with hierarchical structures. *Chem. Soc. Rev.* **2015**, *44*, 6018−6034.
(7) Wang, Y.; Arandiyan, H.; Scott, J.; Bagheri, A.; Dai, H.; Amal, R. Recent advances in ordered meso/macroporous metal oxides for heterogeneous catalysis: a review. *J. Mater. Chem. A* **2017**, *5*, 8825−8846.
(8) Tian, Y.; Zhu, G. Porous aromatic frameworks (PAFs). *Chem. Rev.* **2020**, *120*, 8934−8986.
(9) Kreno, L. E.; Leong, K.; Farha, O. K.; Allendorf, M.; Van Duyne, R. P.; Hupp, J. T. Metal-organic framework materials as chemical sensors. *Chem. Rev.* **2012**, *112*, 1105−1125.
(10) Furukawa, H.; Cordova, K. E.; O'Keeffe, M.; Yaghi, O. M. The chemistry and applications of metal-organic frameworks. *Science* **2013**, *341*, 1230444.
(11) Dhakshinamoorthy, A.; Li, Z.; Garcia, H. Catalysis and photocatalysis by metal organic frameworks. *Chem. Soc. Rev.* **2018**, *47*, 8134−8172.
(12) Xiao, J.-D.; Jiang, H.-L. Metal-organic frameworks for photocatalysis and photothermal catalysis. *Acc. Chem. Res.* **2019**, *52*, 356−366.
(13) Jiao, L.; Seow, J. Y. R.; Skinner, W. S.; Wang, Z. U.; Jiang, H.-L. Metal-organic frameworks: Structures and functional applications. *Mater. Today* **2019**, *27*, 43−68.
(14) Chen, L.; Xu, Q. Metal-organic framework composites for catalysis. *Matter* **2019**, *1*, 57−89.
(15) Li, B.; Wen, H. M.; Cui, Y.; Zhou, W.; Qian, G.; Chen, B. Emerging multifunctional metal-organic framework materials. *Adv. Mater.* **2016**, *28*, 8819−8860.
(16) Islamoglu, T.; Goswami, S.; Li, Z.; Howarth, A. J.; Farha, O. K.; Hupp, J. T. Postsynthetic tuning of metal-organic frameworks for targeted applications. *Acc. Chem. Res.* **2017**, *50*, 805−813.

(17) Zhou, H.-C.; Kitagawa, S. Metal-organic frameworks (MOFs). *Chem. Soc. Rev.* **2014**, *43*, 5415−5418.
(18) Xu, W.; Thapa, K. B.; Ju, Q.; Fang, Z.; Huang, W. Heterogeneous catalysts based on mesoporous metal-organic frameworks. *Coord. Chem. Rev.* **2018**, *373*, 199−232.
(19) Bradshaw, D.; El-Hankari, S.; Lupica-Spagnolo, L. Supramolecular templating of hierarchically porous metal-organic frameworks. *Chem. Soc. Rev.* **2014**, *43*, 5431−5443.
(20) Yue, Y.; Fulvio, P. F.; Dai, S. Hierarchical metal-organic framework hybrids: perturbation-assisted nanofusion synthesis. *Acc. Chem. Res.* **2015**, *48*, 3044−3052.
(21) Khan, N. A.; Hasan, Z.; Jhung, S. H. Beyond pristine metal-organic frameworks: Preparation and application of nanostructured, nanosized, and analogous MOFs. *Coord. Chem. Rev.* **2018**, *376*, 20−45.
(22) Feng, L.; Wang, K.-Y.; Lv, X.-L.; Yan, T.-H.; Zhou, H.-C. Hierarchically porous metal-organic frameworks: synthetic strategies and applications. *Natl. Sci. Rev.* **2020**, *7*, 1743−1758.
(23) Kabtamu, D. M.; Wu, Y.-N.; Li, F. Hierarchically porous metal-organic frameworks: synthesis strategies, structure (s), and emerging applications in decontamination. *J. Hazard. Mater.* **2020**, *397*, 122765.
(24) Jiang, H.-L.; Makal, T. A.; Zhou, H.-C. Interpenetration control in metal-organic frameworks for functional applications. *Coord. Chem. Rev.* **2013**, *257*, 2232−2249.
(25) Liu, D.; Zou, D.; Zhu, H.; Zhang, J. Mesoporous metal-organic frameworks: synthetic strategies and emerging applications. *Small* **2018**, *14*, 1801454.
(26) Guan, H.-Y.; LeBlanc, R. J.; Xie, S.-Y.; Yue, Y. Recent progress in the syntheses of mesoporous metal-organic framework materials. *Coord. Chem. Rev.* **2018**, *369*, 76−90.
(27) Xuan, W.; Zhu, C.; Liu, Y.; Cui, Y. Mesoporous metal-organic framework materials. *Chem. Soc. Rev.* **2012**, *41*, 1677−1695.
(28) Chen, C.; Kuang, Y.; Zhu, S.; Burgert, I.; Keplinger, T.; Gong, A.; Li, T.; Berglund, L.; Eichhorn, S. J.; Hu, L. Structure-property-function relationships of natural and engineered wood. *Nat. Rev. Mater.* **2020**, *5*, 642−666.
(29) Yu, Z.-L.; Yang, N.; Zhou, L.-C.; Ma, Z.-Y.; Zhu, Y.-B.; Lu, Y.-Y.; Qin, B.; Xing, W.-Y.; Ma, T.; Li, S.-C.; et al. Bioinspired polymeric woods. *Sci. Adv.* **2018**, *4*, No. eaat7223.
(30) Wegst, U. G.; Bai, H.; Saiz, E.; Tomsia, A. P.; Ritchie, R. O. Bioinspired structural materials. *Nat. Mater.* **2015**, *14*, 23−36.
(31) Yang, X.-Y.; Chen, L.-H.; Li, Y.; Rooke, J. C.; Sanchez, C.; Su, B.-L. Hierarchically porous materials: synthesis strategies and structure design. *Chem. Soc. Rev.* **2017**, *46*, 481−558.
(32) Li, Y.; Fu, Z. Y.; Su, B. L. Hierarchically structured porous materials for energy conversion and storage. *Adv. Funct. Mater.* **2012**, *22*, 4634−4667.
(33) Zheng, M.; Tang, H.; Li, L.; Hu, Q.; Zhang, L.; Xue, H.; Pang, H. Hierarchically nanostructured transition metal oxides for lithium-ion batteries. *Adv. Sci.* **2018**, *5*, 1700592.
(34) Kalaj, M.; Bentz, K. C.; Ayala, S., Jr; Palomba, J. M.; Barcus, K. S.; Katayama, Y.; Cohen, S. M. MOF−polymer hybrid materials: from simple composites to tailored architectures. *Chem. Rev.* **2020**, *120*, 8267−8302.
(35) Li, Y.; Xu, Y.; Yang, W.; Shen, W.; Xue, H.; Pang, H. MOF-derived metal oxide composites for advanced electrochemical energy storage. *Small* **2018**, *14*, 1704435.
(36) Kempahanumakkagari, S.; Vellingiri, K.; Deep, A.; Kwon, E. E.; Bolan, N.; Kim, K.-H. Metal-organic framework composites as electrocatalysts for electrochemical sensing applications. *Coord. Chem. Rev.* **2018**, *357*, 105−129.
(37) Liang, X.; Zhang, F.; Feng, W.; Zou, X.; Zhao, C.; Na, H.; Liu, C.; Sun, F.; Zhu, G. From metal-organic framework (MOF) to MOF−polymer composite membrane: enhancement of low-humidity proton conductivity. *Chem. Sci.* **2013**, *4*, 983−992.
(38) Dang, S.; Zhu, Q.-L.; Xu, Q. Nanomaterials derived from metal-organic frameworks. *Nat. Rev. Mater.* **2018**, *3*, 17075.
(39) Lee, K. J.; Lee, J. H.; Jeoung, S.; Moon, H. R. Transformation of metal-organic frameworks/coordination polymers into functional nanostructured materials: experimental approaches based on mechanistic insights. *Acc. Chem. Res.* **2017**, *50*, 2684−2692.
(40) Wu, H. B.; Lou, X. W. D. Metal-organic frameworks and their derived materials for electrochemical energy storage and conversion: Promises and challenges. *Sci. Adv.* **2017**, *3*, No. eaap9252.
(41) Chen, Y.; Ji, S.; Chen, C.; Peng, Q.; Wang, D.; Li, Y. Single-atom catalysts: synthetic strategies and electrochemical applications. *Joule* **2018**, *2*, 1242−1264.
(42) Chen, Y.-Z.; Zhang, R.; Jiao, L.; Jiang, H.-L. Metal-organic framework-derived porous materials for catalysis. *Coord. Chem. Rev.* **2018**, *362*, 1−23.
(43) Song, L.; Zhang, J.; Sun, L.; Xu, F.; Li, F.; Zhang, H.; Si, X.; Jiao, C.; Li, Z.; Liu, S.; et al. Mesoporous metal-organic frameworks: design and applications. *Energy Environ. Sci.* **2012**, *5*, 7508−7520.
(44) Ding, M.; Flaig, R. W.; Jiang, H.-L.; Yaghi, O. M. Carbon capture and conversion using metal-organic frameworks and MOF-based materials. *Chem. Soc. Rev.* **2019**, *48*, 2783−2828.
(45) Zhao, R.; Wu, Y.; Liang, Z.; Gao, L.; Xia, W.; Zhao, Y.; Zou, R. Metal-organic frameworks for solid-state electrolytes. *Energy Environ. Sci.* **2020**, *13*, 2386−2403.
(46) Eddaoudi, M.; Kim, J.; Rosi, N.; Vodak, D.; Wachter, J.; O'Keeffe, M.; Yaghi, O. M. Systematic design of pore size and functionality in isoreticular MOFs and their application in methane storage. *Science* **2002**, *295*, 469−472.
(47) Li, H.; Eddaoudi, M.; O'Keeffe, M.; Yaghi, O. M. Design and synthesis of an exceptionally stable and highly porous metal-organic framework. *Nature* **1999**, *402*, 276−279.
(48) Deng, H.; Grunder, S.; Cordova, K. E.; Valente, C.; Furukawa, H.; Hmadeh, M.; Gándara, F.; Whalley, A. C.; Liu, Z.; Asahina, S.; et al. Large-pore apertures in a series of metal-organic frameworks. *Science* **2012**, *336*, 1018−1023.
(49) Zhang, Y.; Li, J.; Yang, X.; Zhang, P.; Pang, J.; Li, B.; Zhou, H.-C. A mesoporous NNN-pincer-based metal-organic framework scaffold for the preparation of noble-metal-free catalysts. *Chem. Commun.* **2019**, *55*, 2023−2026.
(50) Feng, D.; Liu, T.-F.; Su, J.; Bosch, M.; Wei, Z.; Wan, W.; Yuan, D.; Chen, Y.-P.; Wang, X.; Wang, K.; Lian, X.; Gu, Z.-Y.; Park, J.; Zou, X.; Zhou, H.-C. Stable metal-organic frameworks containing single-molecule traps for enzyme encapsulation. *Nat. Commun.* **2015**, *6*, 5979.
(51) Yuan, D.; Zhao, D.; Sun, D.; Zhou, H. C. An isoreticular series of metal-organic frameworks with dendritic hexacarboxylate ligands and exceptionally high gas-uptake capacity. *Angew. Chem., Int. Ed.* **2010**, *49*, 5357−5361.
(52) Feng, D.; Wang, K.; Su, J.; Liu, T. F.; Park, J.; Wei, Z.; Bosch, M.; Yakovenko, A.; Zou, X.; Zhou, H. C. A highly stable zeotype mesoporous zirconium metal-organic framework with ultralarge pores. *Angew. Chem., Int. Ed.* **2015**, *54*, 149−154.
(53) Wang, B.; Lv, X.-L.; Feng, D.; Xie, L.-H.; Zhang, J.; Li, M.; Xie, Y.; Li, J.-R.; Zhou, H.-C. Highly stable Zr(IV)-based metal-organic frameworks for the detection and removal of antibiotics and organic explosives in water. *J. Am. Chem. Soc.* **2016**, *138*, 6204−6216.
(54) Farha, O. K.; Özgür Yazaydın, A.; Eryazici, I.; Malliakas, C. D.; Hauser, B. G.; Kanatzidis, M. G.; Nguyen, S. T.; Snurr, R. Q.; Hupp, J. T. De novo synthesis of a metal-organic framework material featuring ultrahigh surface area and gas storage capacities. *Nat. Chem.* **2010**, *2*, 944−948.
(55) Li, P.; Vermeulen, N. A.; Malliakas, C. D.; Gómez-Gualdrón, D. A.; Howarth, A. J.; Mehdi, B. L.; Dohnalkova, A.; Browning, N. D.; O'Keeffe, M.; Farha, O. K. Bottom-up construction of a superstructure in a porous uranium-organic crystal. *Science* **2017**, *356*, 624−627.
(56) Wang, X.; Zhang, X.; Li, P.; Otake, K.-I.; Cui, Y.; Lyu, J.; Krzyaniak, M. D.; Zhang, Y.; Li, Z.; Liu, J.; et al. Vanadium catalyst on isostructural transition metal, lanthanide, and actinide based metal-organic frameworks for alcohol oxidation. *J. Am. Chem. Soc.* **2019**, *141*, 8306−8314.
(57) Reinares-Fisac, D.; Aguirre-Díaz, L. M.; Iglesias, M.; Snejko, N.; Gutiérrez-Puebla, E.; Monge, M. A. N.; Gándara, F. A mesoporous

indium metal-organic framework: remarkable advances in catalytic activity for strecker reaction of ketones. *J. Am. Chem. Soc.* **2016**, *138*, 9089−9092.
(58) Liu, Q.; Song, Y.; Ma, Y.; Zhou, Y.; Cong, H.; Wang, C.; Wu, J.; Hu, G.; O'Keeffe, M.; Deng, H. Mesoporous cages in chemically robust MOFs created by a large number of vertices with reduced connectivity. *J. Am. Chem. Soc.* **2019**, *141*, 488−496.
(59) Liang, C.-C.; Shi, Z.-L.; He, C.-T.; Tan, J.; Zhou, H.-D.; Zhou, H.-L.; Lee, Y.; Zhang, Y.-B. Engineering of pore geometry for ultrahigh capacity methane storage in mesoporous metal-organic frameworks. *J. Am. Chem. Soc.* **2017**, *139*, 13300−13303.
(60) Morris, W.; Volosskiy, B.; Demir, S.; Gándara, F.; McGrier, P. L.; Furukawa, H.; Cascio, D.; Stoddart, J. F.; Yaghi, O. M. Synthesis, structure, and metalation of two new highly porous zirconium metal-organic frameworks. *Inorg. Chem.* **2012**, *51*, 6443−6445.
(61) Pang, J.; Yuan, S.; Qin, J.; Liu, C.; Lollar, C.; Wu, M.; Yuan, D.; Zhou, H.-C.; Hong, M. Control the structure of Zr-tetracarboxylate frameworks through steric tuning. *J. Am. Chem. Soc.* **2017**, *139*, 16939−16945.
(62) Liu, T.-F.; Feng, D.; Chen, Y.-P.; Zou, L.; Bosch, M.; Yuan, S.; Wei, Z.; Fordham, S.; Wang, K.; Zhou, H.-C. Topology-guided design and syntheses of highly stable mesoporous porphyrinic zirconium metal-organic frameworks with high surface area. *J. Am. Chem. Soc.* **2015**, *137*, 413−419.
(63) Feng, D.; Gu, Z. Y.; Li, J. R.; Jiang, H. L.; Wei, Z.; Zhou, H. C. Zirconium-metalloporphyrin PCN-222: mesoporous metal-organic frameworks with ultrahigh stability as biomimetic catalysts. *Angew. Chem., Int. Ed.* **2012**, *51*, 10307−10310.
(64) Zhang, Q.; Su, J.; Feng, D.; Wei, Z.; Zou, X.; Zhou, H.-C. Piezofluorochromic metal-organic framework: A microscissor lift. *J. Am. Chem. Soc.* **2015**, *137*, 10064−10067.
(65) Liu, T.-F.; Vermeulen, N. A.; Howarth, A. J.; Li, P.; Sarjeant, A. A.; Hupp, J. T.; Farha, O. K. Adding to the arsenal of zirconium-based metal-organic frameworks: the topology as a platform for solvent-assisted metal incorporation. *Eur. J. Inorg. Chem.* **2016**, *2016*, 4349−4352.
(66) Lyu, J.; Zhang, X.; Li, P.; Wang, X.; Buru, C. T.; Bai, P.; Guo, X.; Farha, O. K. Exploring the role of hexanuclear clusters as lewis acidic sites in isostructural metal-organic frameworks. *Chem. Mater.* **2019**, *31*, 4166−4172.
(67) Li, P.; Chen, Q.; Wang, T. C.; Vermeulen, N. A.; Mehdi, B. L.; Dohnalkova, A.; Browning, N. D.; Shen, D.; Anderson, R.; Gómez-Gualdrón, D. A.; et al. Hierarchically engineered mesoporous metal-organic frameworks toward cell-free immobilized enzyme systems. *Chem.* **2018**, *4*, 1022−1034.
(68) Li, P.; Moon, S.-Y.; Guelta, M. A.; Lin, L.; Gómez-Gualdrón, D. A.; Snurr, R. Q.; Harvey, S. P.; Hupp, J. T.; Farha, O. K. Nanosizing a metal-organic framework enzyme carrier for accelerating nerve agent hydrolysis. *ACS Nano* **2016**, *10*, 9174−9182.
(69) Mondloch, J. E.; Bury, W.; Fairen-Jimenez, D.; Kwon, S.; DeMarco, E. J.; Weston, M. H.; Sarjeant, A. A.; Nguyen, S. T.; Stair, P. C.; Snurr, R. Q.; et al. Vapor-phase metalation by atomic layer deposition in a metal-organic framework. *J. Am. Chem. Soc.* **2013**, *135*, 10294−10297.
(70) Park, S. S.; Hendon, C. H.; Fielding, A. J.; Walsh, A.; O'Keeffe, M.; Dincă, M. The organic secondary building unit: strong intermolecular π interactions define topology in MIT-25, a mesoporous MOF with proton-replete channels. *J. Am. Chem. Soc.* **2017**, *139*, 3619−3622.
(71) Ma, J.; Tran, L. D.; Matzger, A. J. Toward topology prediction in zr-based microporous coordination polymers: the role of linker geometry and flexibility. *Cryst. Growth Des.* **2016**, *16*, 4148−4153.
(72) An, J.; Farha, O. K.; Hupp, J. T.; Pohl, E.; Yeh, J. I.; Rosi, N. L. Metal-adeninate vertices for the construction of an exceptionally porous metal-organic framework. *Nat. Commun.* **2012**, *3*, 604.
(73) Loiseau, T.; Serre, C.; Huguenard, C.; Fink, G.; Taulelle, F.; Henry, M.; Bataille, T.; Férey, G. A rationale for the large breathing of the porous aluminum terephthalate (MIL-53) upon hydration. *Chem. - Eur. J.* **2004**, *10*, 1373−1382.
(74) Serre, C.; Millange, F.; Thouvenot, C.; Nogues, M.; Marsolier, G.; Louër, D.; Férey, G. Very large breathing effect in the first nanoporous chromium(III)-based solids: MIL-53 or $Cr^{III}(OH)\cdot\{O_2C\text{-}C_6H_4\text{-}CO_2\}\cdot\{HO_2C\text{-}C_6H_4\text{-}CO_2H\}_x\cdot H_2O_y$. *J. Am. Chem. Soc.* **2002**, *124*, 13519−13526.
(75) Serre, C.; Millange, F.; Surblé, S.; Férey, G. A route to the synthesis of trivalent transition-metal porous carboxylates with trimeric secondary building units. *Angew. Chem., Int. Ed.* **2004**, *43*, 6285−6289.
(76) Horcajada, P.; Chevreau, H.; Heurtaux, D.; Benyettou, F.; Salles, F.; Devic, T.; Garcia-Marquez, A.; Yu, C.; Lavrard, H.; Dutson, C. L.; et al. Extended and functionalized porous iron (iii) tri-or dicarboxylates with MIL-100/101 topologies. *Chem. Commun.* **2014**, *50*, 6872−6874.
(77) Férey, G.; Mellot-Draznieks, C.; Serre, C.; Millange, F.; Dutour, J.; Surblé, S.; Margiolaki, I. A chromium terephthalate-based solid with unusually large pore volumes and surface area. *Science* **2005**, *309*, 2040−2042.
(78) Du, M.; Wang, X.; Chen, M.; Li, C. P.; Tian, J. Y.; Wang, Z. W.; Liu, C. S. Ligand symmetry modulation for designing a mesoporous metal-organic framework: dual reactivity to transition and lanthanide metals for enhanced functionalization. *Chem. - Eur. J.* **2015**, *21*, 9713−9719.
(79) Koh, K.; Wong-Foy, A. G.; Matzger, A. J. A crystalline mesoporous coordination copolymer with high microporosity. *Angew. Chem., Int. Ed.* **2008**, *47*, 677−680.
(80) Klein, N.; Senkovska, I.; Gedrich, K.; Stoeck, U.; Henschel, A.; Mueller, U.; Kaskel, S. A mesoporous metal-organic framework. *Angew. Chem., Int. Ed.* **2009**, *48*, 9954−9957.
(81) Klein, N.; Senkovska, I.; Baburin, I. A.; Gruenker, R.; Stoeck, U.; Schlichtenmayer, M.; Streppel, B.; Mueller, U.; Leoni, S.; Hirscher, M.; et al. Route to a family of robust, non-interpenetrated metal-organic frameworks with pto-like topology. *Chem. - Eur. J.* **2011**, *17*, 13007−13016.
(82) Grünker, R.; Bon, V.; Heerwig, A.; Klein, N.; Müller, P.; Stoeck, U.; Baburin, I. A.; Mueller, U.; Senkovska, I.; Kaskel, S. Dye encapsulation inside a new mesoporous metal-organic framework for multifunctional solvatochromic-response function. *Chem. - Eur. J.* **2012**, *18*, 13299−13303.
(83) Grünker, R.; Bon, V.; Müller, P.; Stoeck, U.; Krause, S.; Mueller, U.; Senkovska, I.; Kaskel, S. A new metal-organic framework with ultra-high surface area. *Chem. Commun.* **2014**, *50*, 3450−3452.
(84) Koh, K.; Wong-Foy, A. G.; Matzger, A. J. A porous coordination copolymer with over 5000 m^2/g BET surface area. *J. Am. Chem. Soc.* **2009**, *131*, 4184−4185.
(85) Furukawa, H.; Ko, N.; Go, Y. B.; Aratani, N.; Choi, S. B.; Choi, E.; Yazaydin, A. Ö.; Snurr, R. Q.; O'Keeffe, M.; Kim, J.; et al. Ultrahigh porosity in metal-organic frameworks. *Science* **2010**, *329*, 424−428.
(86) Roy, X.; Thompson, L. K.; Coombs, N.; MacLachlan, M. J. Mesostructured prussian blue analogues. *Angew. Chem., Int. Ed.* **2008**, *47*, 511−514.
(87) Qiu, L. G.; Xu, T.; Li, Z. Q.; Wang, W.; Wu, Y.; Jiang, X.; Tian, X. Y.; Zhang, L. D. Hierarchically micro-and mesoporous metal-organic frameworks with tunable porosity. *Angew. Chem., Int. Ed.* **2008**, *47*, 9487−9491.
(88) Sun, L.-B.; Li, J.-R.; Park, J.; Zhou, H.-C. Cooperative template-directed assembly of mesoporous metal-organic frameworks. *J. Am. Chem. Soc.* **2012**, *134*, 126−129.
(89) Ma, T.-Y.; Li, H.; Deng, Q.-F.; Liu, L.; Ren, T.-Z.; Yuan, Z.-Y. Ordered mesoporous metal-organic frameworks consisting of metal disulfonates. *Chem. Mater.* **2012**, *24*, 2253−2255.
(90) Yu, H.; Xu, D.; Xu, Q. Dual template effect of supercritical CO_2 in ionic liquid to fabricate a highly mesoporous cobalt metal-organic framework. *Chem. Commun.* **2015**, *51*, 13197−13200.
(91) Li, K.; Lin, S.; Li, Y.; Zhuang, Q.; Gu, J. Aqueous-phase synthesis of mesoporous Zr-Based MOFs templated by amphoteric surfactants. *Angew. Chem., Int. Ed.* **2018**, *57*, 3439−3443.

https://doi.org/10.1021/acs.chemrev.1c00243
Chem. Rev. 2021, 121, 12278−12326

(92) Li, K.; Yang, J.; Huang, R.; Lin, S.; Gu, J. Ordered large-pore mesoMOFs based on synergistic effects of triblock polymer and Hofmeister Ion. *Angew. Chem., Int. Ed.* **2020**, *59*, 14124−14128.
(93) Dutta, S.; Kumari, N.; Dubbu, S.; Jang, S. W.; Kumar, A.; Ohtsu, H.; Kim, J.; Cho, S. H.; Kawano, M.; Lee, I. S. Highly mesoporous metal-organic frameworks as synergistic multimodal catalytic platforms for divergent cascade reactions. *Angew. Chem., Int. Ed.* **2020**, *59*, 3416−3422.
(94) Kirchon, A.; Li, J.; Xia, F.; Day, G. S.; Becker, B.; Chen, W.; Sue, H. J.; Fang, Y.; Zhou, H. C. Modulation versus templating: fine-tuning of hierarchally porous PCN-250 using fatty acids to engineer guest adsorption. *Angew. Chem., Int. Ed.* **2019**, *58*, 12425−12430.
(95) Duan, C.; Zhang, H.; Yang, M.; Li, F.; Yu, Y.; Xiao, J.; Xi, H. Templated fabrication of hierarchically porous metal-organic frameworks and simulation of crystal growth. *Nanoscale Adv.* **2019**, *1*, 1062−1069.
(96) Wang, C.; Liu, X.; Li, W.; Huang, X.; Luan, S.; Hou, X.; Zhang, M.; Wang, Q. CO_2 mediated fabrication of hierarchically porous metal-organic frameworks. *Microporous Mesoporous Mater.* **2019**, *277*, 154−162.
(97) Duan, C.; Huo, J.; Li, F.; Yang, M.; Xi, H. Ultrafast room-temperature synthesis of hierarchically porous metal-organic frameworks by a versatile cooperative template strategy. *J. Mater. Sci.* **2018**, *53*, 16276−16287.
(98) Duan, C.; Zhang, H.; Peng, A.; Li, F.; Xiao, J.; Zou, J.; Luo, S.; Xi, H. Synthesis of hierarchically structured metal-organic frameworks by a dual-functional surfactant. *ChemistrySelect* **2018**, *3*, 5313−5320.
(99) Zhang, P.; Chen, C.; Kang, X.; Zhang, L.; Wu, C.; Zhang, J.; Han, B. In situ synthesis of sub-nanometer metal particles on hierarchically porous metal-organic frameworks via interfacial control for highly efficient catalysis. *Chem. Sci.* **2018**, *9*, 1339−1343.
(100) Li, H.; Sun, Y.; Yuan, Z. Y.; Zhu, Y. P.; Ma, T. Y. Titanium phosphonate based metal-organic frameworks with hierarchical porosity for enhanced photocatalytic hydrogen evolution. *Angew. Chem., Int. Ed.* **2018**, *57*, 3222−3227.
(101) Duan, C.; Li, F.; Zhang, H.; Li, J.; Wang, X.; Xi, H. Template synthesis of hierarchical porous metal-organic frameworks with tunable porosity. *RSC Adv.* **2017**, *7*, 52245−52251.
(102) Zhu, H.; Zhang, Q.; Zhu, S. Assembly of a metal-organic framework into 3D hierarchical porous monoliths using a pickering high internal phase emulsion template. *Chem. - Eur. J.* **2016**, *22*, 8751−8755.
(103) McNamara, N. D.; Hicks, J. C. Chelating agent-free, vapor-assisted crystallization method to synthesize hierarchical micro-porous/mesoporous MIL-125(Ti). *ACS Appl. Mater. Interfaces* **2015**, *7*, 5338−5346.
(104) Wu, Y.-N.; Zhou, M.; Zhang, B.; Wu, B.; Li, J.; Qiao, J.; Guan, X.; Li, F. Amino acid assisted templating synthesis of hierarchical zeolitic imidazolate framework-8 for efficient arsenate removal. *Nanoscale* **2014**, *6*, 1105−1112.
(105) Abedi, S.; Morsali, A. Ordered mesoporous metal-organic frameworks incorporated with amorphous TiO_2 as photocatalyst for selective aerobic oxidation in sunlight irradiation. *ACS Catal.* **2014**, *4*, 1398−1403.
(106) Cao, S.; Gody, G.; Zhao, W.; Perrier, S.; Peng, X.; Ducati, C.; Zhao, D.; Cheetham, A. K. Hierarchical bicontinuous porosity in metal-organic frameworks templated from functional block co-oligomer micelles. *Chem. Sci.* **2013**, *4*, 3573−3577.
(107) Wee, L. H.; Wiktor, C.; Turner, S.; Vanderlinden, W.; Janssens, N.; Bajpe, S. R.; Houthoofd, K.; Van Tendeloo, G.; De Feyter, S.; Kirschhock, C. E.; et al. Copper benzene tricarboxylate metal-organic framework with wide permanent mesopores stabilized by keggin polyoxometallate ions. *J. Am. Chem. Soc.* **2012**, *134*, 10911−10919.
(108) Pham, M.-H.; Vuong, G.-T.; Fontaine, F. D. R.-G.; Do, T.-O. A route to bimodal micro-mesoporous metal-organic frameworks nanocrystals. *Cryst. Growth Des.* **2012**, *12*, 1008−1013.
(109) Huang, X.-X.; Qiu, L.-G.; Zhang, W.; Yuan, Y.-P.; Jiang, X.; Xie, A.-J.; Shen, Y.-H.; Zhu, J.-F. Hierarchically mesostructured MIL-101 metal-organic frameworks: supramolecular template-directed synthesis and accelerated adsorption kinetics for dye removal. *CrystEngComm* **2012**, *14*, 1613−1617.
(110) Peng, L.; Zhang, J.; Li, J.; Han, B.; Xue, Z.; Yang, G. Surfactant-directed assembly of mesoporous metal-organic framework nanoplates in ionic liquids. *Chem. Commun.* **2012**, *48*, 8688−8690.
(111) Do, X.-D.; Hoang, V.-T.; Kaliaguine, S. MIL-53(Al) mesostructured metal-organic frameworks. *Microporous Mesoporous Mater.* **2011**, *141*, 135−139.
(112) Li, Y.; Zhang, D.; Guo, Y.-N.; Guan, B.; Tang, D.; Liu, Y.; Huo, Q. Design and synthesis of novel mesostructured metal-organic frameworks templated by cationic surfactants via cooperative self-organization. *Chem. Commun.* **2011**, *47*, 7809−7811.
(113) Zhao, Y.; Zhang, J.; Han, B.; Song, J.; Li, J.; Wang, Q. Metal-organic framework nanospheres with well-ordered mesopores synthesized in an ionic liquid/CO_2/surfactant system. *Angew. Chem., Int. Ed.* **2011**, *50*, 636−639.
(114) Roy, X.; MacLachlan, M. J. Coordination chemistry: new routes to mesostructured materials. *Chem. - Eur. J.* **2009**, *15*, 6552−6559.
(115) Li, K.; Yang, J.; Gu, J. Spatially organized functional bioreactors in nanoscale mesoporous MOFs for cascade scavenging of intracellular ROS. *Chem. Mater.* **2021**, *33*, 2198−2205.
(116) Li, K.; Yang, J.; Gu, J. Salting-in species induced self-assembly of stable MOFs. *Chem. Sci.* **2019**, *10*, 5743−5748.
(117) Wu, Y. N.; Li, F.; Zhu, W.; Cui, J.; Tao, C. A.; Lin, C.; Hannam, P. M.; Li, G. Metal-organic frameworks with a three-dimensional ordered macroporous structure: dynamic photonic materials. *Angew. Chem., Int. Ed.* **2011**, *50*, 12518−12522.
(118) Zhang, W.; Liu, Y.; Lu, G.; Wang, Y.; Li, S.; Cui, C.; Wu, J.; Xu, Z.; Tian, D.; Huang, W.; DuCheneu, J. S.; Wei, W. D.; Chen, H.; Yang, Y.; Huo, F. Mesoporous metal-organic frameworks with size-, shape-, and space-distribution-controlled pore structure. *Adv. Mater.* **2015**, *27*, 2923−2929.
(119) Wang, S.; Fan, Y.; Teng, J.; Fan, Y. Z.; Jiang, J. J.; Wang, H. P.; Grützmacher, H.; Wang, D.; Su, C. Y. Nanoreactor based on macroporous single crystals of metal-organic framework. *Small* **2016**, *12*, 5702−5709.
(120) Cui, J.; Gao, N.; Yin, X.; Zhang, W.; Liang, Y.; Tian, L.; Zhou, K.; Wang, S.; Li, G. Microfluidic synthesis of uniform single-crystalline MOF microcubes with a hierarchical porous structure. *Nanoscale* **2018**, *10*, 9192−9198.
(121) Jing, P.; Zhang, S. Y.; Chen, W.; Wang, L.; Shi, W.; Cheng, P. A macroporous metal-organic framework with enhanced hydrophobicity for efficient oil adsorption. *Chem. - Eur. J.* **2018**, *24*, 3754−3759.
(122) Shen, K.; Zhang, L.; Chen, X.; Liu, L.; Zhang, D.; Han, Y.; Chen, J.; Long, J.; Luque, R.; Li, Y.; et al. Ordered macro-microporous metal-organic framework single crystals. *Science* **2018**, *359*, 206−210.
(123) Huang, H.; Li, J.-R.; Wang, K.; Han, T.; Tong, M.; Li, L.; Xie, Y.; Yang, Q.; Liu, D.; Zhong, C. An in situ self-assembly template strategy for the preparation of hierarchical-pore metal-organic frameworks. *Nat. Commun.* **2015**, *6*, 5028.
(124) Chen, S.; Zhang, L.; Zhang, Z.; Qian, G.; Liu, Z.; Cui, Q.; Wang, H. Study on the desorption process of n-heptane and methyl cyclohexane using UiO-66 with hierarchical pores. *ACS Appl. Mater. Interfaces* **2018**, *10*, 21612−21618.
(125) Teng, J.; Chen, M.; Xie, Y.; Wang, D.; Jiang, J.-J.; Li, G.; Wang, H.-P.; Fan, Y.; Wei, Z.-W.; Su, C.-Y. Hierarchically porous single nanocrystals of bimetallic metal-organic framework for nanoreactors with enhanced conversion. *Chem. Mater.* **2018**, *30*, 6458−6468.
(126) Reboul, J.; Furukawa, S.; Horike, N.; Tsotsalas, M.; Hirai, K.; Uehara, H.; Kondo, M.; Louvain, N.; Sakata, O.; Kitagawa, S. Mesoscopic architectures of porous coordination polymers fabricated by pseudomorphic replication. *Nat. Mater.* **2012**, *11*, 717−723.
(127) Chou, L.-Y.; Hu, P.; Zhuang, J.; Morabito, J. V.; Ng, K. C.; Kao, Y.-C.; Wang, S.-C.; Shieh, F.-K.; Kuo, C.-H.; Tsung, C.-K.

Formation of hollow and mesoporous structures in single-crystalline microcrystals of metal-organic frameworks via double-solvent mediated overgrowth. *Nanoscale* **2015**, *7*, 19408−19412.
(128) Moitra, N.; Fukumoto, S.; Reboul, J.; Sumida, K.; Zhu, Y.; Nakanishi, K.; Furukawa, S.; Kitagawa, S.; Kanamori, K. Mechanically stable, hierarchically porous $Cu_3(btc)_2$(HKUST-1) monoliths via direct conversion of copper(ii) hydroxide-based monoliths. *Chem. Commun.* **2015**, *51*, 3511−3514.
(129) Bo, R.; Taheri, M.; Liu, B.; Ricco, R.; Chen, H.; Amenitsch, H.; Fusco, Z.; Tsuzuki, T.; Yu, G.; Ameloot, R.; et al. Hierarchical metal-organic framework films with controllable meso/macroporosity. *Adv. Sci.* **2020**, *7*, 2002368.
(130) Xin, Z.; Bai, J.; Pan, Y.; Zaworotko, M. J. Synthesis and enhanced H_2 adsorption properties of a mesoporous nanocrystal of MOF-5: controlling nano-/mesostructures of MOFs to improve their H_2 heat of adsorption. *Chem. - Eur. J.* **2010**, *16*, 13049−13052.
(131) Xin, Z.; Bai, J.; Shen, Y.; Pan, Y. Hierarchically micro-and mesoporous coordination polymer nanostructures with high adsorption performance. *Cryst. Growth Des.* **2010**, *10*, 2451−2454.
(132) Du, H.; Bai, J.; Zuo, C.; Xin, Z.; Hu, J. A hierarchical supra-nanostructure of HKUST-1 featuring enhanced H_2 adsorption enthalpy and higher mesoporosity. *CrystEngComm* **2011**, *13*, 3314−3316.
(133) Yue, Y.; Qiao, Z.-A.; Fulvio, P. F.; Binder, A. J.; Tian, C.; Chen, J.; Nelson, K. M.; Zhu, X.; Dai, S. Template-free synthesis of hierarchical porous metal-organic frameworks. *J. Am. Chem. Soc.* **2013**, *135*, 9572−9575.
(134) Peng, L.; Zhang, J.; Xue, Z.; Han, B.; Sang, X.; Liu, C.; Yang, G. Highly mesoporous metal-organic framework assembled in a switchable solvent. *Nat. Commun.* **2014**, *5*, 4465.
(135) Yue, Y.; Binder, A. J.; Song, R.; Cui, Y.; Chen, J.; Hensley, D. K.; Dai, S. Encapsulation of large dye molecules in hierarchically superstructured metal-organic frameworks. *Dalton Trans.* **2014**, *43*, 17893−17898.
(136) Zhan, G.; Zeng, H. C. An alternative synthetic approach for macro-meso-microporous metal-organic frameworks via a "domain growth" mechanism. *Chem. Commun.* **2016**, *52*, 8432−8435.
(137) Du, P.; Dong, Y.; Liu, C.; Wei, W.; Liu, D.; Liu, P. Fabrication of hierarchical porous nickel based metal-organic framework (Ni-MOF) constructed with nanosheets as novel pseudo-capacitive material for asymmetric supercapacitor. *J. Colloid Interface Sci.* **2018**, *518*, 57−68.
(138) Hao, L.; Li, X.; Hurlock, M. J.; Tu, X.; Zhang, Q. Hierarchically porous UiO-66: facile synthesis, characterization and application. *Chem. Commun.* **2018**, *54*, 11817−11820.
(139) Park, J.; Wang, Z. U.; Sun, L.-B.; Chen, Y.-P.; Zhou, H.-C. Introduction of functionalized mesopores to metal-organic frameworks via metal-ligand-fragment coassembly. *J. Am. Chem. Soc.* **2012**, *134*, 20110−20116.
(140) Li, L.; Xiang, S.; Cao, S.; Zhang, J.; Ouyang, G.; Chen, L.; Su, C.-Y. A synthetic route to ultralight hierarchically micro/mesoporous Al(III)-carboxylate metal-organic aerogels. *Nat. Commun.* **2013**, *4*, 1774.
(141) Cai, G.; Jiang, H. L. A modulator-induced defect-formation strategy to hierarchically porous metal-organic frameworks with high stability. *Angew. Chem., Int. Ed.* **2017**, *56*, 563−567.
(142) Huang, J.-Y.; Xu, H.; Peretz, E.; Wu, D.-Y.; Ober, C. K.; Hanrath, T. Three-dimensional printing of hierarchical porous architectures. *Chem. Mater.* **2019**, *31*, 10017−10022.
(143) Choi, K. M.; Jeon, H. J.; Kang, J. K.; Yaghi, O. M. Heterogeneity within order in crystals of a porous metal-organic framework. *J. Am. Chem. Soc.* **2011**, *133*, 11920−11923.
(144) He, S.; Chen, Y.; Zhang, Z.; Ni, B.; He, W.; Wang, X. Competitive coordination strategy for the synthesis of hierarchical-pore metal-organic framework nanostructures. *Chem. Sci.* **2016**, *7*, 7101−7105.
(145) Fang, Z.; Dürholt, J. P.; Kauer, M.; Zhang, W.; Lochenie, C.; Jee, B.; Albada, B.; Metzler-Nolte, N.; Pöppl, A.; Weber, B.; et al. Structural complexity in metal-organic frameworks: simultaneous modification of open metal sites and hierarchical porosity by systematic doping with defective linkers. *J. Am. Chem. Soc.* **2014**, *136*, 9627−9636.
(146) Liu, B.; Li, Y.; Oh, S. C.; Fang, Y.; Xi, H. Fabrication of a hierarchically structured HKUST-1 by a mixed-ligand approach. *RSC Adv.* **2016**, *6*, 61006−61012.
(147) Perez-Yanez, S.; Beobide, G.; Castillo, O.; Cepeda, J.; Fröba, M.; Hoffmann, F.; Luque, A.; Román, P. Improving the performance of a poorly adsorbing porous material: template mediated addition of microporosity to a crystalline submicroporous MOF. *Chem. Commun.* **2012**, *48*, 907−909.
(148) Wang, Z.; Hu, S.; Yang, J.; Liang, A.; Li, Y.; Zhuang, Q.; Gu, J. Nanoscale Zr-based MOFs with tailorable size and introduced mesopore for protein delivery. *Adv. Funct. Mater.* **2018**, *28*, 1707356.
(149) Liang, W.; Li, L.; Hou, J.; Shepherd, N. D.; Bennett, T. D.; D'Alessandro, D. M.; Chen, V. Linking defects, hierarchical porosity generation and desalination performance in metal-organic frameworks. *Chem. Sci.* **2018**, *9*, 3508−3516.
(150) Lohe, M. R.; Rose, M.; Kaskel, S. Metal-organic framework (MOF) aerogels with high micro-and macroporosity. *Chem. Commun.* **2009**, 6056−6058.
(151) Xia, W.; Zhang, X.; Xu, L.; Wang, Y.; Lin, J.; Zou, R. Facile and economical synthesis of metal-organic framework MIL-100(Al) gels for high efficiency removal of microcystin-LR. *RSC Adv.* **2013**, *3*, 11007−11013.
(152) Ahmed, A.; Forster, M.; Clowes, R.; Myers, P.; Zhang, H. Hierarchical porous metal-organic framework monoliths. *Chem. Commun.* **2014**, *50*, 14314−14316.
(153) Liu, X.; Shen, Z.-Q.; Xiong, H.-H.; Chen, Y.; Wang, X.-N.; Li, H.-Q.; Li, Y.-T.; Cui, K.-H.; Tian, Y.-Q. Hierarchical porous materials based on nanoscale metal-organic frameworks dominated with permanent interparticle porosity. *Microporous Mesoporous Mater.* **2015**, *204*, 25−33.
(154) Mahmood, A.; Xia, W.; Mahmood, N.; Wang, Q.; Zou, R. Hierarchical heteroaggregation of binary metal-organic gels with tunable porosity and mixed valence metal sites for removal of dyes in water. *Sci. Rep.* **2015**, *5*, 10556.
(155) Vilela, S. M.; Salcedo-Abraira, P.; Micheron, L.; Solla, E. L.; Yot, P. G.; Horcajada, P. A robust monolithic metal-organic framework with hierarchical porosity. *Chem. Commun.* **2018**, *54*, 13088−13091.
(156) Hara, Y.; Kanamori, K.; Nakanishi, K. Self-assembly of metal-organic frameworks into monolithic materials with highly controlled trimodal pore structures. *Angew. Chem., Int. Ed.* **2019**, *58*, 19047−19053.
(157) Liu, D.; Jiang, P.; Li, X.; Liu, J.; Zhou, L.; Wang, X.; Zhou, F. 3D printing of metal-organic frameworks decorated hierarchical porous ceramics for high-efficiency catalytic degradation. *Chem. Eng. J.* **2020**, *397*, 125392.
(158) Li, R.; Yuan, S.; Zhang, W.; Zheng, H.; Zhu, W.; Li, B.; Zhou, M.; Wing-Keung Law, A.; Zhou, K. 3D printing of mixed matrix films based on metal-organic frameworks and thermoplastic polyamide 12 by selective laser sintering for water applications. *ACS Appl. Mater. Interfaces* **2019**, *11*, 40564−40574.
(159) Li, T.; Kozlowski, M. T.; Doud, E. A.; Blakely, M. N.; Rosi, N. L. Stepwise ligand exchange for the preparation of a family of mesoporous MOFs. *J. Am. Chem. Soc.* **2013**, *135*, 11688−11691.
(160) Liu, C.; Luo, T.-Y.; Feura, E. S.; Zhang, C.; Rosi, N. L. Orthogonal ternary functionalization of a mesoporous metal-organic framework via sequential postsynthetic ligand exchange. *J. Am. Chem. Soc.* **2015**, *137*, 10508−10511.
(161) Yuan, S.; Zou, L.; Qin, J.-S.; Li, J.; Huang, L.; Feng, L.; Wang, X.; Bosch, M.; Alsalme, A.; Cagin, T.; et al. Construction of hierarchically porous metal-organic frameworks through linker labilization. *Nat. Commun.* **2017**, *8*, 15356.
(162) Feng, L.; Yuan, S.; Zhang, L.-L.; Tan, K.; Li, J.-L.; Kirchon, A.; Liu, L.-M.; Zhang, P.; Han, Y.; Chabal, Y. J.; Zhou, H.-C. Creating hierarchical pores by controlled linker thermolysis in multivariate metal-organic frameworks. *J. Am. Chem. Soc.* **2018**, *140*, 2363−2372.

https://doi.org/10.1021/acs.chemrev.1c00243
Chem. Rev. 2021, 121, 12278−12326

(163) Lyu, J.; Gong, X.; Lee, S.-J.; Gnanasekaran, K.; Zhang, X.; Wasson, M. C.; Wang, X.; Bai, P.; Guo, X.; Gianneschi, N. C.; et al. Phase transitions in metal-organic frameworks directly monitored through in situ variable temperature liquid-cell transmission electron microscopy and in situ X-ray diffraction. *J. Am. Chem. Soc.* **2020**, *142*, 4609−4615.
(164) Park, J.; Feng, D.; Zhou, H.-C. Dual exchange in PCN-333: a facile strategy to chemically robust mesoporous chromium metal-organic framework with functional groups. *J. Am. Chem. Soc.* **2015**, *137*, 11801−11809.
(165) Zou, L.; Feng, D.; Liu, T.-F.; Chen, Y.-P.; Yuan, S.; Wang, K.; Wang, X.; Fordham, S.; Zhou, H.-C. A versatile synthetic route for the preparation of titanium metal-organic frameworks. *Chem. Sci.* **2016**, *7*, 1063−1069.
(166) Ding, M.; Cai, X.; Jiang, H.-L. Improving MOF stability: approaches and applications. *Chem. Sci.* **2019**, *10*, 10209−10230.
(167) Zhang, W.; Hu, Y.; Ge, J.; Jiang, H.-L.; Yu, S.-H. A facile and general coating approach to moisture/water-resistant metal-organic frameworks with intact porosity. *J. Am. Chem. Soc.* **2014**, *136*, 16978−16981.
(168) Ding, M.; Jiang, H.-L. Improving water stability of metal-organic frameworks by a general surface hydrophobic polymerization. *CCS Chem.* **2020**, *2*, 2740−2748.
(169) Yoo, Y.; Jeong, H.-K. Generation of covalently functionalized hierarchical IRMOF-3 by post-synthetic modification. *Chem. Eng. J.* **2012**, *181*, 740−745.
(170) Wang, G.; Xu, Z.; Chen, Z.; Niu, W.; Zhou, Y.; Guo, J.; Tan, L. Sequential binding of large molecules to hairy MOFs. *Chem. Commun.* **2013**, *49*, 6641−6643.
(171) Wee, L. H.; Lescouet, T.; Ethiraj, J.; Bonino, F.; Vidruk, R.; Garrier, E.; Packet, D.; Bordiga, S.; Farrusseng, D.; Herskowitz, M.; et al. Hierarchical zeolitic imidazolate framework-8 catalyst for monoglyceride synthesis. *ChemCatChem* **2013**, *5*, 3562−3566.
(172) Ahmed, A.; Hodgson, N.; Barrow, M.; Clowes, R.; Robertson, C. M.; Steiner, A.; McKeown, P.; Bradshaw, D.; Myers, P.; Zhang, H. Macroporous metal-organic framework microparticles with improved liquid phase separation. *J. Mater. Chem. A* **2014**, *2*, 9085−9090.
(173) El-Hankari, S.; Huo, J.; Ahmed, A.; Zhang, H.; Bradshaw, D. Surface etching of HKUST-1 promoted via supramolecular interactions for chromatography. *J. Mater. Chem. A* **2014**, *2*, 13479−13485.
(174) Kim, Y.; Yang, T.; Yun, G.; Ghasemian, M. B.; Koo, J.; Lee, E.; Cho, S. J.; Kim, K. Hydrolytic transformation of microporous metal-organic frameworks to hierarchical micro-and mesoporous MOFs. *Angew. Chem., Int. Ed.* **2015**, *54*, 13273−13278.
(175) Mao, Y.; Chen, D.; Hu, P.; Guo, Y.; Ying, Y.; Ying, W.; Peng, X. Hierarchical mesoporous metal-organic frameworks for enhanced CO_2 capture. *Chem. - Eur. J.* **2015**, *21*, 15127−15132.
(176) Abdelhamid, H. N.; Huang, Z.; El-Zohry, A. M.; Zheng, H.; Zou, X. A fast and scalable approach for synthesis of hierarchical porous zeolitic imidazolate frameworks and one-pot encapsulation of target molecules. *Inorg. Chem.* **2017**, *56*, 9139−9146.
(177) Dou, S.; Dong, C. L.; Hu, Z.; Huang, Y. C.; Chen, J. L.; Tao, L.; Yan, D.; Chen, D.; Shen, S.; Chou, S.; et al. Atomic-scale CoO_x species in metal-organic frameworks for oxygen evolution reaction. *Adv. Funct. Mater.* **2017**, *27*, 1702546.
(178) Koo, J.; Hwang, I.-C.; Yu, X.; Saha, S.; Kim, Y.; Kim, K. Hollowing out MOFs: hierarchical micro-and mesoporous MOFs with tailorable porosity via selective acid etching. *Chem. Sci.* **2017**, *8*, 6799−6803.
(179) Guillerm, V.; Xu, H.; Albalad, J.; Imaz, I.; Maspoch, D. Postsynthetic selective ligand cleavage by solid-gas phase ozonolysis fuses micropores into mesopores in metal-organic frameworks. *J. Am. Chem. Soc.* **2018**, *140*, 15022−15030.
(180) Liu, T.; Liu, Y.; Yao, L.; Yang, W.; Tian, L.; Liu, H.; Liu, D.; Wang, C. Controllable formation of meso-and macropores within metal-organic framework crystals via a citric acid modulator. *Nanoscale* **2018**, *10*, 13194−13201.
(181) Yang, P.; Mao, F.; Li, Y.; Zhuang, Q.; Gu, J. Hierarchical porous Zr-based MOFs synthesized by a facile monocarboxylic acid etching strategy. *Chem. - Eur. J.* **2018**, *24*, 2962−2970.
(182) Yang, X.; Wu, S.; Wang, P.; Yang, L. Hierarchical 3D ordered meso-/macroporous metal-organic framework produced through a facile template-free self-assembly. *J. Solid State Chem.* **2018**, *258*, 220−224.
(183) Chang, G. G.; Ma, X. C.; Zhang, Y. X.; Wang, L. Y.; Tian, G.; Liu, J. W.; Wu, J.; Hu, Z. Y.; Yang, X. Y.; Chen, B. Construction of hierarchical metal-organic frameworks by competitive coordination strategy for highly efficient CO_2 conversion. *Adv. Mater.* **2019**, *31*, 1904969.
(184) Doan, H. V.; Sartbaeva, A.; Eloi, J.-C.; Davis, S. A.; Ting, V. P. Defective hierarchical porous copper-based metal-organic frameworks synthesised via facile acid etching strategy. *Sci. Rep.* **2019**, *9*, 10887.
(185) Qi, S. C.; Qian, X. Y.; He, Q. X.; Miao, K. J.; Jiang, Y.; Tan, P.; Liu, X. Q.; Sun, L. B. Generation of hierarchical porosity in metal-organic frameworks by the modulation of cation valence. *Angew. Chem., Int. Ed.* **2019**, *58*, 10104−10109.
(186) Lee, S.; Oh, S.; Oh, M. Atypical hybrid metal-organic frameworks (MOFs): a combinative process for MOF-on-MOF growth, etching, and structure transformation. *Angew. Chem., Int. Ed.* **2020**, *59*, 1327−1333.
(187) Gadipelli, S.; Guo, Z. Postsynthesis annealing of MOF-5 remarkably enhances the framework structural stability and CO_2 uptake. *Chem. Mater.* **2014**, *26*, 6333−6338.
(188) Bueken, B.; Van Velthoven, N.; Krajnc, A.; Smolders, S.; Taulelle, F.; Mellot-Draznieks, C.; Mali, G.; Bennett, T. D.; De Vos, D. Tackling the defect conundrum in UiO-66: a mixed-linker approach to engineering missing linker defects. *Chem. Mater.* **2017**, *29*, 10478−10486.
(189) Chen, S.; Mukherjee, S.; Lucier, B. E.; Guo, Y.; Wong, Y. A.; Terskikh, V. V.; Zaworotko, M. J.; Huang, Y. Cleaving carboxyls: understanding thermally triggered hierarchical pores in the metal-organic framework MIL-121. *J. Am. Chem. Soc.* **2019**, *141*, 14257−14271.
(190) Jeong, G.-Y.; Singh, A. K.; Kim, M.-G.; Gyak, K.-W.; Ryu, U.; Choi, K. M.; Kim, D.-P. Metal-organic framework patterns and membranes with heterogeneous pores for flow-assisted switchable separations. *Nat. Commun.* **2018**, *9*, 3968.
(191) Meng, F.; Zhang, S.; Ma, L.; Zhang, W.; Li, M.; Wu, T.; Li, H.; Zhang, T.; Lu, X.; Huo, F.; Lu, J. Construction of hierarchically porous nanoparticles@metal-organic frameworks composites by inherent defects for the enhancement of catalytic efficiency. *Adv. Mater.* **2018**, *30*, 1803263.
(192) Junggeburth, S. C.; Schwinghammer, K.; Virdi, K. S.; Scheu, C.; Lotsch, B. V. Towards mesostructured zinc imidazolate frameworks. *Chem. - Eur. J.* **2012**, *18*, 2143−2152.
(193) Wee, L. H.; Meledina, M.; Turner, S.; Van Tendeloo, G.; Zhang, K.; Rodriguez-Albelo, L. M.; Masala, A.; Bordiga, S.; Jiang, J.; Navarro, J. A.; et al. 1D-2D-3D transformation synthesis of hierarchical metal-organic framework adsorbent for multicomponent alkane separation. *J. Am. Chem. Soc.* **2017**, *139*, 819−828.
(194) Liu, D.; Wan, J.; Pang, G.; Tang, Z. Hollow metal-organic-framework micro/nanostructures and their derivatives: emerging multifunctional materials. *Adv. Mater.* **2019**, *31*, 1803291.
(195) Kim, H.; Lah, M. S. Templated and template-free fabrication strategies for zero-dimensional hollow MOF superstructures. *Dalton Trans.* **2017**, *46*, 6146−6158.
(196) Xu, X.; Zhang, Z.; Wang, X. Well-defined metal-organic-framework hollow nanostructures for catalytic reactions involving gases. *Adv. Mater.* **2015**, *27*, 5365−5371.
(197) Qiu, T.; Gao, S.; Liang, Z.; Wang, D.-G.; Tabassum, H.; Zhong, R.; Zou, R. Pristine hollow metal-organic frameworks: design, synthesis and application. *Angew. Chem., Int. Ed.* **2021**, DOI: 10.1002/anie.202012699.
(198) Nai, J.; Zhang, J.; Lou, X. W. D. Construction of single-crystalline Prussian blue analog hollow nanostructures with tailorable topologies. *Chem* **2018**, *4*, 1967−1982.

(199) Wang, J.; Wan, J.; Yang, N.; Li, Q.; Wang, D. Hollow multishell structures exercise temporal-spatial ordering and dynamic smart behaviour. *Nat. Rev. Chem.* **2020**, *4*, 159−168.
(200) Xie, X.-C.; Huang, K.-J.; Wu, X. Metal-organic framework derived hollow materials for electrochemical energy storage. *J. Mater. Chem. A* **2018**, *6*, 6754−6771.
(201) Lee, H. J.; Cho, W.; Oh, M. Advanced fabrication of metal-organic frameworks: template-directed formation of polystyrene@ZIF-8 core-shell and hollow ZIF-8 microspheres. *Chem. Commun.* **2012**, *48*, 221−223.
(202) Zhang, F.; Wei, Y.; Wu, X.; Jiang, H.; Wang, W.; Li, H. Hollow zeolitic imidazolate framework nanospheres as highly efficient cooperative catalysts for [3 + 3] cycloaddition reactions. *J. Am. Chem. Soc.* **2014**, *136*, 13963−13966.
(203) Wan, M.; Zhang, X.; Li, M.; Chen, B.; Yin, J.; Jin, H.; Lin, L.; Chen, C.; Zhang, N. Hollow Pd/MOF nanosphere with double shells as multifunctional catalyst for hydrogenation reaction. *Small* **2017**, *13*, 1701395.
(204) Kuo, C.-H.; Tang, Y.; Chou, L.-Y.; Sneed, B. T.; Brodsky, C. N.; Zhao, Z.; Tsung, C.-K. Yolk-shell nanocrystal@ZIF-8 nanostructures for gas-phase heterogeneous catalysis with selectivity control. *J. Am. Chem. Soc.* **2012**, *134*, 14345−14348.
(205) Liu, Y.; Zhang, W.; Li, S.; Cui, C.; Wu, J.; Chen, H.; Huo, F. Designable yolk-shell nanoparticle@MOF petalous heterostructures. *Chem. Mater.* **2014**, *26*, 1119−1125.
(206) Lee, J.; Kwak, J. H.; Choe, W. Evolution of form in metal-organic frameworks. *Nat. Commun.* **2017**, *8*, 14070.
(207) Kim, H.; Oh, M.; Kim, D.; Park, J.; Seong, J.; Kwak, S. K.; Lah, M. S. Single crystalline hollow metal-organic frameworks: a metal-organic polyhedron single crystal as a sacrificial template. *Chem. Commun.* **2015**, *51*, 3678−3681.
(208) Chuan Tan, Y.; Chun Zeng, H. Self-templating synthesis of hollow spheres of MOFs and their derived nanostructures. *Chem. Commun.* **2016**, *52*, 11591−11594.
(209) He, T.; Xu, X.; Ni, B.; Lin, H.; Li, C.; Hu, W.; Wang, X. Metal-organic framework based microcapsules. *Angew. Chem., Int. Ed.* **2018**, *57*, 10148−10152.
(210) Hirai, K.; Reboul, J.; Morone, N.; Heuser, J. E.; Furukawa, S.; Kitagawa, S. Diffusion-coupled molecular assembly: structuring of coordination polymers across multiple length scales. *J. Am. Chem. Soc.* **2014**, *136*, 14966−14973.
(211) Zhang, Z.; Chen, Y.; He, S.; Zhang, J.; Xu, X.; Yang, Y.; Nosheen, F.; Saleem, F.; He, W.; Wang, X. Hierarchical Zn/Ni-MOF-2 nanosheet-assembled hollow nanocubes for multicomponent catalytic reactions. *Angew. Chem., Int. Ed.* **2014**, *53*, 12517−12521.
(212) Yang, J.; Zhang, F.; Lu, H.; Hong, X.; Jiang, H.; Wu, Y.; Li, Y. Hollow Zn/Co ZIF particles derived from core-shell ZIF-67@ZIF-8 as selective catalyst for the semi-hydrogenation of acetylene. *Angew. Chem., Int. Ed.* **2015**, *54*, 10889−10893.
(213) Liu, X. Y.; Zhang, F.; Goh, T. W.; Li, Y.; Shao, Y. C.; Luo, L.; Huang, W.; Long, Y. T.; Chou, L. Y.; Tsung, C. K. Using a multi-shelled hollow metal-organic framework as a host to switch the guest-to-host and guest-to-guest interactions. *Angew. Chem., Int. Ed.* **2018**, *57*, 2110−2114.
(214) Liu, W.; Huang, J.; Yang, Q.; Wang, S.; Sun, X.; Zhang, W.; Liu, J.; Huo, F. Multi-shelled hollow metal-organic frameworks. *Angew. Chem., Int. Ed.* **2017**, *56*, 5512−5516.
(215) Ameloot, R.; Vermoortele, F.; Vanhove, W.; Roeffaers, M. B.; Sels, B. F.; De Vos, D. E. Interfacial synthesis of hollow metal-organic framework capsules demonstrating selective permeability. *Nat. Chem.* **2011**, *3*, 382−387.
(216) Yang, Y.; Wang, F.; Yang, Q.; Hu, Y.; Yan, H.; Chen, Y.-Z.; Liu, H.; Zhang, G.; Lu, J.; Jiang, H.-L.; Xu, H. Hollow metal-organic framework nanospheres via emulsion-based interfacial synthesis and their application in size-selective catalysis. *ACS Appl. Mater. Interfaces* **2014**, *6*, 18163−18171.
(217) Jeong, G.-Y.; Ricco, R.; Liang, K.; Ludwig, J.; Kim, J.-O.; Falcaro, P.; Kim, D.-P. Bioactive MIL-88A framework hollow spheres via interfacial reaction in-droplet microfluidics for enzyme and nanoparticle encapsulation. *Chem. Mater.* **2015**, *27*, 7903−7909.
(218) Huo, J.; Marcello, M.; Garai, A.; Bradshaw, D. MOF−polymer composite microcapsules derived from pickering emulsions. *Adv. Mater.* **2013**, *25*, 2717−2722.
(219) Huo, J.; Aguilera-Sigalat, J.; El-Hankari, S.; Bradshaw, D. Magnetic MOF microreactors for recyclable size-selective biocatalysis. *Chem. Sci.* **2015**, *6*, 1938−1943.
(220) Pang, M.; Cairns, A. J.; Liu, Y.; Belmabkhout, Y.; Zeng, H. C.; Eddaoudi, M. Synthesis and integration of Fe-soc-MOF cubes into colloidosomes via a single-step emulsion-based approach. *J. Am. Chem. Soc.* **2013**, *135*, 10234−10237.
(221) Zhu, X.; Zhang, S.; Zhang, L.; Liu, H.; Hu, J. Interfacial synthesis of magnetic PMMA@Fe_3O_4/$Cu_3(BTC)_2$ hollow microspheres through one-pot Pickering emulsion and their application as drug delivery. *RSC Adv.* **2016**, *6*, 58511−58515.
(222) Yang, Y.; Jin, S.; Zhang, Z.; Du, Z.; Liu, H.; Yang, J.; Xu, H.; Ji, H. Nitrogen-doped hollow carbon nanospheres for high-performance Li-ion batteries. *ACS Appl. Mater. Interfaces* **2017**, *9*, 14180−14186.
(223) Hu, M.; Furukawa, S.; Ohtani, R.; Sukegawa, H.; Nemoto, Y.; Reboul, J.; Kitagawa, S.; Yamauchi, Y. Synthesis of prussian blue nanoparticles with a hollow interior by controlled chemical etching. *Angew. Chem., Int. Ed.* **2012**, *51*, 984−988.
(224) Cai, X.; Deng, X.; Xie, Z.; Bao, S.; Shi, Y.; Lin, J.; Pang, M.; Eddaoudi, M. Synthesis of highly monodispersed Ga-soc-MOF hollow cubes, colloidosomes and nanocomposites. *Chem. Commun.* **2016**, *52*, 9901−9904.
(225) Hu, M.; Ju, Y.; Liang, K.; Suma, T.; Cui, J.; Caruso, F. Void engineering in metal-organic frameworks via synergistic etching and surface functionalization. *Adv. Funct. Mater.* **2016**, *26*, 5827−5834.
(226) Tang, L.; Zhang, S.; Wu, Q.; Wang, X.; Wu, H.; Jiang, Z. Heterobimetallic metal-organic framework nanocages as highly efficient catalysts for CO_2 conversion under mild conditions. *J. Mater. Chem. A* **2018**, *6*, 2964−2973.
(227) Hu, M.; Torad, N. L.; Yamauchi, Y. Preparation of various prussian blue analogue hollow nanocubes with single crystalline shells. *Eur. J. Inorg. Chem.* **2012**, *2012*, 4795−4799.
(228) Zhou, M.; Li, J.; Zhang, M.; Wang, H.; Lan, Y.; Wu, Y.-N.; Li, F.; Li, G. A polydopamine layer as the nucleation center of MOF deposition on "inert" polymer surfaces to fabricate hierarchically structured porous films. *Chem. Commun.* **2015**, *51*, 2706−2709.
(229) Yu, L.; Yang, J. F.; Lou, X. W. Formation of CoS_2 nanobubble hollow prisms for highly reversible lithium storage. *Angew. Chem., Int. Ed.* **2016**, *55*, 13422−13426.
(230) Alizadeh, S.; Nematollahi, D. Electrochemically assisted self-assembly technique for the fabrication of mesoporous metal-organic framework thin films: composition of 3D hexagonally packed crystals with 2D honeycomb-like mesopores. *J. Am. Chem. Soc.* **2017**, *139*, 4753−4761.
(231) Xu, X.; Chen, S.; Chen, Y.; Sun, H.; Song, L.; He, W.; Wang, X. Polyoxometalate cluster-incorporated metal-organic framework hierarchical nanotubes. *Small* **2016**, *12*, 2982−2990.
(232) Tang, J.; Chen, X.; Zhang, L.; Yang, M.; Wang, P.; Dong, W.; Wang, G.; Yu, F.; Tao, J. Alkylated meso-macroporous metal-organic framework hollow tubes as nanocontainers of octadecane for energy storage and thermal regulation. *Small* **2018**, *14*, 1801970.
(233) Li, W.; Zhang, Y.; Li, Q.; Zhang, G. Metal-organic framework composite membranes: synthesis and separation applications. *Chem. Eng. Sci.* **2015**, *135*, 232−257.
(234) Li, S.; Huo, F. Metal-organic framework composites: from fundamentals to applications. *Nanoscale* **2015**, *7*, 7482−7501.
(235) Li, S.; Yang, K.; Tan, C.; Huang, X.; Huang, W.; Zhang, H. Preparation and applications of novel composites composed of metal-organic frameworks and two-dimensional materials. *Chem. Commun.* **2016**, *52*, 1555−1562.
(236) Liu, X.-W.; Sun, T.-J.; Hu, J.-L.; Wang, S.-D. Composites of metal-organic frameworks and carbon-based materials: preparations, functionalities and applications. *J. Mater. Chem. A* **2016**, *4*, 3584−3616.

https://doi.org/10.1021/acs.chemrev.1c00243
Chem. Rev. 2021, 121, 12278−12326

(237) Zheng, Y.; Zheng, S.; Xue, H.; Pang, H. Metal-organic frameworks/graphene-based materials: preparations and applications. *Adv. Funct. Mater.* **2018**, *28*, 1804950.
(238) Ma, X.; Chai, Y.; Li, P.; Wang, B. Metal-organic framework films and their potential applications in environmental pollution control. *Acc. Chem. Res.* **2019**, *52*, 1461−1470.
(239) Xiao, X.; Zou, L.; Pang, H.; Xu, Q. Synthesis of micro/nanoscaled metal-organic frameworks and their direct electrochemical applications. *Chem. Soc. Rev.* **2020**, *49*, 301−331.
(240) Yi, F. Y.; Zhang, R.; Wang, H.; Chen, L. F.; Han, L.; Jiang, H. L.; Xu, Q. Metal-organic frameworks and their composites: synthesis and electrochemical applications. *Small Methods* **2017**, *1*, 1700187.
(241) Górka, J.; Fulvio, P. F.; Pikus, S.; Jaroniec, M. Mesoporous metal organic framework-boehmite and silica composites. *Chem. Commun.* **2010**, *46*, 6798−6800.
(242) Seo, Y.-K.; Yoon, J. W.; Lee, U.-H.; Hwang, Y. K.; Jun, C.-H.; Chang, J.-S. Formation of a nanohybrid composite between mesostructured cellular silica foam and microporous copper trimesate. *Microporous Mesoporous Mater.* **2012**, *155*, 75−81.
(243) Cirujano, F. G.; Luz, I.; Soukri, M.; Van Goethem, C.; Vankelecom, I. F.; Lail, M.; De Vos, D. E. Boosting the catalytic performance of metal-organic frameworks for steroid transformations by confinement within a mesoporous scaffold. *Angew. Chem., Int. Ed.* **2017**, *56*, 13302−13306.
(244) Schwab, M. G.; Senkovska, I.; Rose, M.; Koch, M.; Pahnke, J.; Jonschker, G.; Kaskel, S. MOF@polyhipes. *Adv. Eng. Mater.* **2008**, *10*, 1151−1155.
(245) O'Neill, L. D.; Zhang, H.; Bradshaw, D. Macro-/microporous MOF composite beads. *J. Mater. Chem.* **2010**, *20*, 5720−5726.
(246) Pinto, M. S. L.; Dias, S.; Pires, J. O. Composite MOF foams: the example of UiO-66/polyurethane. *ACS Appl. Mater. Interfaces* **2013**, *5*, 2360−2363.
(247) Kovačič, S.; Mazaj, M.; Ješelnik, M.; Pahovnik, D.; Žagar, E.; Slugovc, C.; Logar, N. Z. Synthesis and catalytic performance of hierarchically porous MIL-100(Fe)@polyHIPE hybrid membranes. *Macromol. Rapid Commun.* **2015**, *36*, 1605−1611.
(248) Jin, P.; Tan, W.; Huo, J.; Liu, T.; Liang, Y.; Wang, S.; Bradshaw, D. Hierarchically porous MOF/polymer composites via interfacial nanoassembly and emulsion polymerization. *J. Mater. Chem. A* **2018**, *6*, 20473−20479.
(249) Jiang, Z.-R.; Ge, J.; Zhou, Y.-X.; Wang, Z. U.; Chen, D.; Yu, S.-H.; Jiang, H.-L. Coating sponge with a hydrophobic porous coordination polymer containing a low-energy CF_3-decorated surface for continuous pumping recovery of an oil spill from water. *NPG Asia Mater.* **2016**, *8*, No. e253.
(250) Huang, N.; Drake, H.; Li, J.; Pang, J.; Wang, Y.; Yuan, S.; Wang, Q.; Cai, P.; Qin, J.; Zhou, H. C. Flexible and hierarchical metal-organic framework composites for high-performance catalysis. *Angew. Chem., Int. Ed.* **2018**, *57*, 8916−8920.
(251) Fu, Q.; Wen, L.; Zhang, L.; Chen, X.; Pun, D.; Ahmed, A.; Yang, Y.; Zhang, H. Preparation of ice-templated MOF−polymer composite monoliths and their application for wastewater treatment with high capacity and easy recycling. *ACS Appl. Mater. Interfaces* **2017**, *9*, 33979−33988.
(252) Li, W.; Zhang, Y.; Xu, Z.; Meng, Q.; Fan, Z.; Ye, S.; Zhang, G. Assembly of MOF microcapsules with size-selective permeability on cell walls. *Angew. Chem., Int. Ed.* **2016**, *55*, 955−959.
(253) Liang, K.; Richardson, J. J.; Cui, J.; Caruso, F.; Doonan, C. J.; Falcaro, P. Metal-organic framework coatings as cytoprotective exoskeletons for living cells. *Adv. Mater.* **2016**, *28*, 7910−7914.
(254) Li, Z.; Zeng, H. C. Armored MOFs: enforcing soft microporous MOF nanocrystals with hard mesoporous silica. *J. Am. Chem. Soc.* **2014**, *136*, 5631−5639.
(255) Bao, S.; Li, J.; Guan, B.; Jia, M.; Terasaki, O.; Yu, J. A green selective water-etching approach to MOF@mesoporous SiO_2 yolk-shell nanoreactors with enhanced catalytic stabilities. *Matter* **2020**, *3*, 498−508.
(256) Zhang, Y.; Feng, X.; Li, H.; Chen, Y.; Zhao, J.; Wang, S.; Wang, L.; Wang, B. Photoinduced postsynthetic polymerization of a metal-organic framework toward a flexible stand-alone membrane. *Angew. Chem., Int. Ed.* **2015**, *54*, 4259−4263.
(257) Li, W.; Zhang, Y.; Xu, Z.; Meng, Q.; Fan, Z.; Ye, S.; Zhang, G. Assembly of MOF microcapsules with size-selective permeability on cell walls. *Angew. Chem.* **2016**, *128*, 967−971.
(258) Zheng, Y.; Zheng, S.; Xue, H.; Pang, H. Metal-organic frameworks for lithium-sulfur batteries. *J. Mater. Chem. A* **2019**, *7*, 3469−3491.
(259) Wisser, D.; Wisser, F. M.; Raschke, S.; Klein, N.; Leistner, M.; Grothe, J.; Brunner, E.; Kaskel, S. Biological chitin-MOF composites with hierarchical pore systems for air-filtration applications. *Angew. Chem., Int. Ed.* **2015**, *54*, 12588−12591.
(260) Zhang, H.; Zhao, W.; Wu, Y.; Wang, Y.; Zou, M.; Cao, A. Dense monolithic MOF and carbon nanotube hybrid with enhanced volumetric and areal capacities for lithium-sulfur battery. *J. Mater. Chem. A* **2019**, *7*, 9195−9201.
(261) Kim, D.; Kim, D. W.; Hong, W. G.; Coskun, A. Graphene/ZIF-8 composites with tunable hierarchical porosity and electrical conductivity. *J. Mater. Chem. A* **2016**, *4*, 7710−7717.
(262) Jayaramulu, K.; Datta, K. K. R.; Rösler, C.; Petr, M.; Otyepka, M.; Zboril, R.; Fischer, R. A. Biomimetic superhydrophobic/superoleophilic highly fluorinated graphene oxide and ZIF-8 composites for oil-water separation. *Angew. Chem., Int. Ed.* **2016**, *55*, 1178−1182.
(263) Jayaramulu, K.; Geyer, F.; Petr, M.; Zboril, R.; Vollmer, D.; Fischer, R. A. Shape controlled hierarchical porous hydrophobic/oleophilic metal-organic nanofibrous gel composites for oil adsorption. *Adv. Mater.* **2017**, *29*, 1605307.
(264) Wang, F.; Chen, X.; Chen, L.; Yang, J.; Wang, Q. High-performance non-enzymatic glucose sensor by hierarchical flower-like nickel(II)-based MOF/carbon nanotubes composite. *Mater. Sci. Eng., C* **2019**, *96*, 41−50.
(265) Ma, X.; Fang, W.; Guo, Y.; Li, Z.; Chen, D.; Ying, W.; Xu, Z.; Gao, C.; Peng, X. Hierarchical porous SWCNT stringed carbon polyhedrons and PSS threaded MOF bilayer membrane for efficient solar vapor generation. *Small* **2019**, *15*, 1900354.
(266) Zhang, Y.; Yuan, S.; Feng, X.; Li, H.; Zhou, J.; Wang, B. Preparation of nanofibrous metal-organic framework filters for efficient air pollution control. *J. Am. Chem. Soc.* **2016**, *138*, 5785−5788.
(267) Chen, Y.; Zhang, S.; Cao, S.; Li, S.; Chen, F.; Yuan, S.; Xu, C.; Zhou, J.; Feng, X.; Ma, X.; et al. Roll-to-roll production of metal-organic framework coatings for particulate matter removal. *Adv. Mater.* **2017**, *29*, 1606221.
(268) Chen, Y.; Zhang, S.; Chen, F.; Cao, S.; Cai, Y.; Li, S.; Ma, H.; Ma, X.; Li, P.; Huang, X.; et al. Defect engineering of highly stable lanthanide metal-organic frameworks by particle modulation for coating catalysis. *J. Mater. Chem. A* **2018**, *6*, 342−348.
(269) Li, P.; Li, J.; Feng, X.; Li, J.; Hao, Y.; Zhang, J.; Wang, H.; Yin, A.; Zhou, J.; Ma, X.; et al. Metal-organic frameworks with photocatalytic bactericidal activity for integrated air cleaning. *Nat. Commun.* **2019**, *10*, 2177.
(270) Wang, H.; Zhao, S.; Liu, Y.; Yao, R.; Wang, X.; Cao, Y.; Ma, D.; Zou, M.; Cao, A.; Feng, X.; et al. Membrane adsorbers with ultrahigh metal-organic framework loading for high flux separations. *Nat. Commun.* **2019**, *10*, 4024.
(271) Zhan, W.-W.; Kuang, Q.; Zhou, J.-Z.; Kong, X.-J.; Xie, Z.-X.; Zheng, L.-S. Semiconductor@metal-organic framework core-shell heterostructures: a case of ZnO@ZIF-8 nanorods with selective photoelectrochemical response. *J. Am. Chem. Soc.* **2013**, *135*, 1926−1933.
(272) Yao, M. S.; Tang, W. X.; Wang, G. E.; Nath, B.; Xu, G. MOF thin film-coated metal oxide nanowire array: significantly improved chemiresistor sensor performance. *Adv. Mater.* **2016**, *28*, 5229−5234.
(273) Deng, T.; Lu, Y.; Zhang, W.; Sui, M.; Shi, X.; Wang, D.; Zheng, W. Inverted design for high-performance supercapacitor via Co $(OH)_2$-derived highly oriented MOF electrodes. *Adv. Energy Mater.* **2018**, *8*, 1702294.

https://doi.org/10.1021/acs.chemrev.1c00243
Chem. Rev. 2021, 121, 12278−12326

(274) Duan, J.; Chen, S.; Zhao, C. Ultrathin metal-organic framework array for efficient electrocatalytic water splitting. *Nat. Commun.* **2017**, *8*, 15341.
(275) Falcaro, P.; Okada, K.; Hara, T.; Ikigaki, K.; Tokudome, Y.; Thornton, A. W.; Hill, A. J.; Williams, T.; Doonan, C.; Takahashi, M. Centimetre-scale micropore alignment in oriented polycrystalline metal-organic framework films via heteroepitaxial growth. *Nat. Mater.* **2017**, *16*, 342−348.
(276) Cai, D.; Liu, B.; Wang, D.; Wang, L.; Liu, Y.; Qu, B.; Duan, X.; Li, Q.; Wang, T. Rational synthesis of metal-organic framework composites, hollow structures and their derived porous mixed metal oxide hollow structures. *J. Mater. Chem. A* **2016**, *4*, 183−192.
(277) Shen, K.; Chen, X.; Chen, J.; Li, Y. Development of MOF-derived carbon-based nanomaterials for efficient catalysis. *ACS Catal.* **2016**, *6*, 5887−5903.
(278) Indra, A.; Song, T.; Paik, U. Metal organic framework derived materials: progress and prospects for the energy conversion and storage. *Adv. Mater.* **2018**, *30*, 1705146.
(279) Zhang, H.; Liu, X.; Wu, Y.; Guan, C.; Cheetham, A. K.; Wang, J. MOF-derived nanohybrids for electrocatalysis and energy storage: current status and perspectives. *Chem. Commun.* **2018**, *54*, 5268−5288.
(280) Zou, G.; Hou, H.; Ge, P.; Huang, Z.; Zhao, G.; Yin, D.; Ji, X. Metal-organic framework-derived materials for sodium energy storage. *Small* **2018**, *14*, 1702648.
(281) Zou, K. Y.; Li, Z. X. Controllable syntheses of MOF-derived materials. *Chem. - Eur. J.* **2018**, *24*, 6506−6518.
(282) Liang, Z.; Zhao, R.; Qiu, T.; Zou, R.; Xu, Q. Metal-organic framework-derived materials for electrochemical energy applications. *EnergyChem.* **2019**, *1*, 100001.
(283) Wen, X.; Guan, J. Recent progress on MOF-derived electrocatalysts for hydrogen evolution reaction. *Appl. Mater. Today* **2019**, *16*, 146−168.
(284) Yang, S.; Peng, L.; Bulut, S.; Queen, W. L. Recent advances of MOFs and MOF-derived materials in thermally driven organic transformations. *Chem. - Eur. J.* **2019**, *25*, 2161−2178.
(285) Yang, W.; Li, X.; Li, Y.; Zhu, R.; Pang, H. Applications of metal-organic-framework-derived carbon materials. *Adv. Mater.* **2018**, *31*, 1804740.
(286) Zhang, X.; Chen, A.; Zhong, M.; Zhang, Z.; Zhang, X.; Zhou, Z.; Bu, X.-H. Metal-organic frameworks (MOFs) and MOF-derived materials for energy storage and conversion. *Electrochem. Energy Rev.* **2019**, *2*, 29−104.
(287) Zhong, M.; Kong, L.; Li, N.; Liu, Y.-Y.; Zhu, J.; Bu, X.-H. Synthesis of MOF-derived nanostructures and their applications as anodes in lithium and sodium ion batteries. *Coord. Chem. Rev.* **2019**, *388*, 172−201.
(288) Konnerth, H.; Matsagar, B. M.; Chen, S. S.; Prechtl, M. H.; Shieh, F.-K.; Wu, K. C.-W. Metal-organic framework (MOF)-derived catalysts for fine chemical production. *Coord. Chem. Rev.* **2020**, *416*, 213319.
(289) Wang, Q.; Astruc, D. State of the art and prospects in metal-organic framework (MOF)-based and MOF-derived nanocatalysis. *Chem. Rev.* **2020**, *120*, 1438−1511.
(290) Yang, H.; Peng, F.; Dang, C.; Wang, Y.; Hu, D.; Zhao, X.; Feng, P.; Bu, X. Ligand charge separation to build highly stable quasi-isomer of MOF-74-Zn. *J. Am. Chem. Soc.* **2019**, *141*, 9808−9812.
(291) Chen, L.; Tsumori, N.; Xu, Q. Quasi-MOF-immobilized metal nanoparticles for synergistic catalysis. *Sci. China: Chem.* **2020**, *63*, 1601−1607.
(292) Tsumori, N.; Chen, L.; Wang, Q.; Zhu, Q.-L.; Kitta, M.; Xu, Q. Quasi-MOF: exposing inorganic nodes to guest metal nanoparticles for drastically enhanced catalytic activity. *Chem* **2018**, *4*, 845−856.
(293) Lu, M.; Hou, H.; Wei, C.; Guan, X.; Wei, W.; Wang, G.-S. Preparation of quasi-MIL-101(Cr) loaded ceria catalysts for the selective catalytic reduction of NO_x at low temperature. *Catalysts* **2020**, *10*, 140.
(294) Liu, B.; Han, W.; Li, X.; Li, L.; Tang, H.; Lu, C.; Li, Y.; Li, X. Quasi metal organic framework with highly concentrated Cr_2O_3 molecular clusters as the efficient catalyst for dehydrofluorination of 1, 1, 1, 3, 3-pentafluoropropane. *Appl. Catal., B* **2019**, *257*, 117939.
(295) Zhu, R.; Ding, J.; Yang, J.; Pang, H.; Xu, Q.; Zhang, D.; Braunstein, P. Quasi-ZIF-67 for boosted oxygen evolution reaction catalytic activity via a low temperature calcination. *ACS Appl. Mater. Interfaces* **2020**, *12*, 25037−25041.
(296) Liao, X.; Zhang, M.; Wang, X.; Zhou, Y.; Wang, F.; Chen, L.; Yao, Y.; Lu, S. Vacuum degassed treatment for fabricating quasi-MIL-125(Ti) with enhanced catalytic oxidative desulfurization activity. *Microporous Mesoporous Mater.* **2020**, *308*, 110529.
(297) Dong, P.; Wang, H.; Liu, W.; Wang, S.; Wang, Y.; Zhang, J.; Lin, F.; Wang, Y.; Zhao, C.; Duan, X.; et al. Quasi-MOF derivative-based electrode for efficient electro-Fenton oxidation. *J. Hazard. Mater.* **2021**, *401*, 123423.
(298) Shen, Y.; Bao, L.-W.; Sun, F.-Z.; Hu, T.-L. A novel Cu-nanowire@quasi-MOF via mild pyrolysis of a bimetal-MOF for the selective oxidation of benzyl alcohol in air. *Mater. Chem. Front.* **2019**, *3*, 2363−2373.
(299) Cui, W.-G.; Li, Y.-T.; Zhang, H.; Wei, Z.-C.; Gao, B.-H.; Dai, J.-J.; Hu, T.-L. In situ encapsulated Co/MnO_x nanoparticles inside quasi-MOF-74 for the higher alcohols synthesis from syngas. *Appl. Catal., B* **2020**, *278*, 119262.
(300) Pan, T.; Shen, Y.; Wu, P.; Gu, Z.; Zheng, B.; Wu, J.; Li, S.; Fu, Y.; Zhang, W.; Huo, F. Thermal shrinkage behavior of metalorganic frameworks. *Adv. Funct. Mater.* **2020**, *30*, 2001389.
(301) Jiao, L.; Jiang, H.-L. Metal-organic-framework-based single-atom catalysts for energy applications. *Chem* **2019**, *5*, 786−804.
(302) Jeoung, S.; Ju, I. T.; Kim, J. H.; Joo, S. H.; Moon, H. R. Hierarchically porous adamantane-shaped carbon nanoframes. *J. Mater. Chem. A* **2018**, *6*, 18906−18911.
(303) Lee, K. J.; Choi, S.; Park, S.; Moon, H. R. General recyclable redox-metallothermic reaction route to hierarchically porous carbon/metal composites. *Chem. Mater.* **2016**, *28*, 4403−4408.
(304) Lee, K. J.; Sa, Y. J.; Jeong, H. Y.; Bielawski, C. W.; Joo, S. H.; Moon, H. R. Simple coordination complex-derived three-dimensional mesoporous graphene as an efficient bifunctional oxygen electrocatalyst. *Chem. Commun.* **2015**, *51*, 6773−6776.
(305) Liu, B.; Shioyama, H.; Akita, T.; Xu, Q. Metal-organic framework as a template for porous carbon synthesis. *J. Am. Chem. Soc.* **2008**, *130*, 5390−5391.
(306) Jiang, H.-L.; Liu, B.; Lan, Y.-Q.; Kuratani, K.; Akita, T.; Shioyama, H.; Zong, F.; Xu, Q. From metal-organic framework to nanoporous carbon: toward a very high surface area and hydrogen uptake. *J. Am. Chem. Soc.* **2011**, *133*, 11854−11857.
(307) Hu, M.; Reboul, J.; Furukawa, S.; Torad, N. L.; Ji, Q.; Srinivasu, P.; Ariga, K.; Kitagawa, S.; Yamauchi, Y. Direct carbonization of Al-based porous coordination polymer for synthesis of nanoporous carbon. *J. Am. Chem. Soc.* **2012**, *134*, 2864−2867.
(308) Kaneti, Y. V.; Tang, J.; Salunkhe, R. R.; Jiang, X.; Yu, A.; Wu, K. C. W.; Yamauchi, Y. Nanoarchitectured design of porous materials and nanocomposites from metal-organic frameworks. *Adv. Mater.* **2017**, *29*, 1604898.
(309) Zhang, W.; Wu, Z.-Y.; Jiang, H.-L.; Yu, S.-H. Nanowire-directed templating synthesis of metal-organic framework nanofibers and their derived porous doped carbon nanofibers for enhanced electrocatalysis. *J. Am. Chem. Soc.* **2014**, *136*, 14385−14388.
(310) Lai, Q.; Zhao, Y.; Liang, Y.; He, J.; Chen, J. In situ confinement pyrolysis transformation of ZIF-8 to nitrogen-enriched meso-microporous carbon frameworks for oxygen reduction. *Adv. Funct. Mater.* **2016**, *26*, 8334−8344.
(311) Zhang, W.; Cai, G.; Wu, R.; He, Z.; Yao, H. B.; Jiang, H. L.; Yu, S. H. Templating synthesis of metal-organic framework nanofiber aerogels and their derived hollow porous carbon nanofibers for energy storage and conversion. *Small* **2021**, 2004140.
(312) Sun, J.-K.; Xu, Q. From metal-organic framework to carbon: toward controlled hierarchical pore structures via a double-template approach. *Chem. Commun.* **2014**, *50*, 13502−13505.

https://doi.org/10.1021/acs.chemrev.1c00243
Chem. Rev. 2021, 121, 12278−12326

(313) Zhang, L.; Wu, H. B.; Madhavi, S.; Hng, H. H.; Lou, X. W. Formation of Fe_2O_3 microboxes with hierarchical shell structures from metal-organic frameworks and their lithium storage properties. *J. Am. Chem. Soc.* **2012**, *134*, 17388−17391.
(314) Jiang, Z.; Li, Z.; Qin, Z.; Sun, H.; Jiao, X.; Chen, D. LDH nanocages synthesized with MOF templates and their high performance as supercapacitors. *Nanoscale* **2013**, *5*, 11770−11775.
(315) He, P.; Yu, X. Y.; Lou, X. W. Carbon-incorporated nickel-cobalt mixed metal phosphide nanoboxes with enhanced electrocatalytic activity for oxygen evolution. *Angew. Chem., Int. Ed.* **2017**, *56*, 3897−3900.
(316) Liu, X.; Liu, Y.; Fan, L.-Z. MOF-derived $CoSe_2$ microspheres with hollow interiors as high-performance electrocatalysts for the enhanced oxygen evolution reaction. *J. Mater. Chem. A* **2017**, *5*, 15310−15314.
(317) Shang, L.; Yu, H.; Huang, X.; Bian, T.; Shi, R.; Zhao, Y.; Waterhouse, G. I.; Wu, L. Z.; Tung, C. H.; Zhang, T. Well-dispersed ZIF-derived Co, N-co-doped carbon nanoframes through mesoporous-silica-protected calcination as efficient oxygen reduction electrocatalysts. *Adv. Mater.* **2016**, *28*, 1668−1674.
(318) Li, Y.; Zhou, Y.-X.; Ma, X.; Jiang, H.-L. A metal-organic framework-templated synthesis of γ-Fe_2O_3 nanoparticles encapsulated in porous carbon for efficient and chemoselective hydrogenation of nitro compounds. *Chem. Commun.* **2016**, *52*, 4199−4202.
(319) Ma, X.; Zhou, Y.-X.; Liu, H.; Li, Y.; Jiang, H.-L. A MOF-derived Co-CoO@N-doped porous carbon for efficient tandem catalysis: dehydrogenation of ammonia borane and hydrogenation of nitro compounds. *Chem. Commun.* **2016**, *52*, 7719−7722.
(320) Khaletskaya, K.; Pougin, A.; Medishetty, R.; Rösler, C.; Wiktor, C.; Strunk, J.; Fischer, R. A. Fabrication of gold/titania photocatalyst for CO_2 reduction based on pyrolytic conversion of the metal-organic framework NH_2-MIL-125(Ti) loaded with gold nanoparticles. *Chem. Mater.* **2015**, *27*, 7248−7257.
(321) Ji, D.; Zhou, H.; Zhang, J.; Dan, Y.; Yang, H.; Yuan, A. Facile synthesis of a metal-organic framework-derived Mn_2O_3 nanowire coated three-dimensional graphene network for high-performance free-standing supercapacitor electrodes. *J. Mater. Chem. A* **2016**, *4*, 8283−8290.
(322) Jiao, L.; Zhou, Y.-X.; Jiang, H.-L. Metal-organic framework-based CoP/reduced graphene oxide: high-performance bifunctional electrocatalyst for overall water splitting. *Chem. Sci.* **2016**, *7*, 1690−1695.
(323) Ma, T. Y.; Dai, S.; Jaroniec, M.; Qiao, S. Z. Metal-organic framework derived hybrid Co_3O_4-carbon porous nanowire arrays as reversible oxygen evolution electrodes. *J. Am. Chem. Soc.* **2014**, *136*, 13925−13931.
(324) Cai, G.; Zhang, W.; Jiao, L.; Yu, S.-H.; Jiang, H.-L. Template-directed growth of well-aligned MOF arrays and derived self-supporting electrodes for water splitting. *Chem* **2017**, *2*, 791−802.
(325) Yang, Q.; Yang, C. C.; Lin, C. H.; Jiang, H. L. Metal-organic-framework-derived hollow N-doped porous carbon with ultrahigh concentrations of single Zn atoms for efficient carbon dioxide conversion. *Angew. Chem., Int. Ed.* **2019**, *58*, 3511−3515.
(326) Yin, P.; Yao, T.; Wu, Y.; Zheng, L.; Lin, Y.; Liu, W.; Ju, H.; Zhu, J.; Hong, X.; Deng, Z.; et al. Single cobalt atoms with precise N-coordination as superior oxygen reduction reaction catalysts. *Angew. Chem., Int. Ed.* **2016**, *55*, 10800−10805.
(327) Crabtree, R. H. Deactivation in homogeneous transition metal catalysis: causes, avoidance, and cure. *Chem. Rev.* **2015**, *115*, 127−150.
(328) Valyaev, D. A.; Lavigne, G.; Lugan, N. Manganese organometallic compounds in homogeneous catalysis: past, present, and prospects. *Coord. Chem. Rev.* **2016**, *308*, 191−235.
(329) Bedioui, F. Zeolite-encapsulated and clay-intercalated metal porphyrin, phthalocyanine and Schiff-base complexes as models for biomimetic oxidation catalysts: an overview. *Coord. Chem. Rev.* **1995**, *144*, 39−68.
(330) Fang, X.; Liu, Z.; Hsieh, M.-F.; Chen, M.; Liu, P.; Chen, C.; Zheng, N. Hollow mesoporous aluminosilica spheres with perpendicular pore channels as catalytic nanoreactors. *ACS Nano* **2012**, *6*, 4434−4444.
(331) Liu, F.; Wang, L.; Sun, Q.; Zhu, L.; Meng, X.; Xiao, F.-S. Transesterification catalyzed by ionic liquids on superhydrophobic mesoporous polymers: heterogeneous catalysts that are faster than homogeneous catalysts. *J. Am. Chem. Soc.* **2012**, *134*, 16948−16950.
(332) Dai, C.; Zhang, A.; Li, J.; Hou, K.; Liu, M.; Song, C.; Guo, X. Synthesis of yolk-shell HPW@hollow silicalite-1 for esterification reaction. *Chem. Commun.* **2014**, *50*, 4846−4848.
(333) Gao, W.-Y.; Chrzanowski, M.; Ma, S. Metal-metalloporphyrin frameworks: a resurging class of functional materials. *Chem. Soc. Rev.* **2014**, *43*, 5841−5866.
(334) Qiao, Z.-A.; Zhang, P.; Chai, S.-H.; Chi, M.; Veith, G. M.; Gallego, N. C.; Kidder, M.; Dai, S. Lab-in-a-shell: encapsulating metal clusters for size sieving catalysis. *J. Am. Chem. Soc.* **2014**, *136*, 11260−11263.
(335) Leenders, S. H.; Gramage-Doria, R.; de Bruin, B.; Reek, J. N. Transition metal catalysis in confined spaces. *Chem. Soc. Rev.* **2015**, *44*, 433−448.
(336) Dai, C.; Zhang, A.; Liu, M.; Gu, L.; Guo, X.; Song, C. Hollow alveolus-like nanovesicle assembly with metal-encapsulated hollow zeolite nanocrystals. *ACS Nano* **2016**, *10*, 7401−7408.
(337) Zhan, G.; Zeng, H. C. Integrated nanocatalysts with mesoporous silica/silicate and microporous MOF materials. *Coord. Chem. Rev.* **2016**, *320*, 181−192.
(338) Chen, L.-J.; Chen, S.; Qin, Y.; Xu, L.; Yin, G.-Q.; Zhu, J.-L.; Zhu, F.-F.; Zheng, W.; Li, X.; Yang, H.-B. Construction of porphyrin-containing metallacycle with improved stability and activity within mesoporous carbon. *J. Am. Chem. Soc.* **2018**, *140*, 5049−5052.
(339) Cirujano, F. G.; Martin, N.; Wee, L. H. Design of hierarchical architectures in metal-oganic frameworks for catalysis and adsorption. *Chem. Mater.* **2020**, *32*, 10268−10295.
(340) Jiao, L.; Wang, Y.; Jiang, H. L.; Xu, Q. Metal-organic frameworks as platforms for catalytic applications. *Adv. Mater.* **2018**, *30*, 1703663.
(341) Horcajada, P.; Surblé, S.; Serre, C.; Hong, D.-Y.; Seo, Y.-K.; Chang, J.-S.; Grenèche, J.-M.; Margiolaki, I.; Férey, G. Synthesis and catalytic properties of MIL-100(Fe), an iron(III) carboxylate with large pores. *Chem. Commun.* **2007**, 2820−2822.
(342) Mondloch, J. E.; Katz, M. J.; Isley, W. C., III; Ghosh, P.; Liao, P.; Bury, W.; Wagner, G. W.; Hall, M. G.; DeCoste, J. B.; Peterson, G. W.; et al. Destruction of chemical warfare agents using metal-organic frameworks. *Nat. Mater.* **2015**, *14*, 512−516.
(343) Akiyama, G.; Matsuda, R.; Sato, H.; Takata, M.; Kitagawa, S. Cellulose hydrolysis by a new porous coordination polymer decorated with sulfonic acid functional groups. *Adv. Mater.* **2011**, *23*, 3294−3297.
(344) Zhou, Y. X.; Chen, Y. Z.; Hu, Y.; Huang, G.; Yu, S. H.; Jiang, H. L. MIL-101-SO_3H: a highly efficient brønsted acid catalyst for heterogeneous alcoholysis of epoxides under ambient conditions. *Chem. - Eur. J.* **2014**, *20*, 14976−14980.
(345) Hwang, Y. K.; Hong, D. Y.; Chang, J. S.; Jhung, S. H.; Seo, Y. K.; Kim, J.; Vimont, A.; Daturi, M.; Serre, C.; Férey, G. Amine grafting on coordinatively unsaturated metal centers of MOFs: consequences for catalysis and metal encapsulation. *Angew. Chem., Int. Ed.* **2008**, *47*, 4144−4148.
(346) Banerjee, M.; Das, S.; Yoon, M.; Choi, H. J.; Hyun, M. H.; Park, S. M.; Seo, G.; Kim, K. Postsynthetic modification switches an achiral framework to catalytically active homochiral metal-organic porous materials. *J. Am. Chem. Soc.* **2009**, *131*, 7524−7525.
(347) Noh, H.; Cui, Y.; Peters, A. W.; Pahls, D. R.; Ortuño, M. A.; Vermeulen, N. A.; Cramer, C. J.; Gagliardi, L.; Hupp, J. T.; Farha, O. K. An exceptionally stable metal-organic framework supported molybdenum(VI) oxide catalyst for cyclohexene epoxidation. *J. Am. Chem. Soc.* **2016**, *138*, 14720−14726.
(348) Li, Z.; Schweitzer, N. M.; League, A. B.; Bernales, V.; Peters, A. W.; Getsoian, A. B.; Wang, T. C.; Miller, J. T.; Vjunov, A.; Fulton, J. L.; et al. Sintering-resistant single-site nickel catalyst supported by metal-organic framework. *J. Am. Chem. Soc.* **2016**, *138*, 1977−1982.

https://doi.org/10.1021/acs.chemrev.1c00243
Chem. Rev. 2021, 121, 12278−12326

(349) Yang, Q.; Xu, Q.; Jiang, H.-L. Metal-organic frameworks meet metal nanoparticles: synergistic effect for enhanced catalysis. *Chem. Soc. Rev.* **2017**, *46*, 4774−4808.
(350) Kockrick, E.; Lescouet, T.; Kudrik, E. V.; Sorokin, A. B.; Farrusseng, D. Synergistic effects of encapsulated phthalocyanine complexes in MIL-101 for the selective aerobic oxidation of tetralin. *Chem. Commun.* **2011**, *47*, 1562−1564.
(351) Aijaz, A.; Karkamkar, A.; Choi, Y. J.; Tsumori, N.; Rönnebro, E.; Autrey, T.; Shioyama, H.; Xu, Q. Immobilizing highly catalytically active Pt nanoparticles inside the pores of metal-organic framework: a double solvents approach. *J. Am. Chem. Soc.* **2012**, *134*, 13926−13929.
(352) Chen, Y.-Z.; Zhou, Y.-X.; Wang, H.; Lu, J.; Uchida, T.; Xu, Q.; Yu, S.-H.; Jiang, H.-L. Multifunctional PdAg@MIL-101 for one-pot cascade reactions: combination of host-guest cooperation and bimetallic synergy in catalysis. *ACS Catal.* **2015**, *5*, 2062−2069.
(353) Chen, Y. Z.; Xu, Q.; Yu, S. H.; Jiang, H. L. Tiny Pd@Co core-shell nanoparticles confined inside a metal-organic framework for highly efficient catalysis. *Small* **2015**, *11*, 71−76.
(354) Chen, Y.-Z.; Gu, B.; Uchida, T.; Liu, J.; Liu, X.; Ye, B.-J.; Xu, Q.; Jiang, H.-L. Location determination of metal nanoparticles relative to a metal-organic framework. *Nat. Commun.* **2019**, *10*, 3462.
(355) Ma, X.; Wang, L.; Zhang, Q.; Jiang, H. L. Switching on the photocatalysis of metal-organic frameworks by engineering structural defects. *Angew. Chem., Int. Ed.* **2019**, *58*, 12175−12179.
(356) Cai, X.; Xie, Z.; Li, D.; Kassymova, M.; Zang, S.-Q.; Jiang, H.-L. Nano-sized metal-organic frameworks: synthesis and applications. *Coord. Chem. Rev.* **2020**, *417*, 213366.
(357) Hu, P.; Morabito, J. V.; Tsung, C.-K. Core-shell catalysts of metal nanoparticle core and metal-organic framework shell. *ACS Catal.* **2014**, *4*, 4409−4419.
(358) Wang, X.; Li, M.; Cao, C.; Liu, C.; Liu, J.; Zhu, Y.; Zhang, S.; Song, W. Surfactant-free palladium nanoparticles encapsulated in ZIF-8 hollow nanospheres for size-selective catalysis in liquid-phase solution. *ChemCatChem* **2016**, *8*, 3224−3228.
(359) Cai, G.; Ding, M.; Wu, Q.; Jiang, H.-L. Encapsulating soluble active species into hollow crystalline porous capsules beyond integration of homogeneous and heterogeneous catalysis. *Natl. Sci. Rev.* **2020**, *7*, 37−45.
(360) Cao, X.; Tan, C.; Sindoro, M.; Zhang, H. Hybrid micro-/nano-structures derived from metal-organic frameworks: preparation and applications in energy storage and conversion. *Chem. Soc. Rev.* **2017**, *46*, 2660−2677.
(361) Liang, Z.; Qu, C.; Xia, D.; Zou, R.; Xu, Q. Atomically dispersed metal sites in MOF-based materials for electrocatalytic and photocatalytic energy conversion. *Angew. Chem., Int. Ed.* **2018**, *57*, 9604−9633.
(362) Bhadra, B. N.; Vinu, A.; Serre, C.; Jhung, S. H. MOF-derived carbonaceous materials enriched with nitrogen: Preparation and applications in adsorption and catalysis. *Mater. Today* **2019**, *25*, 88−111.
(363) Zhan, W.; Sun, L.; Han, X. Recent progress on engineering highly efficient porous semiconductor photocatalysts derived from metal-organic frameworks. *Nano-Micro Lett.* **2019**, *11*, 1.
(364) Chen, Z.; Qing, H.; Zhou, K.; Sun, D.; Wu, R. Metal-organic framework-derived nanocomposites for electrocatalytic hydrogen evolution reaction. *Prog. Mater. Sci.* **2020**, *108*, 100618.
(365) Cheng, N.; Ren, L.; Xu, X.; Du, Y.; Dou, S. X. Recent development of zeolitic imidazolate frameworks (ZIFs) derived porous carbon based materials as electrocatalysts. *Adv. Energy Mater.* **2018**, *8*, 1801257.
(366) Yang, L.; Zeng, X.; Wang, W.; Cao, D. Recent progress in MOF-derived, heteroatom-doped porous carbons as highly efficient electrocatalysts for oxygen reduction reaction in fuel cells. *Adv. Funct. Mater.* **2018**, *28*, 1704537.
(367) Song, Z.; Zhang, L.; Doyle-Davis, K.; Fu, X.; Luo, J. L.; Sun, X. Recent advances in MOF-derived single-atom catalysts for electrochemical applications. *Adv. Energy Mater.* **2020**, *10*, 2001561.
(368) Zhou, W.; Huang, D. D.; Wu, Y. P.; Zhao, J.; Wu, T.; Zhang, J.; Li, D. S.; Sun, C.; Feng, P.; Bu, X. Stable hierarchical bimetal-organic nanostructures as highperformance electrocatalysts for the oxygen evolution reaction. *Angew. Chem., Int. Ed.* **2019**, *58*, 4227−4231.
(369) Bai, C.; Yao, X.; Li, Y. Easy access to amides through aldehydic C-H bond functionalization catalyzed by heterogeneous Co-based catalysts. *ACS Catal.* **2015**, *5*, 884−891.
(370) Jagadeesh, R. V.; Murugesan, K.; Alshammari, A. S.; Neumann, H.; Pohl, M.-M.; Radnik, J.; Beller, M. MOF-derived cobalt nanoparticles catalyze a general synthesis of amines. *Science* **2017**, *358*, 326−332.
(371) Gao, X.; Ding, Y.; Sheng, Y.; Hu, M.; Zhai, Q.; Li, S.; Jiang, Y.; Chen, Y. Enzyme immobilization in MOF-derived porous NiO with hierarchical structure: an efficient and stable enzymatic reactor. *ChemCatChem* **2019**, *11*, 2828−2836.
(372) Guo, Y.; Feng, L.; Wu, C.; Wang, X.; Zhang, X. Confined pyrolysis transformation of ZIF-8 to hierarchically ordered porous Zn-NC nanoreactor for efficient CO_2 photoconversion under mild conditions. *J. Catal.* **2020**, *390*, 213−223.
(373) Xiao, J. D.; Jiang, H. L. Thermally stable metal-organic framework-templated synthesis of hierarchically porous metal sulfides: enhanced Photocatalytic hydrogen production. *Small* **2017**, *13*, 1700632.
(374) Jiao, L.; Wan, G.; Zhang, R.; Zhou, H.; Yu, S. H.; Jiang, H. L. From metal-organic frameworks to single-atom Fe implanted N-doped porous carbons: efficient oxygen reduction in both alkaline and acidic media. *Angew. Chem., Int. Ed.* **2018**, *57*, 8525−8529.
(375) Zhou, J.; Dou, Y.; Zhou, A.; Shu, L.; Chen, Y.; Li, J.-R. Layered metal-organic framework-derived metal oxide/carbon nanosheet arrays for catalyzing the oxygen evolution reaction. *ACS Energy Lett.* **2018**, *3*, 1655−1661.
(376) Wu, Y. L.; Li, X.; Wei, Y. S.; Fu, Z.; Wei, W.; Wu, X. T.; Zhu, Q. L.; Xu, Q. Ordered macroporous superstructure of nitrogen-doped nanoporous carbon implanted with ultrafine Ru nanoclusters for efficient pH-universal hydrogen evolution reaction. *Adv. Mater.* **2021**, *33*, 2006965.
(377) Li, H.; Wang, K.; Sun, Y.; Lollar, C. T.; Li, J.; Zhou, H.-C. Recent advances in gas storage and separation using metal-organic frameworks. *Mater. Today* **2018**, *21*, 108−121.
(378) Sumida, K.; Rogow, D. L.; Mason, J. A.; McDonald, T. M.; Bloch, E. D.; Herm, Z. R.; Bae, T.-H.; Long, J. R. Carbon dioxide capture in metal-organic frameworks. *Chem. Rev.* **2012**, *112*, 724−781.
(379) Yu, G.; Zou, X.; Sun, L.; Liu, B.; Wang, Z.; Zhang, P.; Zhu, G. Constructing connected paths between UiO-66 and PIM-1 to improve membrane CO_2 separation with crystal-like gas selectivity. *Adv. Mater.* **2019**, *31*, 1806853.
(380) Wang, Y.; Jia, X.; Yang, H.; Wang, Y.; Chen, X.; Hong, A. N.; Li, J.; Bu, X.; Feng, P. A strategy for constructing pore-space-partitioned MOFs with high uptake capacity for C_2 Hydrocarbons and CO_2. *Angew. Chem., Int. Ed.* **2020**, *59*, 19027−19030.
(381) Lieb, A.; Leclerc, H.; Devic, T.; Serre, C.; Margiolaki, I.; Mahjoubi, F.; Lee, J. S.; Vimont, A.; Daturi, M.; Chang, J.-S. MIL-100(V)-a mesoporous vanadium metal organic framework with accessible metal sites. *Microporous Mesoporous Mater.* **2012**, *157*, 18−23.
(382) Barea, E.; Montoro, C.; Navarro, J. A. Toxic gas removal-metal-organic frameworks for the capture and degradation of toxic gases and vapours. *Chem. Soc. Rev.* **2014**, *43*, 5419−5430.
(383) DeCoste, J. B.; Peterson, G. W. Metal-organic frameworks for air purification of toxic chemicals. *Chem. Rev.* **2014**, *114*, 5695−5727.
(384) Chen, Y.; Chen, F.; Zhang, S.; Cai, Y.; Cao, S.; Li, S.; Zhao, W.; Yuan, S.; Feng, X.; Cao, A.; et al. Facile fabrication of multifunctional metal-organic framework hollow tubes to trap pollutants. *J. Am. Chem. Soc.* **2017**, *139*, 16482−16485.
(385) Khan, N. A.; Hasan, Z.; Jhung, S. H. Adsorptive removal of hazardous materials using metal-organic frameworks (MOFs): a review. *J. Hazard. Mater.* **2013**, *244*, 444−456.

https://doi.org/10.1021/acs.chemrev.1c00243
Chem. Rev. 2021, 121, 12278−12326

(386) Dias, E. M.; Petit, C. Towards the use of metal-organic frameworks for water reuse: a review of the recent advances in the field of organic pollutants removal and degradation and the next steps in the field. *J. Mater. Chem. A* **2015**, *3*, 22484−22506.
(387) Hasan, Z.; Jhung, S. H. Removal of hazardous organics from water using metal-organic frameworks (MOFs): plausible mechanisms for selective adsorptions. *J. Hazard. Mater.* **2015**, *283*, 329−339.
(388) Bobbitt, N. S.; Mendonca, M. L.; Howarth, A. J.; Islamoglu, T.; Hupp, J. T.; Farha, O. K.; Snurr, R. Q. Metal-organic frameworks for the removal of toxic industrial chemicals and chemical warfare agents. *Chem. Soc. Rev.* **2017**, *46*, 3357−3385.
(389) Li, J.; Wang, X.; Zhao, G.; Chen, C.; Chai, Z.; Alsaedi, A.; Hayat, T.; Wang, X. Metal-organic framework-based materials: superior adsorbents for the capture of toxic and radioactive metal ions. *Chem. Soc. Rev.* **2018**, *47*, 2322−2356.
(390) Zhu, B.-J.; Yu, X.-Y.; Jia, Y.; Peng, F.-M.; Sun, B.; Zhang, M.-Y.; Luo, T.; Liu, J.-H.; Huang, X.-J. Iron and 1, 3, 5-benzenetricarboxylic metal-organic coordination polymers prepared by solvothermal method and their application in efficient As(V) removal from aqueous solutions. *J. Phys. Chem. C* **2012**, *116*, 8601−8607.
(391) Nuzhdin, A. L.; Kovalenko, K. A.; Dybtsev, D. N.; Bukhtiyarova, G. A. Removal of nitrogen compounds from liquid hydrocarbon streams by selective sorption on metal-organic framework MIL-101. *Mendeleev Commun.* **2010**, *20*, 57−58.
(392) Hedegaard, M. J.; Arvin, E.; Corfitzen, C. B.; Albrechtsen, H.-J. Mecoprop (MCPP) removal in full-scale rapid sand filters at a groundwater-based waterworks. *Sci. Total Environ.* **2014**, *499*, 257−264.
(393) Zhang, N.; Qi, Y.; Zhang, Y.; Luo, J.; Cui, P.; Jiang, W. A Review on oil/water mixture separation material. *Ind. Eng. Chem. Res.* **2020**, *59*, 14546−14568.
(394) Wang, X.; Yu, J.; Sun, G.; Ding, B. Electrospun nanofibrous materials: a versatile medium for effective oil/water separation. *Mater. Today* **2016**, *19*, 403−414.
(395) Xue, Z.; Cao, Y.; Liu, N.; Feng, L.; Jiang, L. Special wettable materials for oil/water separation. *J. Mater. Chem. A* **2014**, *2*, 2445−2460.
(396) Padaki, M.; Surya Murali, R.; Abdullah, M.S.; Misdan, N.; Moslehyani, A.; Kassim, M.A.; Hilal, N.; Ismail, A.F. Membrane technology enhancement in oil-water separation. A review. *Desalination* **2015**, *357*, 197−207.
(397) Gupta, R. K.; Dunderdale, G. J.; England, M. W.; Hozumi, A. Oil/water separation techniques: a review of recent progresses and future directions. *J. Mater. Chem. A* **2017**, *5*, 16025−16058.
(398) Lustig, W. P.; Mukherjee, S.; Rudd, N. D.; Desai, A. V.; Li, J.; Ghosh, S. K. Metal-organic frameworks: functional luminescent and photonic materials for sensing applications. *Chem. Soc. Rev.* **2017**, *46*, 3242−3285.
(399) Dolgopolova, E. A.; Rice, A. M.; Martin, C. R.; Shustova, N. B. Photochemistry and photophysics of MOFs: steps towards MOF-based sensing enhancements. *Chem. Soc. Rev.* **2018**, *47*, 4710−4728.
(400) Zhang, Y.; Yuan, S.; Day, G.; Wang, X.; Yang, X.; Zhou, H.-C. Luminescent sensors based on metal-organic frameworks. *Coord. Chem. Rev.* **2018**, *354*, 28−45.
(401) Amini, A.; Kazemi, S.; Safarifard, V. Metal-organic framework-based nanocomposites for sensing applications-a review. *Polyhedron* **2020**, *177*, 114260.
(402) Li, H.-Y.; Zhao, S.-N.; Zang, S.-Q.; Li, J. Functional metal-organic frameworks as effective sensors of gases and volatile compounds. *Chem. Soc. Rev.* **2020**, *49*, 6364−6401.
(403) Deibert, B. J.; Li, J. A distinct reversible colorimetric and fluorescent low pH response on a water-stable zirconium-porphyrin metal-organic framework. *Chem. Commun.* **2014**, *50*, 9636−9639.
(404) Cao, Y.; Wang, L.; Shen, C.; Wang, C.; Hu, X.; Wang, G. An electrochemical sensor on the hierarchically porous Cu-BTC MOF platform for glyphosate determination. *Sens. Actuators, B* **2019**, *283*, 487−494.
(405) Cai, G.; Holoubek, J.; Xia, D.; Li, M.; Yin, Y.; Xing, X.; Liu, P.; Chen, Z. An ester electrolyte for lithium-sulfur batteries capable of ultra-low temperature cycling. *Chem. Commun.* **2020**, *56*, 9114−9117.
(406) D'Alessandro, D. Exploiting redox activity in metal-organic frameworks: concepts, trends and perspectives. *Chem. Commun.* **2016**, *52*, 8957−8971.
(407) Zhang, Y.; Riduan, S. N.; Wang, J. Redox active metal-and covalent organic frameworks for energy storage: balancing porosity and electrical conductivity. *Chem. - Eur. J.* **2017**, *23*, 16419−16431.
(408) Zhao, R.; Liang, Z.; Zou, R.; Xu, Q. Metal-organic frameworks for batteries. *Joule* **2018**, *2*, 2235−2259.
(409) Baumann, A. E.; Burns, D. A.; Liu, B.; Thoi, V. S. Metal-organic framework functionalization and design strategies for advanced electrochemical energy storage devices. *Commun. Chem.* **2019**, *2*, 86.
(410) He, Y.; Qiao, Y.; Chang, Z.; Zhou, H. The potential of electrolyte filled MOF membranes as ionic sieves in rechargeable batteries. *Energy Environ. Sci.* **2019**, *12*, 2327−2344.
(411) Li, C.; Liu, L.; Kang, J.; Xiao, Y.; Feng, Y.; Cao, F.-F.; Zhang, H. Pristine MOF and COF materials for advanced batteries. *Energy Storage Mater.* **2020**, *31*, 115−134.
(412) Shin, J.; Kim, M.; Cirera, J.; Chen, S.; Halder, G. J.; Yersak, T. A.; Paesani, F.; Cohen, S. M.; Meng, Y. S. MIL-101 (Fe) as a lithium-ion battery electrode material: a relaxation and intercalation mechanism during lithium insertion. *J. Mater. Chem. A* **2015**, *3*, 4738−4744.
(413) Férey, G.; Millange, F.; Morcrette, M.; Serre, C.; Doublet, M. L.; Grenèche, J. M.; Tarascon, J. M. Mixed-valence Li/Fe-based metal-organic frameworks with both reversible redox and sorption properties. *Angew. Chem., Int. Ed.* **2007**, *46*, 3259−3263.
(414) Bai, S.; Liu, X.; Zhu, K.; Wu, S.; Zhou, H. Metal-organic framework-based separator for lithium-sulfur batteries. *Nat. Energy* **2016**, *1*, 16094.
(415) Guo, Y.; Sun, M.; Liang, H.; Ying, W.; Zeng, X.; Ying, Y.; Zhou, S.; Liang, C.; Lin, Z.; Peng, X. Blocking polysulfides and facilitating lithium-ion transport: polystyrene sulfonate@HKUST-1 membrane for lithium-sulfur batteries. *ACS Appl. Mater. Interfaces* **2018**, *10*, 30451−30459.
(416) Wang, Z.; Huang, W.; Hua, J.; Wang, Y.; Yi, H.; Zhao, W.; Zhao, Q.; Jia, H.; Fei, B.; Pan, F. An anionic-MOF-based bifunctional separator for regulating lithium deposition and suppressing polysulfides shuttle in Li-S batteries. *Small Methods* **2020**, *4*, 2000082.
(417) Cai, G.; Yin, Y.; Xia, D.; Chen, A. A.; Holoubek, J.; Scharf, J.; Yang, Y.; Koh, K. H.; Li, M.; Davies, D. M.; Mayer, M.; Han, T. H.; Meng, Y. S.; Pascal, T. A.; Chen, Z. Sub-nanometer confinement enables facile condensation of gas electrolyte for low-temperature batteries. *Nat. Commun.* **2021**, *12*, 3395.
(418) Rustomji, C. S.; Yang, Y.; Kim, T. K.; Mac, J.; Kim, Y. J.; Caldwell, E.; Chung, H.; Meng, Y. S. Liquefied gas electrolytes for electrochemical energy storage devices. *Science* **2017**, *356*, No. eaal4263.
(419) Aukett, P.; Quirke, N.; Riddiford, S.; Tennison, S. Methane adsorption on microporous carbons—a comparison of experiment, theory, and simulation. *Carbon* **1992**, *30*, 913−924.

https://doi.org/10.1021/acs.chemrev.1c00243
Chem. Rev. 2021, 121, 12278−12326